Chapter 1

Table S1-1. Target gene selection and comparisons between target genes conducted in insects.

Abbreviations: GPCR, G-protein-coupled receptor; COPB, Coatome Protein Complex Subunit Beta; vATPase A, vacuolar H+-ATPase subunit A; RPL9, Ribosomal Protein L9; arf1, ADP-ribosylation factor 1; Nrg, Neuregulin; PPO2, Polyphenol oxidase 2 precursor; Prosα2, proteasome subunit alpha type 2; Snf7, vacuolar-sorting protein Snf7; CHY, chymotrypsin; Cpcul1, cullin-1; jhamt, juvenile hormone acid methyl transferase; IAP1, inhibitor of apoptosis protein 1; VTE, v-type ATPase subunit E; IAP, inhibitor of apoptosis.

Order	Species	Genes screened	Results	Best target gene(s)	Function	Expression	Comments & Citation(s)
Coleoptera	Red flour beetle, *Tribolium castaneum*	111 non-sensory GPCRs (Bai et al., 2011); 5,000 random genes from iBeetle screened (Ulrich et al., 2015); Two critical genes for insect development that had previously been good	8 genes (Bai et al., 2011) and 100 (Ulrich et al., 2015) genes caused >90% mortality; 100% mortality and >80% suppression after feeding and injection of *VTE* and *IAP* (Cao et al., 2018)	11 highly efficient targets, but *dopamine-2 like receptor* & *latrophilin receptor* best (Bai et al., 2011); 11 genes with 100% mortality by day 8 (Ulrich et al., 2015); Higher mortality for *VTE* than *IAP* with injection even though	Non-sensory GPCRs involved in crucial physiological processes (Bai et al., 2011); Genes identified by name; Go terms that are predictive of good targets identified (protesome & cytoskeleton) (Ulrich et al., 2015); Name and function	Basal stage-specific expression shown for six genes; suppression checked for four genes (Bai et al., 2011); Tissue-specific and basal expression not presented (Ulrich et al., 2015); lifestage specific	Stage-specific mortality for different genes; more than 50% silencing for 95% of genes (Bai et al., 2011). Proteasomal genes are most predictive (over 70% caused mortality). Better mortality than genes from Baum et al.,

		targets (Cao et al., 2018)		knockdown was similar (Cao et al., 2018)	of target genes discussed (Cao et al., 2018)	expression presented (Cao et al., 2018)	2007 (Ulrich et al., 2015); Uses flour discs for oral delivery; notes a difference in the expression of critical genes in different insect species (Cao et al., 2018)
Coleoptera	Colorado potato beetle, *Leptinotarsa decemlineata*	5 genes with essential functions	All five knocked down >60%; significant mortality & weight loss for all five genes	Actin reduced body weight most, but LC_{50} was lowest for *COPB*	Functions of each gene discussed in detail	Tissue-specific and basal expression not presented	Compared suppression between synthesized dsRNA and *E. coli* produced/encapsulated dsRNA (Zhu et al., 2011).
Coleoptera	Western corn rootworm, *Diabrotica virgifera virgifera*	290 genes with essential functions (Baum et al., 2007); Four genes expected to generate pigmentation defects	125 exhibited stunting & mortality at 52 ng/cm^2 and 67 exhibited stunting & mortality at 5.2 ng/cm;^{2} (Baum et al., 2007)	Four genes with LC_{50} near 0.52 ng/cm^2; Most suppression for *vATPase A* (Baum et al., 2007); *Laccase 2* and *ebony* are suitable as	Names of 26 target genes provided; functions not discussed (Baum et al., 2007); Names and functions discussed	Tissue-specific and basal expression not presented (Baum et al., 2007; Miyata et al., 2014)	Six dsRNAs targeting different regions of *v-ATPase* gene tested and all worked equally well (Baum et al., 2007). No phenotype observed for

		(Miyata et al., 2014)	Clear phenotypes observed for *Laccase 2* and *ebony*	marker genes (Miyata et al., 2014)	(Miyata et al., 2014)		two *yellow* genes (Miyata et al., 2014).
Coleoptera	African sweet potato weevil, *Cylas puncticollis*	First screened 24 genes with injection, and then chose three genes for oral delivery	>50% mortality for all 24 genes after 14 days; almost 100% morality for 12 genes at 14 days post injection	Significant suppression after oral feeding for *Prosα2* and *Snf7*, with ~70% mortality	Names of all target genes provided; function of top three targets discussed	Tissue-specific or basal expression not presented	Lower mortality after feeding than injection (Prentice et al., 2017).
Diptera	Yellow fever mosquito, *Aedes aegypti*	3'UTR, 5'UTR, CDS of *IAP1*	Highest mortality when 3'UTR targeted or when a combination of all three is used	Targeting 3'UTR region and using a transfection reagent was most effective (43% mortality)	Name and function of target gene discussed	Tissue-specific expression of splicing variants discussed	Topical application was used to deliver dsRNA instead of injection or feeding. The region of the gene targeted and the carrier effect suppression (Pridgeon et al., 2008).

Hemipteran	Brown marmorated stink bug, *Halyomorpha halys*	13 genes that were effective in other species	70% mortality for 5/13 genes with injection; 70% mortality for 3/5 genes after feeding	*IAP*, *ATPase*, *SNF7*, *GPCR*, and *PPI* used for feeding; *ATPase* caused highest mortality	Names of target genes given and functions of some discussed	Tissue-specific or basal expression not presented	ATPase caused highest mortality but dsSNF7 had lower transcript levels after feeding (Mogilicherla et al., 2018).
Hemiptera	Gran aphid, *Sitobion avenae*	16 genes significantly up or down regulated in gut	Five genes with significant mortality and stunting	Three highly expressed and two low expressed genes identified as good targets	Names of targets given; function not discussed	Basal expression investigated in gut, and tissue specific expression presented	Choose target genes based on gene regulation in gut, before and after feeding on wheat plants (Zhang et al., 2013).
Hemiptera	Whitefly, *Bemisia tabaci*	Five genes selected based on Baum et al., 2007	Mortality observed for all five genes with dsRNA and siRNA	*RPL9* and *vATPase A* (LC_{50} 11.21 & 3.08 ug/ml)	Genes identified but functions not discussed	Tissue-specific or basal expression not presented	Higher mortality for highly "active" genes (*RPL9 and V-ATPase A*) rather than the structural and less "active" genes (*actin ortholog* and *α-tubulin*) (Upadhyay et al., 2011)

Hemiptera	Pea aphid, *Acyrthosi-phon pisum*	Two critical genes for insect development that had previously been good targets	*VTE* but not *IAP* resulted in 65% mortality and 40% suppression after injection Feeding of VTE reduced growth and fecundity but no gene suppression was observed	*VTE* with injection but not feeding	Name and function of target genes discussed	Lifestage-specific expression presented	*IAP* mRNA levels were more variable during the lifecycle than *VTE;* notes a difference in the expression of critical genes in different insect species; suppression is weak and transient (i.e., suppression at 24 h but not 72 h) (Cao et al., 2018).
Lepidoptera	Tomato leafminer, *Tuta absoluta*	Eight highly expressed genes	Suppression of five genes, significant weight loss for all eight	All eight ruled as good targets, but mortality was not mentioned	Gene identities not presented	Tissue-specific not presented; basal expression discussed	Genes with high expression likely have essential functions (Camargo et al., 2015).
Lepidoptera	Beet armyworm, *Spodoptera exigua*	Nine genes involved in important cellular processes (worked in	20-95% suppression & mortality with eight genes; retarded development	Highest mortality (28.3%) with *tubulin2* and *arf1* (Li et al., 2013);	Genes identified but functions not discussed (Li et al., 2013);	Tissue-specific and basal expression not presented	Duration and degree of knockdown varies between nine genes. Five genes

		rootworms) (Li et al., 2013); Seven *CHY* genes (Vatanparast and Kim, 2017)	for five genes (Li et al., 2013); Five of seven genes suppressed in gut after feeding, and eight suppressed after injection (Vatanparast and Kim, 2017)	Highest mortality & suppression for *CHY2* after feeding and injection (Vatanparast and Kim, 2017)	Genes identified and functions discussed (Vatanparast and Kim, 2017)	(Li et al., 2013); Life stage-specific basal expression and tissue-specific expression presented and discussed (Vatanparast and Kim, 2017)	significantly upregulated at different time points (Li et al., 2013); RNAi is not systemic, and dsRNA delivered in sonicated bacteria enhanced RNAi efficiency (Vatanparast and Kim, 2017).
Lepidoptera	Asian corn borer, *Ostrinia furnalalis*	Ten genes with high expression	Nine genes with mortality between 73-100% & nine genes with suppression	5 genes >90% mortality	Genes are identified by name and functions in various tissues discussed	Life stage-specific basal expression shown but not tissue-specific	Expression increased at first then decreased to different levels at different rates. Highest expressed genes make best targets (Wang et al., 2011).
Lepidoptera	Armyworm, *Mythimna separata*	Five genes with distinct tissue-specific	All genes refractory despite being expressed in	30% knockdown in adhering	Genes are identified by name; Two immune genes	Tissue-specific expression and basal	Only adhering (phagocytic) hemocytes exhibited

		expression; two dsRNAs targeting different gene regions tested	different tissues	hemocytes with *Nrg*	(*Nrg & PPO2*) but those did not work any better than others	expression in each tissue presented	suppression when the abdomen was ligated to prevent replacement of blood cells (Yokoi et al., 2013).
Lepidoptera	Codling moth, *Cydia pomonella*	Five target genes with well-defined phenotypes in *Drosophila*	Mortality and phenotypes only for *Cpcul1*	*Cpcul1* significantly affected larval growth	Genes identified by name and function of best gene discussed	Life stage-specific basal expression shown but not tissue-specific	Labeled dsRNA accumulated in gut and did not spread to other tissues. SiRNA has similar RNAi efficiency as dsRNA (Wang et al., 2015a).
Lepidoptera	Cotton bollworm, *Helicoverpa armigera*	Five genes with crucial roles in daily biological functions of insects	Significant suppression of three genes with a 10 µg dose and 4 genes with 20 µg dose	*CHY* significantly affected larval and pupal weight while *jhamt* severely affected pupation	Genes identified by name and functions discussed	Tissue-specific or basal expression not presented	(Asokan et al., 2014)
Orthoptera	Migratory locust, *Locusta migratoria*	Nine genes with essential functions	Seven genes resulted in mortality and suppression	40-60% mortality for *vATPase*	Genes identified by name and	Tissue-specific expression and basal	Two midgut-specific genes and three broadly

				subunits A & *E*	functions discussed	expression discussed	expressed genes were suppressed with injection but not oral feeding (with or without a transfection reagent) (Luo et al., 2013).

Table S1-2. Assessments of dsRNA stability conducted in insects.

Abbreviations: RNAi, RNA interference; dsRNase, double-stranded ribonucleases; ssRNase, single-stranded RNase; Eri-1, Enhanced RNA Interference-1 3'-5' exonuclease; CB_{50}, concentration of body fluid to degrade 50% of dsRNA in 1 hour; REase, RNAi efficiency-related nuclease; h, hour; min, minute; Tsal, tsetse salivary gland protein; Endo, nonspecific endonuclease.

Order	Species	Stability/Tissue(s)	Cause(s) implicated	RNAi Efficiency	Comments & Reference(s)
Blattodae	American cockroach, *Periplaneta americana*	Stable in hemolymph & gut after 1 h (Wang et al., 2016); 54.72 & 0.12 RFU mg^{-1} protein $s^{-1}$of nuclease activity in gut fluid and hemolymph, respectively under physiological conditions	Uninvestigated	High	(Wang et al., 2016). Higher RFU mg^{-1} protein s^{-1} values indicate higher dsRNase activity; Highest dsRNA degrading activity in gut; pH of gut and hemolymph is 6.23 and 7.16, respectively (Peng et al., 2018).
Blattodae	German cockroach,	Stable in hemolymph for 6-24 h (Garbutt et al., 2013); Degraded	Enzymatic activity	High with injeciton but not	(Garbutt et al., 2013).

	Blattella germanica	in gut in less than 12 h (Lin et al., 2017)	(Garbutt et al., 2013)	feeding; Variable	Lipoplexes increase stability and enhance oral RNAi efficiency (Lin et al., 2017).
Coleoptera	Giant mealworm beetle, *Zophobas atratus*	Stable in gut & fairly stable in hemolymph after 1 h (Wang et al., 2016); 15.72 & 0.04 RFU mg^{-1} protein $s^{-1}$of nuclease activity in gut fluid and hemolymph, respectively under physiological conditions (Peng et al., 2018)	Uninvestigated	High	(Wang et al., 2016). Highest dsRNA degrading activity in gut; pH of gut and hemolymph is 5.74 and 6.84, respectively (Peng et al., 2018).
Coleoptera	Colorado potato beetle, *Leptinotarsa decemlineata*	Degraded in gut after 10 min (Spit et al., 2017); Degraded in gut after 3 h (Prentice et al., 2017); CB_{50} 2.27 mg/ml (Singh et al., 2017); dsRNA completely digested after 90 min in hemolymph diluted up to 12.5% & in undiluted gut contents (Shukla et al., 2016)	dsRNase1 & 2 (Spit et al., 2017)	Variable (Spit et al., 2017)	*DsRNases* are mainly expresed in gut, and more highly expressed in adults. Knockdown of both dsRNase 1 & 2 increased RNAi efficiency (Spit et al., 2017). DsRNA degradation in this species is slow compared to other beetles (Prentice et al., 2017). DsRNA degradation in this species is average compared to other beetles (Singh et al., 2017); Hemolymph and gut contents of *H. virescens* more efficiently degrade dsRNA compared to *L. decemlineata* (Shukla et al., 2016).

Coleoptera	Sweet potato weevil, *Cylas brunneus*	Degraded in gut after 1 h	Uninvestigated	Higher oral RNAi effiency than *C. puncticollis*	(Prentice et al., 2017).
Coleoptera	African sweet potato weevil, *Cylas puncticollis*	Degraded in gut after 5 min	Enzymatic activity	High with injection but low with feeding	Degradation in *C. puncticollis* gut juice happens rapidly comared to *C. brunneus* and *L. decemlineata* (Prentice et al., 2017).
Coleoptera	Western corn rootworm, *Diabrotica virgifera virgifera*	Stable in hemolymph & gut for at least 1 h (AMW Cooper, unpublished)	Presumed enzymatic activity & pH (Baum and Roberts, 2014)	High	DsRNA degradation becomes visible after 60 min at pH of 10.5 but not pH 7.5 (Baum and Roberts, 2014) . Two d*sRNases* identified; one is mainly expressed in egg and the other in the gut of larvae (AMW Cooper, unpublished).
Coleoptera	Cotton Boll weevil, *Anthonomus grandis*	Degraded in gut in <10 min at pH 5.5) (Gillet et al., 2017); DsRNA completely degraded in gut juice after 30 min (Garcia et al., 2017)	Presumed enzymatic activity (Gillet et al., 2017); *Nuc2* nucleases (Garcia et al., 2017)	High with injeciton but not feeding	Feeding ribonucleoprotein-dsRNA particles improves RNAi efficency 2-fold (Gillet et al., 2017). Optimal ph range is 5.5-6.5. RNAi of Nuc2, but not Nuc1or Ncu3, enhanced RNAi effiency of a reporter. Silencing of all 3 nucleases enhanced dsRNA stability in gut juice. Nuc2 & 3 are expressed in gut, but Nuc 1 is expressed in carcus and gut. Nucleases may be more active at antierior midgut at acidic pH and inactive in posterior sections at nutral pH (Garcia et al., 2017).

Coleoptera	Small hive beetle, *Aethina tumida*	Stable in gut up to 1 h but totally degraded after 8 h	Presumably dsRNases	High with injeciton but not feeding	DsRNA is unstable in gut, regurgitant & frass, but not in tissues from wondering stage larvae (Powell et al., 2017).
Coleoptera	Japanese beetle, *Popillia japonica*	CB_{50} 0.05 mg/ml	Uninvestigated	Unknown	(Singh et al., 2017).
Coleoptera	Mexican bean beetle, *Epilachna varivestis*	CB_{50} 0.42 mg/ml	Uninvestigated	Unknown	(Singh et al., 2017).
Coleoptera	Seven-spot ladybird, *Coccinella septempunctata*	CB_{50} 0.49 mg/ml	Uninvestigated	Unknown	(Singh et al., 2017).
Coleoptera	Striped flea beetle, *Disonycha glabrata*	CB_{50} 0.52 mg/ml	Uninvestigated	Unknown	(Singh et al., 2017).
Coleoptera	Striped cucumber beetle, *Acalymma vittatum*	CB_{50} 2.56 mg/ml	Uninvestigated	Unknown	(Singh et al., 2017).
Coleoptera	Eggplant flea beetle, *Epitrix fuscula*	CB_{50} 2.56 mg/ml	Uninvestigated	Unknown	(Singh et al., 2017).
Coleoptera	Spotted cucumber beetle, *Diabrotica undecimpunctata*	CB_{50} 3.54 mg/ml	Uninvestigated	High	(Singh et al., 2017).
Coleoptera	Goldenrod soldier beetle, *Chauliognathus pensylvanicus*	CB_{50} 4.12 mg/ml	Uninvestigated	Unknown	(Singh et al., 2017).

Coleoptera	Red flour beetle, *Tribolium castaneum*	CB_{50} 4.68 mg/ml (Singh et al., 2017); Stable in hemolymph and gut contents for >30min (Cao et al., 2018)	Uninvestigated (Singh et al., 2017); Nuclease activity- possibly exonuclease activity (Cao et al., 2018)	High with injection	(Singh et al., 2017). DsRNA is stable in diet fed on by *T. castaneum* for up to 14 days; uses heating and EDTA to implecate nuclease activity; change in dsRNA size when incubated with different concentrations of gut juice is likely an artifact. Identify a Rrp44-like sequence possibly responsible for exonculease activity (Cao et al., 2018) .
Coleoptera	Korean black chafer, *Holotrichia diomphalia*	Stable in gut for >6 h but <18 h	Uninvestigated	Unknown	DsRNA is more stable in gut contents of *H. diomphalia* than in gut contents of *O. furnacalis* or *H. armigera* (Guan et al., 2018).
Coleoptera	Emerald, ash borer, Agrilus planipennis	CB_{50} 36.9 mg/ml	Uninvestigated	High with injeciton	Highest CB_{50} reported (i.e., dsRNA is more stable in body fluids from this species than in other insect) (Singh et al., 2017).
Diptera	Yellow Fever mosquito, *Aedes aegypti*	Stable in body for 24 h (Coy et al., 2012); CB_{50} 4.98 mg/ml (Singh et al., 2017)	Uninvestigated	High with injection but not feeding	(Coy et al., 2012; Singh et al., 2017).
Diptera	Southern house mosquito, *Culex pipiens quinquefasciatus*	DsDNA, but not ssDNA or dsRNA, degraded in saliva	*Endo*		*Endo* is a DNA/RNA non-specific nuclease that is most active from pH 7.5-8.5 but has no RNase activity (Calvo and Ribeiro, 2006).
Diptera	Tsetse fly, *Glossina* sp.	DsDNA, but not dsRNA or ssDNA, degraded in saliva	*Tsal1*, *Tsal2*		*Tsal1* and *2* are DNA/RNA non-specific nuclelic acid binding proteins with only residual nuclease activity over a broad pH range (Caljon et al., 2012).

Diptera	Hoverfly, *Allograpta obliqua*	CB_{50} 2.83 mg/ml	Uninvestigated	unknown	(Singh et al., 2017).
Diptera	Fruit fly, *Drosophila melanogaster*	CB_{50} 3.02 mg/ml	Uninvestigated	Variable	(Singh et al., 2017).
Diptera	Housefly, *Musca domestica*	CB_{50} 3.03 mg/ml	Uninvestigated	High with injection but not feeding in larvae; ineffective in adults	(Singh et al., 2017). (Powell et al., 2017).
Diptera	Cabbage root fly, *Delia radicum*	Stable in homogenized gut for <5 min		High with injection but not feeding in larvae; ineffective in adults	Stable in diet for <5 min also (Powell et al., 2017).
Diptera	Caribbean fruit fly, *Anastrepha suspensa*	CB_{50} 4.44 mg/ml	Uninvestigated	Embryonic RNAi is fuctional	(Singh et al., 2017).
Hemiptera	Pea aphid, *Acyrthosiphon pisum*	Slightly degraded in saliva after 48 h; stable in hemolymph for 1 h but mostly degraded after 3 h (Christiaens et al., 2014); CB_{50} 0.07 mg/ml (Singh et al., 2017);	Inconclusive (Singh et al., 2017); Nuclease activity- possibly endonuclease activity (Cao et al., 2018)	Variable, low	DsRNA could be detected in the body after 2 h, but not 5 h post injection. DsRNA is stabel in diet for at least 84 h (Christiaens et al., 2014). Lowest CB_{50} reported (i.e., dsRNA is less stable in body fluids from this species than in other insects).(Singh et al., 2017).

		Degraded in hemolymph in <5 min & degraded in gut contents in <5 min (Cao et al., 2018)			DsRNA is stable in diet fed on by *A. pisum* for <72 hr; used heating and EDTA to implicate nuclease activity (Cao et al., 2018).
Hemiptera	Brown marmorated stink bug, *Halyomorpha halys*	CB_{50} 3.07 mg/ml (Singh et al., 2017); dsRNA stable in hemolymph & saliva (Mogilicherla et al., 2018)	Uninvestigated	High with injection & feeding	(Singh et al., 2017). Less dsRNA degradation in saliva and hemolymph compared to *H. virescence* hemolymph (Mogilicherla et al., 2018).
Hemiptera	Harlequin cabbage bug, *Murgantia histrionica*	CB_{50} 6.57 mg/ml	Uninvestigated	Unknown	(Singh et al., 2017).
Hemiptera	Squash bug, *Anasa tristis*	CB50 3.66 mg/ml	Uninvestigated	Unknown	(Singh et al., 2017).
Hemiptera	Southern green stink bug, *Nezara viridula*	Degradation in saliva after 5 min, but stable in salivary glands & gut for at least 20 min (Lomate and Bonning, 2016); CB_{50} 4.86 mg/ml (Singh et al., 2017)	nuclease (i.e., exonuclease Rrp44-like protein) (Lomate and Bonning, 2016)	High with injection	Nuclease activity in saliva, but not gut or salivary glands. Exosome complex exonuclease RRP44-like expressed in salivary glands (Lomate and Bonning, 2016). (Singh et al., 2017)
Hemiptera	Tarnished plant bug, *Lygus lineolaris*	Completely degraded in saliva but not hemolymph after 30 min; partial degradation in	dsRNase presumed	High with injeciton but low with feeding	SsRNase inhibitor did not affect dsRNase activity, but heat treatment did. RNA but not DNA was degraded (Allen and Walker, 2012)

		hemolymph after 24 h			
Lepidoptera	Silkworm, *Bombyx mori*	Degraded in midgut in <10 min & mostly degraded in hemolymph after 3 h (Liu et al., 2013)	Alkaline nucleases (dsRNases) (Arimatsu et al., 2007)	Variable	*DsRNase* is upregulated 3 h after injection of dsRNA, and may constitute a defense mechanism (Liu et al., 2013). (Arimatsu et al., 2007)
Lepidoptera	Tobacco hornworm, *Manduca sexta*	Complete degradation in hemolymph after 4 h (Garbutt et al., 2013) CB_{50} 1.75 mg/ml (Singh et al., 2017)	Enzymatic activity (Garbutt et al., 2013)	Low	*DsRNase2* is expressed in gut and *dsRNase1* is expressed in fat body, hemocytes, and midgut (Garbutt et al., 2013). (Singh et al., 2017).
Lepidoptera	Fall armworm, *Spodoptera frugiperda*	Degraded in gut <10 min (Baum and Roberts, 2014; Christiaens et al., 2018); Degraded after 1 h in gut of fed larvae but not starved; (Rodríguez-Cabrera et al., 2010) CB_{50} 0.11 mg/ml (Singh et al., 2017)	Presumed enzymatic activity & pH (Baum and Roberts, 2014)	Low	DsRNA degradation becomes visible after 20 min at pH 7.4 but dsRNA is completely degraded after 10 min at pH 10.5 (Baum and Roberts, 2014). Higher efficiency with oral delivery than injection (Rodríguez-Cabrera et al., 2010). (Singh et al., 2017). The pH of midgut is >9.0, and use of dsRNA–guanylated polymer complexes enhance dsRNA stability and RNAi efficiency (Christiaens et al., 2018).
Lepidoptera	Tobacco budworm, *Heliothis virescens*	CB_{50} 0.17 mg/ml (Singh et al., 2017); Degradation in hemolymph (Mogilicherla et al., 2018);	Uninvestigated	Low	(Singh et al., 2017). DsRNA degrades more rapidly in hemolymph of *H. virescens* than in hemolymph or salivary gland secretions of *H. halys* (Mogilicherla et al., 2018).

		dsRNA completely digested after 90 min in hemolymph or gut contents diluted up to 25% (Shukla et al., 2016)			Hemolymph and gut contents of *H. virescens* degraded dsRNA more efficiently compared to *L. decemlineata* (Shukla et al., 2016).
Lepidoptera	Yellow woolly bear, *Spilosoma virginica*	CB_{50} 1.62 mg/ml	Uninvestigated	Unknown	(Singh et al., 2017).
Lepidoptera	Cotton bollworm, *Helicoverpa armigera*	Stable in gut <4 min; <16 min in hemolymph (Yang and Han, 2014); Stable in gut for <2 h (Guan et al., 2018)	Uninvestigated (Yang and Han, 2014); REase (Guan et al., 2018)	Low efficiency with injection but worse with feeding	Feeding of dsRNA-expressing bacteria enhances oral RNAi efficiency (Yang and Han, 2014). *In vivo* treatment with dsRNA targeting *dsREase* extended *ex vivo* dsRNA stability in gut juice slightly (Guan et al., 2018).
Lepidoptera	Tobacco cutworm, *Spodoptera litura*	Highly degraded in gut & hemolymph after 1 h (Wang et al., 2016); 6923.6 & 0.80 RFU mg^{-1} protein $s^{-1}$of nuclease activity in gut fluid and hemolymph, respectively under physiological conditions; dsRNA completely degraded in gut fluids in <2 min and stable in hemolymph for	Uninvestigated	Low	(Wang et al., 2016). Highest dsRNA degrading activity in gut; pH of gut and hemolymph is 8.72 and 6.69, respectively (Peng et al., 2018).

		nearly 120 min (Peng et al., 2018)			
Lepidoptera	European corn borer, *Ostrinia nubilalis*	Completely degraded in gut after 10 min, completely degraded in hemolymph after 60 min	Enzymatic activity	Low	One *dsRNase* gene identified so far; expressed in gut and larvae; expression increases in older larvae (AMW Cooper, unpublished)
Lepidoptera	Asian corn borer, *Ostrinia furnacalis*	Stable in gut for <1 h; (Guan et al., 2018)	REase (Guan et al., 2018)	Low, variable	*REase* is induced in gut and other body tissues upon dsRNA exposure. Suppression of *REase* enhances RNAi effiency (Guan et al., 2018).
Lepidoptera	Beet armyworm, *Spodoptera exigua*	Stable in hemolymph for at least 40 min but partially degraded after 1 h; stable in gut for 20 min to1 h in old larvae, & for 6-24 h in young larvae	Enzymatic activity	Sensitive to feeding; high quantities of dsRNA required for lethality	Feeding of sonicated dsRNA-expressing bacteria enhances RNAi efficiency, as does targeting young larvae with low *dsRNase* expression (Vatanparast and Kim, 2017).
Orthoptera	Desert locust, *Schistocerca gregaria*	Degraded in gut in less than 3 min (Wynant et al., 2014d); Degraded in gut after 10 min (Spit et al., 2017)	dsRNase2	High with injeciton but low with feeding	Four *dsRNases* are expressed in gut; but knockdown of *dsRNase2* improves dsRNA stability and RNAi efficiency (Wynant et al., 2014d). Parital suppression of all four *dsRNases* did not enhance oral efficiency (Spit et al., 2017).
Orthoptera	Migratory locust, *Locusta migratoria*	Low persistence in gut or hemolymph after 1 h (Wang et al., 2016); Mostly degraded in gut juice after 10 min	dsRNase2	High with injeciton but low with feeding	*DsRNase2* & *dsRNase3* expressed in gut, but dsRNase2 causes degradation. Suppression of *dsRNase2* enhances RNAi effeicincy. Optimal pH is 5.0-ll.0 for dsRNase3 and below pH 5 for dsRNase2 (Song et al., 2017). Liposomes did not

		at natural pH (6.8) (Luo et al., 2013); Stable in hemolymph for at least 20 min, but degrades in gut < 5 min (Song et al., 2017); Degraded in hemolymph after 4 h, but not fat body or ovarian homogenate (Ren et al., 2014); 49.36 & 0.66 RFU mg^{-1} protein $s^{-1}$of nuclease activity in gut fluid and hemolymph, respectively under physiological conditions (Peng et al., 2018)			protect dsRNA from degradation in gut. Degridaiton of dsRNA occurred in gut between pH 6.8-9.9, but not at pH 10.7, 5.5 or 4.2 (Luo et al., 2013). (Ren et al., 2014; Wang et al., 2016). Highest dsRNA degrading activity in gut; pH of gut and hemolymph is 5.79 and 6.82, respectively (Peng et al., 2018).
Orthoptera	Admirable Grasshopper, *Syrbula admirabilis*	CB_{50} 2.47 mg/ml	Uninvestigated	Unknown	(Singh et al., 2017).
Orthoptera	Field cricket, *Gryllus texensis*	CB_{50} 11.02 mg/ml	Uninvestigated	High	(Singh et al., 2017).

Table S1-3. Investigations of *Snipper* genes in insects.

Abbreviations: RNAi, RNA interference; Eri-1, Enhanced RNAi 1; Snp, Snipper.

Order	Species	*Snipper* genes	Comments & citation(s)
Coleoptera	Red flour beetle, *Tribolium castaneum*	1 *Snp*	(Tomoyasu et al., 2008).
Diptera	Fruit fly, *Drosophila melanogaster*	1 *Snp*	Transgenic flies lacking *Snp* do not show improved RNAi efficiency (Kupsco et al., 2006).
Hemiptera	Brown plant hopper, *Nilaparvata lugens*	2 *Eri-1* homologs	Suppression of each *Eri-1* individually and in combination did not improve RNAi efficiency (Xu et al., 2013).
Hemiptera	Pea aphid, *Acyrthosiphon pisum*	1 *Eri-1* homolog	*Eri-1* not upregulated in response to dsRNA treatment (Christiaens et al., 2014).
Orthoptera	Migratory locust, *Locusta migratoria*	1 *Snp*	*Snp* not upregulated in response to dsRNA treatment (Wynant et al., 2012).

Table S1-4. Reports of dsRNA binding activity in insect hemolymph.

Abbreviations: Apo1, Apolipophorin 1; Apo2, Apolipophorin 2; Apo3, Apolipophorin 3; PAMPs, pathogen associated molecular patterns.

Order	Species	Components implicated	Comments & references
Blattodea	American cockroach, *Periplaneta americana*	Putative lipophorins	Electrophoretic shift observed when dsRNA incubated in hemolymph (Wynant et al., 2014a).
Diptera	Flesh fly, *Sarcophaga crassipalpis*	Putative lipophorins	Electrophoretic shift observed when dsRNA incubated in hemolymph (Wynant et al., 2014a).
Lepidoptera	Silkworm, *Bombyx mori*	Apo1	Mobility shift observed after dsRNA incubated in hemolymph (Sakashita et al., 2009).
Orthoptera	House circket, *Acheta domesticus*	Putative lipophorins	Electrophoretic shift observed when dsRNA incubated in hemolymph (Wynant et al., 2014a).
Orthoptera	Desert locust, *Schistocerca gregaria*	Apo3, and possibly Apo1 & Apo2	Lipophorins also adhere to bacterial and fungal pathogens. dsRNA may function as PAMPs (Wynant et al., 2014a).

Table S1-5. Investigations of dsRNA uptake and internalization in insects.

Abbreviations: dsRNA, double stranded RNA; RNAi, RNA interference; siRNA, short interfering RNA; CDE, clathrin-dependent endocytosis; RME, receptor-mediated endocytosis; Sil, sid-1-like; Chc, clathrin heavy chain; AP50, clathrin coat assembly protein AP50; VhaSFD, vacuolar (H+)-ATPase subunit H; Rab7, ras-related protein 7; Arf72A, ARF-like 1 orthologue; light, vacuolar protein sorting Vsp41 orthologue; V-H-ATPase, vacuolar H^{+}-ATPase; IdlCp, Cog2 ortholog; CG3248, Cog3 orthologue; CG3911, transport protein particle –TRAPP- component 3 orthologue; ninaC, neither inactivation nor afterpotential protein C; Pi3K, phosphoinositide 3-kinase; Saposin-r, saposin–related; SR, scavenger receptors; SR-Cl, class C scavenger receptor; eater, epidermal growth factor repeat-containing scavenger receptor; Vha16, 16kDa subunit of the vacuolar H1 ATPase; Epn-1, Epsin-1 ; Rsd-3, regulator of sigma D ; TRF3, tricorn protease-interacting factor F3 ; SLR, Somatolactin receptor; SC-R2, Scarecrow 2; HPS4, Hermansky-Pudlak syndrome 4 protein; FBX011, F-Box protein 11; Sid1, Systemic RNA interference defective protein 1; RNP, ribonucleoprotein particle; cog3, component of oligomeric Golgi complex 3; bet3, trafficking protein particle complex submunit bet3; ldlCp; conserv3ed oligomeric Goligi complex subunit 2; Hsc70, Endoplasmic reticulum chaperone BiP; HK2, hexo kinase 2; MAP2K1, Mitogen-Activated Protein Kinase Kinase 1; pgk1, Phosphoglycerate Kinase 1; fasn, fatty acid synthase; MVBs, multivesicular bodies; ESCRT6; Endosomal sorting complex required for transport protein 6.

Order	Species	Pathway(s) implicated	Molecular component(s) implicated	Comments & Reference(s)
Coleoptera	Cotton boll weevil, *Anthonomus grandis*	Endocytosis, possibly macropinocytosis		Two-fold increase in RNAi efficiency when RNPs are used to deliver dsRNA. Large plasma membrane extensions and large vesicular bodies observed, indicating Macropinocytosis (Gillet et al., 2017).
Coleoptera	Western corn rootworm, *Diabrotica virgifera vigifera*	*Sils*	*SilA* & *SilC*	DsRNA under 100 bp is not taken up. DsRNA uptake is saturable. Suppression of *SilA* or *SilC* partially blocks RNAi of a marker gene (Miyata et al., 2014). DsRNA under 60 bp not taken up (Bolognesi et al., 2012; Li et al., 2015a). DsRNA uptake is saturable (Bolognesi et al., 2012).
Coleoptera	Red flour beetle & TcA cells, *Tribolium castaneum*	CDE	*Chc, AP50, VhaSFD, Rab7*	Phagocytosis and caveolae-dependent endocytosis not involved (Xiao et al., 2015). *Sils* are not involved (Tomoyasu et al., 2008). DsRNA under 60 bp are not taken up. DsRNA uptake is saturable. The number of siRNAs produced

				determines RNAi efficiency, not the initial number of dsRNA molecules (Miller et al., 2012). SiRNA is less effective than dsRNA but still triggers gene suppression for a short period (Wang et al., 2013a). Fluorescein-labeled dsRNA is taken up TcA cells and is converted into siRNA (Shukla et al., 2016).
Coleoptera	Colorado potato beetle & Lepd-SL1 cells, *Leptinotarsa decemlineata*	CDE, *Sils* (Cappelle et al., 2016a; Yoon et al., 2016); endosomal acidification & escape (Yoon et al., 2016)	*SilA*, *SilC*, *Vha16*, *Chc* (Cappelle et al., 2016a; Yoon et al., 2016); *Epn-1*, *Rsd-3*, *TRF3*, *SLR*, *HPS4*, *FBX011*, *SC-R2*, *Rab7*, *Arf72*, *Armitage*, *Neuron-Specific Staufen*, *sortlin-like receptor*, *transferrin receptor 3*, *innexin2* (Yoon et al., 2016)	*SilB* is not involved in RNAi (Cappelle et al., 2016a). Suppression of 29 components effected RNAi efficiency, but *Vha16* was one of 5 genes that blocked RNAi. However, suppression *of VhaSFD*, *Belle*, etc. did not impact RNAi effiency (Yoon et al., 2016). Fluorescein-labeled dsRNA is taken up cells and is converted into siRNA (Shukla et al., 2016).
Diptera	Two spotted drosophila, *Drosophila suzukii*			RNAi-mediated gene suppression can be achieved after dsRNA injection but not feeding. However, oral RNAi works if dsRNA is combined with a transfection reagent (Taning et al., 2016a). Oral RNAi was achieved using genetically modified *Saccharomyces cerevisiae* expressing dsRNA (Murphy et al., 2016).

Diptera	African malaria mosquito, *Anopheles gambiae*			High doses of injected dsRNA are required for RNAi in salivary tissues compared to other tissues. Fluorescently labeled siRNA not detected in salivary tissues after injection (Boisson et al., 2006). Oral RNAi is possible when Chitosan/dsRNA nanoparticles are used (Zhang et al., 2010).
Diptera	Fruit fly & S2 cells, *Drosophila melanogaster*	CDE, RME, enovesicular trafficking, protein sorting, Golgi complex, cytoskeletion organization, lipid metabolism (Saleh et al., 2006); CDE, RME (Ulvila et al., 2006); Phagocytosis* (Rocha et al., 2011)	*Chc, AP50, Rab7, Arf72A, Light, V-H-ATPase, IdlCp, CG3248, CG3911, ninaC, Pi3K, Saposin-r, SR* (Saleh et al., 2006); *Chc, SR-CI, eater* (Ulvila et al., 2006); *HPS4, ESCRT* (Lee et al., 2010)	DsRNA uptake in S2 cells is size & temperature dependent. 23 genes are required for RNAi silencing. Phagocytosis and caveolae-dependent endocytosis are not involved, nor Toll receptors (Saleh et al., 2006). Simultaneous suppression of *SR-Ci* & *eater* decreased internalization of dsRNA by >90% (Ulvila et al., 2006). *Phagocytosis can be exploited when dsRNA is expressed in *E. coli* (Rocha et al., 2011). Injected extracellular dsRNA is not taken up by any larval tissues except hemocytes (Miller et al., 2008). GW-bodies associate with MVBs (Lee et al., 2010). Expression of Sid1 from *Caenorhabditis elegans* in S2 cells promotes uptake of dsRNA from the media (Feinberg and Hunter, 2003).
Diptera	Oriental fruit fly, *Bactrocera dorsalis*	CDE, Golgi complex, F-actin polymerization (Li et al., 2015b); polyunsaturated fatty acids (Dong et al., 2017)	*Chc, rab7, arf72a, V-H-ATPase saposin, ninaC, ldlCp, cog3, light, bet3, hsc70, actin 3, actin 4, actin 5, HK2, map2k1, pgk1* (Li et al., 2015b);	Endocytosis and endocytosis genes down-regulated upon dsRNA feeding; promoting F-actin polymerization with H_2O_2 reverses refractoriness (Li et al., 2015b). Injecting arachidonic acid facilitates endocytotic uptake of dsRNA but injection of linoleic acid inhibits endocytic uptake of dsRNA; Silencing of *fasn* reverses RNAi refractoriness (Dong et al., 2017).

			Fasn (Dong et al., 2017)	
Hemiptera	Brown planthopper, *Nilaparvata lugens*	*Sils*	*Sid1*	*Sid1* is expressed in all life stages and tissues. *Sid1* is highly expressed compared to *Aub* (Zha et al., 2011). Suppression of *Sid1* abolishes phenotype of reporter gene (Xu et al., 2013).
Hymenoptera	Honey bee, *Apis mellifera*	*Sils* (Aronstein et al., 2006)	*Sid1*(Aronstein et al., 2006)	*Sid1* is upregulated in response to dsRNA feeding (Aronstein et al., 2006). Injected siRNA is not taken up by any tissue but fat body. Injection of dsRNA or siRNA induces gene suppression in fat body but not ovary (Jarosch and Moritz, 2011).
Lepidoptera	Silkmoth BmN4 cells, *Bombyx mori*	*Sils*	Sid1	Expression of *Sid1* but not *Sid2* from *C. elegans* in BmN4 cells promotes uptake of dsRNA from the media; however *in vivo* expression of *Sid1* in larvae did not enhance RNAi (Kobayashi et al., 2012).
Lepidoptera	Fall armyworm & Sf9 cells, *Spodoptera frugiperda*	Endosomal acidification & escape		Fluorescein-labeled dsRNA is taken up bySf9 cells and midgut tissue, and accumulates in endocytic compartments. DsRNA is never converted into siRNA (Shukla et al., 2016).
Lepidoptera	Choristoneura fumiferana			See Christeianes 2018.
Lepidoptera	Tobacco budworm & Hv-E6, *Heliothis virescens*	Endosomal acidification & escape		Fluorescein-labeled dsRNA is taken up by Hv-E6 cells and accumulates in endocytic compartments. DsRNA is never converted into siRNA (Shukla et al., 2016).
Orthoptera	Migratory locust, *Locusta migratoria*	CDE (Ren et al., 2014)	*Chc* (Ren et al., 2014)	*Sid1* not involved in uptake (Luo et al., 2012; Ren et al., 2014). Sid1 expression increases throughout development and is enriched in gonad (Luo et al., 2012).

				Deficient uptake in ovary and follicle cells limits RNAi efficiency (Ren et al., 2014).
Orthoptera	Desert locust, *Schistocerca gregaria*	CDE, RME	*Vha16, Chc, SR*	*Sid1* not involved in dsRNA uptake (Wynant et al., 2014b).

Table S1-6. Core RNAi enzymes identified in insects.

Duplicated enzymes and enzymes not found are bolded. (+) sign indicates upregulated enzymes and (–) sign indicates downregulated enzymes. Also see the following references for tables containing core RNAi enzyme information for 86 dipterans (Lewis et al., 2016), and for 100 insect species from all recognized insect orders (Dowling et al., 2016). The information from those tables have not been duplicated here. *Abbreviations*: RNAi, RNA interference; miRNA, Micro-RNA pathway; piRNA, Piwi-Interacting-RNA pathway; siRNA, Small-interfering-RNA pathway; Dcr, Dicer; Ago, Argonaute; R2D2, two dsRNA-binding domains associated with Dicer2; Trsn, translin; Trax, Translin associated factor X; Loqs, Loquacious; Aub, Aubergine; Piwi, P-element induced wimpy testis; Drosha, Double-stranded RNA-specific endoribonuclease; Pasha, Partner of Drosha; RISC, RNA-Induced Silencing Complex; C3PO, Component 3 Promoter of RISC; vATPase, vacuolar H^+- ATPase; Vha16, vacuolar H+ ATP synthase 16 kDa proteolipid subunit; DCGR8, Microprocessor complex subunit DGCR8; REase, RNAi efficiency-related nuclease; Sid1, Systemic RNA interference defective protein 1;

Order	Species	siRNA pathway	miRNA pathway	piRNA pathway	RNAi efficiency	Comments & Reference(s)
Blattodea	German cockroach, *Blattella germanica*	1 *Dcr2* +	1 *Dcr1*		High with injeciton but not feeding; Variable	*Dcr2* is upregulated in response to dsRNA but not siRNA targeting *Dcr2* or mimicking a virus (Lozano et al., 2012).
Coleoptera	Red flour beetle, *Tribolium castaneum*	1 *Dcr2* **2 *Ago2*** **2 *R2D2***	1 *Dcr1* 1 *Drosha* 1 *Pasha* 1 *Ago1* 1 *Loqs*	1 *Ago3* 1 *Aub* 1 *Piwi*	High by Injection	Domain structure suggests Dcr1 may serve the same purpose as Dcr2. Two *Agos* may affect RNAi efficiency. Suppressing *Dcr2*, but not *Dcr1* reduced RNAi efficiency (Dowling et al., 2016; Tomoyasu et al., 2008).

Coleoptera	Colorado potato beetle, *Leptinotarsa decemlineata*	**2 *Dcr2* +** **2 *Ago2* +** 1 *R2D2* 1 *Trsn*	1 *Dcr1* 1 *Drosha* 1 *Pasha* 1 *Ago1* 1 *Loqs*	1 *Ago3* 1 *Aub/Piwi*	Variable	*Ago1* but not *Ago2s* are involved. Expression of *Ago2*s and *Dcr2* is highest in young larvae; however long exposure decreases expression (Guo et al., 2015). RNAi of *Ago1*, both *Ago2s*, *Aub* and *vATPase* block RNAi of a reporter gene. *Ago2* is not involved in siRNA generation but other *Ago*s are (Yoon et al., 2016). Suppression of *Ago1*, *both Ago2s*, *Aub* & *Vha16* totally block RNAi. *Ago2* associated with other small noncoding RNAs (Swevers et al., 2013).
Coleoptera	Emerald ash borer, *Agrilus planipennis*	1 *Dcr2* 1 *Ago2* 1 *R2D2*			High	(Zhao et al., 2015).
Coleoptera	Mountain pine beetle, *Dendroctonus ponderosae*	1 *Ago2*			High	(Zhao et al., 2015).
Coleoptera	Asian longhorned beetle, *Anoplophora glabripennis*	1 *Dcr2* 1 *Ago2* 1 *R2D2*	1 *Dcr1* 1 *Drosha* 1 *Pasha* 1 *Loqs*	1 *Ago3* 1 *Aub*	High	(Rodrigues et al., 2017).
Coleoptera	Western corn rootworm, *Diabrotica virgifera virgifera*	1 *Dcr2* 1 *Ago2* **2 *R2D2***	1 *Dcr1* 1 *Ago1*	1 *Piwi*	High	(H Song, unpublished).

Coleoptera	citrus leaf-mining beetle,, Podagricomela weisei	1 *Dcr2* 1 *Ago2* 1 *R2D2*	1 *Dcr1* 1 *Drosha* 1 *Pasha* 1 *Ago1*	1 *Ago3* 1 *Aub* 1 *Piwi*	unknown	(Ding et al., 2019).
Diptera	Fruit fly and S2 cells, *Drosophila melanogaster*	1 *Dcr2* + 1 *Ago2* + 1 *R2D2* + 1 *Trsn* + 1 *Trax*+	1 *Dcr1* 1 *Drosha* 1 *Pasha* 1 *Ago1* 1 *Loqs* +	1 *Ago3* 1 *Aub* 1 *Piwi*	Variable	Both siRNA and dsRNA upregulate core RNAi enzymes. C3PO activates RISC, and RNAi efficiency is reduced when this complex is not active (Liu et al., 2009). *Ago2* is indispensable and *Loqs* gene also necessary (Marques et al., 2010). In S2 cells, *Ago2* and *Dcr2* are not upregulated by viral infection, and feeding and injection of adults does not change expression of the core enzymes (Mongelli and Saleh, 2016). One of each core enzyme from all 3 pathways (Dowling et al., 2016). *Ago2* & *Dcr2*, but not *Ago1* or *Dcr1* required for exogenous siRNAi (Saleh et al., 2006).
Diptera	Two spotted drosophila, *Drosophila suzukii*	1 *Dcr2* 1 *Ago2* 1 *R2D2*	1 *Ago1*	1 *Ago3* 1 *Aub* 1 *Piwi*	Low by feeding	(Lewis et al., 2016; Taning et al., 2016a).
Diptera	Oriental fruit fly, *Bactrocera dorsalis*	1 *Dcr2* + 1 *Ago2* + 1 *R2D2* +	1 *Ago1*	1 *Ago3* 1 *Aub* 1 *Piwi*	High	All core enzymes upregulated in response to viruses and iron, but down regulated by *E. coli*, high and low temps, and starvation. All core enzymes expressed in all tissues. *Ago2* & *Dcr2* highest expressed in adults.

						R2D2 is highest expressed in eggs and adults (Xie et al., 2016). (Lewis et al., 2016).
Diptera	Housefly, *Musca domestica*	**2 *Ago2***	**2 *Dcr1*** 1 *Drosha* 1 *Ago1*	1 *Ago3* 1 *Aub* 1 *Piwi*	High	(Lewis et al., 2016; Mongelli and Saleh, 2016).
Diptera	Tsetse fly, *Glossina morsitans*	**3 *Ago2***	1 *Ago1*	**3* *Ago3*** 1 *Aub* 1 *Piwi*	Low but functional	*Three copies of *Ago3* reported (Mongelli and Saleh, 2016). Two copies of *Ago3* reported (Lewis et al., 2016).
Diptera	Yellow fever mosquito, *Aedes aegypti*	1 *Dcr2* 1 *Ago2*	1 *Dcr1* 1 *Drosha* **2* *Ago1***	1 *Ago3* 1 *Aub* **7 *Piwi***	High with injection but not feeding	(Mongelli and Saleh, 2016). One copy of *Ago1* reported (Lewis et al., 2016). *Two copies of *Ago1* reported (Dowling et al., 2016).
Diptera	Malaria mosquito, *Anopheles gambiae*	1 *Dcr2* 1 *Ago2*	1 *Dcr1* 1 *Drosha* 1 *Ago1*	1 *Ago3* 1 *Aub* **7 *Piwi*** **2 *Aub/Piwi***	Variable	(Lewis et al., 2016; Mongelli and Saleh, 2016).
Diptera	House mosquito, *Culex pipiens*	1 *Dcr2* **2 *Ago2***	1 *Dcr1* 1 *Drosha* 1 *Ago1*	1 *Ago3* **0 *Aub*** **6 *Piwi***	Variable (highest in adult with injection)	(Dowling et al., 2016; Mongelli and Saleh, 2016).
Hemiptera	Russian wheat aphid, *Diuraphis noxia*	1 *Dcr2* **2 *Ago2***	1 *Dcr1* 1 *Drosha* **2 *Ago 1***	1 *Ago3* **0 *Aub*** **5 *Piwi***	Unknown	(Mongelli and Saleh, 2016).
Hemiptera	Pea aphid, *Acyrthosiphon pisum*	1 *Dcr2* - 1 *Ago2* - 1 *R2D2* -	**2 *Dcr1*** 1 *Drosha* **2 *Ago1*** **2 *Loqs***	**2 *Ago3*** **0 *Aub*** **8 *Piwi***	Variable, low	*Dcr2*, *Ago2*, and *R2D2* are not upregulated in response to dsRNA (Christiaens et al., 2014). (Dowling et al., 2016; Jaubert-Possamai et al., 2010; Mongelli and Saleh, 2016)

Hemiptera	Brown plant hopper, *Nilaparvata lugens*	1 *Dcr2* 1 *Ago2* 1 *R2D2*	1 *Dcr1* 1 *Drosha* 1 *Pasha* 1 *Loqs*	1 *Ago3* 1 *Aub* 1 *Piwi*	High	Variations in domain structure are not enough to reduce RNAi efficiency (Xu et al., 2013). *Aub* is expressed in all life stages and tissues. Expression of *Aub* is low compared to *Sid* (Zha et al., 2011).
Hemiptera	Asian citrus Psyllid, *Diaphorina citri*	1 *Dcr2* 1 *Ago2* **0 *R2D2***	1 *Dcr1* 1 *Drosha* 1 *Ago1* 1 *Loqs* 1 *Loq-like* 1 *DGCR8*	1 *Ago3* 1 *Aug/Piwi*	High	Did not look for interactions between pathways; Loqs replaces R2D2 (Taning et al., 2016b).
Hemiptera	Soybean aphid, *Aphis glycines*	1 *Dcr2* 1 *Ago2* 1 *R2D2*			Unknown	Core enzymes are expressed in all tissues and life stages, but highest in early larvae (Bansal and Michel, 2013).
Hemiptera	White fly, *Bemisia tabaci*	1 *Dcr2* 1 *Ago2* 1 *R2D2*			High	Core enzymes expressed in all life stages (Upadhyay et al., 2013).
Hymenoptera	Bumblebee, *Bombus terrestris,*	1 *Dcr2* + 1 *Ago2* -			High	Viral infections or dsGFP cause upregulation of *Dcr2* but not *Ago2*. Knockout of *Dcr2* does not alter viral replication but does inhibit RNAi (Niu et al., 2016).
Hymenoptera	Honey bee, *Apis mellifera*	1 *Dcr2* + 1 *Ago2* + 1 *R2D2*	1 *Dcr1* 1 *Pasha* 1 *Drosha* 1 *Ago1*	1 *Ago3* 1 *Aub*	Variable	Almost all genes were down regulated in bees with high virus loads (De Smet et al., 2016). *Dcr2* and *Ago2* are upregulated in response to acute viruses (Galbraith et al., 2015).
Hymenoptera	Parasitoid wasp, *Nasonia vitripennis*	1 *Dcr2* **2 *Ago2***	1 *Dcr1* 1 *Drosha* 1 *Ago1*	1 *Ago3* **3 *Aub*** **0 *Piwi***	High	(Mongelli and Saleh, 2016).

Hymenoptera	Bull ant, *Camponotus floridanus*	*1 Dcr2* 1 *Ago2*	1 *Dcr1* 1 *Drosha* 1 *Ago1*	1 *Ago3* **2 *Aub*** 1 *Piwi*	Unknown	(Mongelli and Saleh, 2016).
Hymenoptera	Indian jumping ant, *Harpegnathos saltator*	1 *Dcr2* 1 *Ago2*	1 *Dcr1* 1 *Drosha* 1 *Ago1*	1 *Ago3* **2 *Aub*** 1 *Piwi*	Unknown	(Mongelli and Saleh, 2016).
Lepidoptera	Tobacco hornworm, *Manduca sexta*	1 *Dcr2* + 1 *Ago2* + 1 *Trsn* -	1 *Dcr1* 1 *Drosha* 1 *Ago1*	1 *Ago3* 1 *Piwi*	Low	Multiple injections further elevate *Ago2* and *Dcr2* expression, but not *Trsn* which is deficiently expressed (Garbutt and Reynolds, 2012). (Mongelli and Saleh, 2016) .
Lepidoptera	Silkmoth and Bm5 cells, *Bombyx mori*	1 *Dcr2* + 1 *Ago2* + 1 *R2D2* - 1 *Trsn* - 1 *Trax*	1 *Dcr1* 1 *Drosha* 1 *Pasha* 1 *Ago1* + 1 *Loqs*	1 *Ago3* + 1 *Piwi* +	Variable	Overexpressing *Ago2* helps efficiency in insects and cell lines, and suppressing it abolishes RNAi (Li et al., 2015c). *Ago1* and *Ago3* are both involved in RNAi (Kolliopoulou and Swevers, 2013). *Ago2* and *Dcr2* are upregulated in response to injection but not feeding. Low expression of *R2D2* insects & cells, and low expression of *Trsn* in Bm5 cells. All other enzymes investigated are expressed constantly between tissues and lifestages (Swevers et al., 2011). Upregulation of *Ago2* and *Dcr2* after injection but not feeding (Liu et al., 2013). Low expression of all *Ago* genes, and all are upregulated upon viral

						infection. Highest expression occurred during the transition from larvae to adult. Lowest expression was in larvae (Wang et al., 2013b).
Lepidoptera	Tobacco cutworm, *Spodoptera litura*	1 *Dcr2* 1 *Ago2* 1 *R2D2*	1 *Dcr1* 1 *Ago1* 1 *Logs*		Low	Sufficient expression of all core enzymes. Highest expression in fat body, and expression increases as age increases (Gong et al., 2015).
Lepidoptera	Fall army worm Sf21 cells, *Spodoptera frugiperda*	1 *Dcr2* **0 *Ago2*** 1 *R2D2*	1 *Dcr1* 1 *Drosha* 1 *Parsha* 1 *Ago1* 1 *Loqs*	1 *Ago3* 1 *Aub*	Low	Ago1 possibly takes the place of Ago2 in the siRNA pathway. 42 components potentially involved in RNAi are identified (Ghosh et al., 2014).
Lepidoptera	Monarch, *Danaus plexippus*	1 *Dcr2* 1 *Ago2* 1 *R2D2*	1 *Dcr1* 1 *Drosha* 1 *Pasha* 1 *Ago1* 1 *Loqs*	1 *Ago3* 1 *Aub* 1 *Piwi*	Unknown	(Mongelli and Saleh, 2016; Zhan et al., 2011).
Lepidoptera	Postman butterfly, *Heliconius melpomene*	1 *Dcr2* 1 *Ago2*	1 *Dcr1* 1 *Drosha* 1 *Ago1*	1 *Ago3* 1 *Aub* 1 *Piwi*	Unknown	(Mongelli and Saleh, 2016).
Lepidoptera	European corn borer, *Ostrinia nubialis*	1 *Dcr2* **2 *Ago2*** 1 *R2D2* 1 *Trsn*	1 *Dcr1* 1 *Ago1*	1 *Ago3* 1 *Piwi*	Low	(H Song, unpublished).
Lepidoptera	Asian corn borer, *Ostrinia furnacalis*	1 *Dcr2+* **2 *Ago2+*** 1 *R2D2*	1 *Dcr1* 1 *Ago1*		Variable, low	2 *Ago2*s reported (J Zhang, unpublished). 1 *Ago2* reported. *Dcr2* and *Ago2* are upregulated in response to dsRNA but *REase* is upregulated first (Guan et al., 2018).

Orthoptera	Desert locust, *Schistocerca gregaria*	**2 *Dcr2* 2 *Ago2*** 1 *R2D2*	1 *Dcr1* 1 *Drosha* 1 *Ago1*		High with injeciton but low with feeding	*Ago2* and *Dcr2* is deficiently expressed in gonads, and suppression of either inhibits RNAi (Wynant et al., 2012). miRNA genes are expressed in all tissues (Wynant et al., 2015).
Orthoptera	Migratory locust, *Locusta migratoria*	**2 *Dcr2* 2 *Ago2*** 1 *R2D2*	1 *Dcr1* 1 *Drosha* 1 *Ago1*		High with injeciton but low with feeding	(J Zhang, unpublished). (Mongelli and Saleh, 2016).

Table S1-7. Investigations documenting effects and mechanisms of systemic RNAi across insect orders.

Abbreviations: Argonaute 2; Ago2, Egghead; Egh, Neither inactivation nor afterpotential C; NinaC; Ras-related protein 11A; Rab11, Reverse transcriptase; RTase, Spreading deficient 1; Sid1, Sid-like; Sil, Syntaxin 1A; syx1A; Diap1, *Drosophila* inhibitor of apoptosis protein 1.

Order	Species	Pathways implicated	Molecular components investigated	RNAi Efficiency	Comments & references
Coleoptera	Colorado potato beetle, *Leptinotarsa delineata*			High	Long dsRNAs were detected in tissues distant from gut following feeding (Ivashuta et al., 2014).
Coleoptera	Red flour beetle, *Tribolium castaneum*		*Sil A-C*	High	All tissues showed reduced transcript levels following dsRNA injection (Miller et al., 2012, 2008). *Sils A-C* are not involved in systemic RNAi (Tomoyasu et al., 2008).

Coleoptera	Western corn rootworm, *Diabrotica virgifera virgifera*			High	Suppression of transcript levels in tissues outside of the midgut within 24 h following dsRNA feeding (Bolognesi et al., 2012). Systemic RNAi does not involve synthesis of secondary siRNAs and relies only on the original sequence (Fishilevich et al., 2016; Li et al., 2015a).
Coleoptera	Cotton boll Weevil, *Anthonomus grandis*			High with injection, low with feeding	Eleven bp in common was enough to induce off-target suppression of other nuclease genes, suggesting an RNAi amplification pathway that results in cross-gene silencing (Garcia et al., 2017).
Diptera	Fruit fly, *Drosophila melanogaster*	Receptor-mediated endocytosis (Saleh et al., 2009); Exosome synthesis (Tassetto et al., 2017); Nanotubes (Karlikow et al., 2016)	*NinaC* (Saleh et al., 2009); *Egh* (Saleh et al., 2009); *CG4572* (Karlikow et al., 2016; Saleh et al., 2009); *Ago2* (Karlikow et al., 2016; Tassetto et al., 2017); *Endogenous RTases* (Tassetto et al., 2017);	Variable	Mutation or silencing of these endocytic pathway components rendered the insect highly susceptible to viral infection, inhibited the ability to mount a dsRNA-based anti-viral immune response, and prevented processing of injected dsRNAs into siRNAs (Saleh et al., 2009). Hemocytes take up viral RNA and synthesize viral DNA to produce secondary viral siRNAs (Ago2-dependent) which are transported to other tissues via exosome-like vesicles (Tassetto et al., 2017). Nanotube structures between cells were found to contain viral dsRNA, Ago2, and tubulin (Karlikow et al., 2016).

			Rab11 (Tassetto et al., 2017); *Syx1A* (Tassetto et al., 2017); *Actin* (Karlikow et al., 2016); *Tubulin* (Karlikow et al., 2016)		
Diptera	Housefly, *Musca domestica*			High with injection but not feeding in larvae, no RNAi in adults	Off-target suppression/cross species effects observed when dsRNA targeting *Delia radicum* Diap1 gene was injected into *M. domestica* larvae (only 15 bp in common) (Powell et al., 2017).
Hemiptera	Grain aphid, *Sitobion avenae* F			Variable	Oral administration of dsRNA resulted in significant suppression of transcript levels, and fluorescently-labeled dsRNA was detected outside of the gut in aphids (Wang et al., 2015b; Zhang et al., 2013).
Hymenoptera	Bumblebee, *Bombus terrestris*			High	Injection of dsRNA results in significant suppression of transcript levels in brain, fat body, and midgut (Cappelle et al., 2016b).
Hymenoptera	Honey bee, *Apis mellifera*			Variable	Injection of long dsRNA or siRNA into abdomen resulted in suppression of transcript levels only in fat body (Jarosch and Moritz, 2011).
Lepidoptera	Asian corn borer,			Low	Topical application of dsRNA resulted in stunting of larval development and suppression

	Ostrinia furnicalis				of transcript levels. Fluorescently-labeled dsRNAs were also detected in gut, hemocytes, and silk fibers (Wang et al., 2011).
Orthoptera	Desert locust, *Schistocerca gregaria*			High with injeciton but low with feeding	Abdominal injection of dsRNA resulted in suppression of transcript levels in fat body, brain, midgut, muscle, and Malpighian tubules (Wynant et al., 2012). Off-target suppression of nuclease genes observed, suggesting an RNAi amplification pathway that results in cross-gene silencing (Garcia et al., 2017; Wynant et al., 2014d).
Orthoptera	Migratory locust, *Locusta migratoria*	Systemic spread of dsRNA	*Sid1*	High with injeciton but low with feeding	Pre-silencing of *Sid-1* transcripts had no effect on suppression of target transcripts via injection (Luo et al., 2012).

Chapter 1 Supplementary references

Allen ML, and Walker WB, Saliva of *Lygus lineolaris* digests double stranded ribonucleic acids. *J Insect Physiol* **58**:391–396 (2012).

Arimatsu Ya, Furuno T, Sugimura Y, Togoh M, Ishihara R, Tokizane M, *et al.*, Purification and properties of double-stranded RNA-degrading nuclease, dsRNase, from the digestive juice of the silkworm, *Bombyx mori. J Insect Biotechnol Sericology* **76**:57–62 (2007).

Aronstein KK, Pankiw T, and Saldivar E, SID-1 is implicated in systemic gene silencing in the honey bee. *J Apic Res* **45**:20–24 (2006).

Asokan R, Sharath Chandra G, Manamohan M, Krishna Kumar NK, and Sita T, Response of various target genes to diet-delivered dsRNA mediated RNA interference in the cotton bollworm, *Helicoverpa armigera*. *J Pest Sci* **87**:163–172 (2014).

Bai H, Zhu F, Shah K, and Palli SR, Large-scale RNAi screen of G protein-coupled receptors involved in larval growth, molting and metamorphosis in the red flour beetle. *BMC Genomics* **12**:388 (2011).

Bansal R, and Michel A, Core RNAi machinery and Sid1, a component for systemic RNAi, in the Hemipteran insect, *Aphis glycines*. *Int J Mol Sci* **14**:3786–3801 (2013).

Baum JA, and Roberts JK, Progress towards RNAi-mediated insect pest management. *Adv Insect Physiol* **47:**249–295 (2014).

Baum JA, Bogaert T, Clinton W, Heck GR, Feldmann P, Ilagan O, *et al.*, Control of coleopteran insect pests through RNA interference. *Nat Biotechnol* **25**:1322–1326 (2007).

Boisson B, Jacques JC, Choumet V, Martin E, Xu J, Vernick K, *et al.*, Gene silencing in mosquito salivary glands by RNAi. *FEBS Lett* **580**:1988–1992 (2006).

Bolognesi R, Ramaseshadri P, Anderson J, Bachman P, Clinton W, Flannagan R, *et al.*, Characterizing the mechanism of action of double-stranded RNA activity against western corn rootworm (*Diabrotica virgifera virgifera* LeConte). *PLoS One* **7**:e47534 (2012).

Caljon G, Ridder, K D, Stijlemans B, Coosemans M, Maez S, Baetselier P D et al., Tsetse salivary gland proteins 1 and 2 are high affinity nucleic acid binding proteins with residual nuclease activity. *PLoS One* **7**: e47233 (2012).

Calvo E, and Ribeiro J M C. A novel secreted endonuclease from *Culex quinquefasciatus* salivary glands. *J Expt Biol* **209**, 2651-2659 (2006).

Camargo R de A, Herai RH, Santos LN, Bento FMM, Lima JE, Marques-Souza H, et al., De novo transcriptome assembly and analysis to identify potential gene targets for RNAi-mediated control of the tomato leafminer (*Tuta absoluta*). *BMC Genomics* **16**:635 (2015).

Cao M, Gatehouse J A, Fitches E C, A systematic study of RNAi effects and dsRNA stability in *Tribolium castaneum* and *Acyrthosiphon pisum*, following injection and ingestion of analogous dsRNAs. *Int J Mol Sci* **19**, 29–31 (2018).

Cappelle K, de Oliveira CFR, Van Eynde B, Christiaens O, and Smagghe G, The involvement of clathrin-mediated endocytosis and two Sid-1-like transmembrane proteins in double-stranded RNA uptake in the Colorado potato beetle midgut. *Insect Mol Biol* **25**:315–323 (2016a).

Cappelle K, Smagghe G, Dhaenens M, and Meeus I, Israeli acute paralysis virus infection leads to an enhanced RNA interference response and not its suppression in the bumblebee *Bombus terrestris. Viruses* **8**:334 (2016b).

Christiaens O, Swevers L, and Smagghe G, DsRNA degradation in the pea aphid (*Acyrthosiphon pisum*) associated with lack of response in RNAi feeding and injection assay. *Peptides* **53**:307–314 (2014).

Christiaens O, Tardajos M G, Reyna Z L M, Dash M, Dubruel P, Smagghe G, Increased RNAi efficacy in *Spodoptera exigua* via the formulation of dsRNA with guanylated polymers. *Front Physiol* **9**, 1–13 (2018).

Coy MR, Sanscrainte ND, Chalaire KC, Inberg A, Maayan I, Glick E, et al., Gene silencing in adult *Aedes aegypti* mosquitoes through oral delivery of double-stranded RNA. *J Appl Entomol* **136**:741–748 (2012).

De Smet L, Ravoet J, Wenseleers T, and de Graaf DC, Expression of key components of the RNAi machinery are suppressed in *Apis mellifera* that suffer a high virus infection. *Entomol Sci* **20**:76–85 (2016).

Ding B-Y, Yang L, Peng Y-Y, Chang T-Y, Ye C, Shang F, et al., RNA-sequencing of a citrus bud-feeder, *Podagricomela weisei* (Coleoptera: Chrysomelidae), reveals xenobiotic metabolism/core RNAi machinery-associated genes and conserved miRNAs. *CBPD* **29**: 339-350 (2019).

Dong X, Li X, Li Q, Jia H, and Zhang H, The inducible blockage of RNAi reveals a role for polyunsaturated fatty acids in the regulation of dsRNA-endocytic capacity in *Bactrocera dorsalis*. *Sci Rep* **7**:5584 (2017).

Dowling D, Pauli T, Donath A, Meusemann K, Podsiadlowski L, Petersen M, *et al.*, Phylogenetic origin and diversification of RNAi pathway genes in insects. *Genome Biol Evol* **8**:3784–3793 (2016).

Feinberg EH and Hunter CP, Transport of dsRNA into cells by the transmembrane protein SID-1. *Science* **301**:1545–1547 (2003).

Fishilevich E, Vélez AM, Storer NP, Li H, Bowling AJ, Rangasamy M, *et al.*, RNAi as a management tool for the western corn rootworm, *Diabrotica virgifera virgifera*. *Pest Manag Sci* **732**:1652-1663 (2016).

Galbraith DA, Yang X, Niño EL, Yi S, and Grozinger C, Parallel epigenomic and transcriptomic responses to viral infection in honey bees (*Apis mellifera*). *PLoS Pathog* **11**:e1004713 (2015).

Garbutt JS and Reynolds SE, Induction of RNA interference genes by double-stranded RNA; implications for susceptibility to RNA interference. *Insect Biochem Mol Biol* **42**:621–628 (2012).

Garbutt JS, Bellés X, Richards EH, and Reynolds SE, Persistence of double-stranded RNA in insect hemolymph as a potential determiner of RNA interference success: Evidence from *Manduca sexta* and *Blattella germanica*. *J Insect Physiol* **59**:171–178 (2013).

Garcia R A, Pepino Macedo L L, Do Nascimento D C, Gillet F X, Moreira-Pinto C E, Faheem M, et al., Nucleases as a barrier to gene silencing in the cotton boll weevil, *Anthonomus grandis*. *PLoS One* **12**, 1–22 (2017).

Ghosh S, Kakumani PK, Kumar A, Malhotra P, Mukherjee SK, and Bhatnagar RK, Genome wide screening of RNAi factors of Sf21 cells reveal several novel pathway associated proteins. *BMC Genomics* **15**:775 (2014).

Gillet F, Garcia RA, and Macedo LLP, Investigating engineered ribonucleoprotein particles to improve oral RNAi delivery in crop insect pests. *Front Physiol* **8**:256 (2017).

Gong L, Wang Z, Wang H, Qi J, Hu M, and Hu Q, Core RNAi machinery and three Sid-1 related genes in *Spodoptera litura* (Fabricius). *Int J Agric Biol* **17**:937–944 (2015).

Guan R-B, Li H-C, Fan Y-J, Hu S-R, Christiaens O, Smagghe G, *et al.*, A nuclease specific to lepidopteran insects suppresses RNAi. *J Biol Chem* **293**:6011-6021 (2018)

Guo W-CC, Fu K-YY, Yang S, Li X-XX, and Li G-QQ, Instar-dependent systemic RNA interference response in *Leptinotarsa decemlineata* larvae. *Pestic Biochem Physiol* **123**:28–33 (2015).

Ivashuta S, Zhang Y, Wiggins BE, Ramaseshadri P, Segers GC, Johnson S, *et al.*, Environmental RNAi in herbivorous insects. *RNA* **21**:840-850 (2015).

Jarosch A and Moritz RF a, Systemic RNA-interference in the honeybee *Apis mellifera*: Tissue dependent uptake of fluorescent siRNA after intra-abdominal application observed by laser-scanning microscopy. *J Insect Physiol* **57**:851–857 (2011).

Jaubert-Possamai S, Rispe C, Tanguy S, Gordon K, Walsh T, Edwards O, *et al.*, Expansion of the miRNA pathway in the hemipteran insect *Acyrthosiphon pisum*. *Mol Biol Evol* **27**:979–987 (2010).

Karlikow M, Goic B, Mongelli V, Salles A, Schmitt C, Bonne I, *et al.*, *Drosophila* cells use nanotube-like structures to transfer dsRNA and RNAi machinery between cells. *Sci Rep* **6**:27085 (2016).

Kobayashi I, Tsukioka H, Kômoto N, Uchino K, Sezutsu H, Tamura T, *et al.*, SID-1 protein of *Caenorhabditis elegans* mediates uptake of dsRNA into *Bombyx cells*. *Insect Biochem Mol Biol* **42**:148–154 (2012).

Kolliopoulou A and Swevers L, Functional analysis of the RNAi response in ovary-derived silkmoth Bm5 cells. *Insect Biochem Mol Biol* **43**:654–663 (2013).

Kupsco JM, Wu M-J, Marzluff WF, Thapar R, and Duronio RJ, Genetic and biochemical characterization of *Drosophila* Snipper: A promiscuous member of the metazoan 3'hExo/ERI-1 family of 3' to 5' exonucleases. *RNA* **12**:2103–2117 (2006).

Lee YS, Pressman S, Andress AP, Kim K, White JL, Cassidy J, *et al.*, Silencing by small RNAs is linked to endosome trafficking. *Cell* **11**:1150–1156 (2010).

Lewis SH, Salmela H, and Obbard DJ, Duplication and diversification of dipteran argonaute genes, and the evolutionary divergence of Piwi and Aubergine. *Genome Biol Evol* **8**:507–518 (2016).

Li H, Jiang W, Zhang Z, Xing Y, and Li F, Transcriptome analysis and screening for potential target genes for RNAi-mediated pest control of the beet armyworm, *Spodoptera exigua*. *PLoS One* **8**:e65931 (2013).

Li H, Khajuria C, Rangasamy M, Gandra P, Fitter M, Gen C, *et al.,* Long dsRNA but not siRNA initiates RNAi in western corn rootworm larvae and adults. *J Appl Entomol* **139**:432-445 (2015a).

Li X, Dong X, Zou C, and Zhang H, Endocytic pathway mediates refractoriness of insect *Bactrocera dorsalis* to RNA interference. *Sci Rep* **5**:8700 (2015b).

Li Z, Zeng B, Ling L, Xu J, You L, Aslam AFM, *et al.*, Enhancement of larval RNAi efficiency by over-expressing Argonaute 2 in *Bombyx mori*. *Int J Biol Sci* **11**:176–185 (2015c).

Lin YH, Huang JH, Liu Y, Belles X, and Lee HJ, Oral delivery of dsRNA lipoplexes to German cockroach protects dsRNA from degradation and induces RNAi response. *Pest Manag Sci* **73**:960–966 (2017).

Liu J, Smagghe G, and Swevers L, Transcriptional response of BmToll9-1 and RNAi machinery genes to exogenous dsRNA in the midgut of *Bombyx mori*. *J Insect Physiol* **59**:646–654 (2013).

Liu Y, Ye X, Jiang F, Liang C, Chen D, Peng J, *et al.*, C3PO, an endoribonuclease that promotes RNAi by facilitating RISC activation. *Science* **325**:750–753 (2009).

Lomate PR and Bonning BC, Distinct properties of proteases and nucleases in the gut, salivary gland and saliva of southern green stink bug, *Nezara viridula*. *Sci Rep* **6**:27587 (2016).

Lozano J, Gomez-Orte E, Lee H-J, and Belles X, Super-induction of Dicer-2 expression by alien double-stranded RNAs: An evolutionary ancient response to viral infection? *Dev Genes Evol* **222**:229–235 (2012).

Luo Y, Wang X, Yu D, and Kang L, The SID-1 double-stranded RNA transporter is not required for systemic RNAi in the migratory locust. *RNA Biol* **9**:663–671 (2012).

Luo Y, Wang X, Yu D, Chen B, and Kang L, Differential responses of migratory locusts to systemic RNA interference via double-stranded RNA injection and feeding. *Insect Mol Biol* **22**:574–583 (2013).

Marques JT, Kim K, Wu PH, Alleyne TM, Jafari N, and Carthew RW, Loqs and R2D2 act sequentially in the siRNA pathway in *Drosophila*. *Nat Struct Mol Biol* **17**:24–31 (2010).

Miller SC, Brown SJ, and Tomoyasu Y, Larval RNAi in *Drosophila*? *Dev Genes Evol* **218**:505–510 (2008).

Miller SC, Miyata K, Brown SJ, and Tomoyasu Y, Dissecting systemic RNA interference in the red flour beetle *Tribolium castaneum*: parameters affecting the efficiency of RNAi. *PLoS One* **7**:e47431 (2012).

Miyata K, Ramaseshadri P, Zhang Y, Segers G, Bolognesi R, and Tomoyasu Y, Establishing an in vivo assay system to identify components involved in environmental RNA interference in the Western corn rootworm. *PLoS One* **9**:e101661 (2014).

Mogilicherla K, Howell JL, and Palli SR, Improving RNAi in the brown marmorated stink bug: Identification of target genes and reference genes for RT-qPCR. *Sci Rep* **8**:3720 (2018).

Mongelli V and Saleh M-C, Bugs are not to be silenced: Small RNA pathways and antiviral responses in insects. *Annu Rev Virol* **3**:573–589 (2016).

Murphy KA, Tabuloc CA, Cervantes KR, and Chiu JC, Ingestion of genetically modified yeast symbiont reduces fitness of an insect pest via RNA interference. *Sci Rep* **6**:22587 (2016).

Niu J, Smagghe G, De Coninck DIMM, Van Nieuwerburgh F, Deforce D, and Meeus I, In vivo study of Dicer-2-mediated immune response of the small interfering RNA pathway upon systemic infections of virulent and avirulent viruses in *Bombus terrestris. Insect Biochem Mol Biol* **70**:127-137 (2016).

Peng Y, Wang K, Fu W, Sheng C, and Han Z, Biochemical comparison of dsRNA degrading nucleases in four different insects. *Front Physicol* **9**, 1–14 (2018).

Powell ME, Bradish HM, Gatehouse JA, and Fitches EC, Systemic RNAi in the small hive beetle *Aethina tumida* Murray (Coleoptera: Nitidulidae), a serious pest of the European honey bee *Apis mellifera*. *Pest Manag Sci* **73**:53–63 (2017).

Prentice K, Christiaens O, Pertry I, Bailey A, Niblett C, Ghislain M, *et al.*, RNAi-based gene silencing through dsRNA injection or ingestion against the African sweet potato weevil *Cylas puncticollis* (Coleoptera: Brentidae). *Pest Manag Sci* **73**:44–52 (2017).

Pridgeon JW, Zhao L, Becnel JJ, Daniel A, Clark GG, Linthicum KJ, *et al.*, Topically applied *AaeIAP1* double-stranded RNA kills female adults of *Aedes aegypti*. *J Med Entomol* **45**:414–420 (2008).

Ren D, Cai Z, Song J, Wu Z, and Zhou S, DsRNA uptake and persistence account for tissue-dependent susceptibility to RNA interference in the migratory locust. *Locusta migratoria*. *Insect Mol Biol* **23**:175–184 (2014).

Rocha JJE, Korolchuk VI, Robinson IM, and O’Kane CJ, A phagocytic route for uptake of double-stranded RNA in RNAi. *PLoS One* **6**:e19087 (2011).

Rodrigues TB, Dhandapani RK, Duan JJ, and Palli SR, RNA interference in the Asian longhorned beetle:Identification of key RNAi genes and reference genes for RT-qPCR. *Sci Rep* **7**:8913 (2017).

Rodríguez-Cabrera L, Trujillo-Bacallao D, Borrás-Hidalgo O, Wright DJ, and Ayra-Pardo C, RNAi-mediated knockdown of a *Spodoptera frugiperda* trypsin-like serine-protease gene reduces susceptibility to a *Bacillus thuringiensis* Cry1Ca1 protoxin. *Environ Microbiol* **12**:2894–2903 (2010).

Sakashita K, Tatsuke T, Masaki Y, Lee JM, Kawaguchi Y, Kusakabe T, *et al.*, dsRNA binding activity of silworm larval hemolymph is mediated by lipophorin complex. *J Fac Agric Kyushu Univ* **54**:401–406 (2009).

Saleh M, Tassetto M, van Rij RP, Goic B, Gausson V, Berry B, *et al.*, Antiviral immunity in *Drosophila* requires systemic RNAi spread. *Nature* **458**:346–350 (2009).

Saleh M-C, Rij RP Van, Hekele A, Gillis A, Foley E, Farrell PHO, *et al.*, The endocytic pathway mediates cell entry of dsRNA to induce RNAi silencing. *Nat Cell Biol* **8**:793–802 (2006).

Shukla JN, Kalsi M, Sethi A, Narva KE, Fishilevich E, Singh S, *et al.*, Reduced stability and intracellular transport of dsRNA contribute to poor RNAi response in lepidopteran insects. *RNA Biol* **13**:656–669 (2016).

Singh IK, Singh S, Mogilicherla K, Shukla JN, and Palli SR, Comparative analysis of double-stranded RNA degradation and processing in insects. *Sci Rep* **7**:17059 (2017).

Song H, Zhang J, Li D, Cooper AMW, Silver K, Li T, *et al.*, A double-stranded RNA degrading enzyme reduces the efficiency of oral RNA interference in migratory locust. *Insect Biochem Mol Biol* **86**:68–80 (2017).

Spit J, Philips A, Wynant N, Santos D, Plaetinck G, and Broeck JV, Knockdown of nuclease activity in the gut enhances RNAi efficiency in the Colorado potato beetle, *Leptinotarsa decemlineata*, but not in the desert locust, *Schistocerca gregaria. Insect Biochem Mol Biol* **81**:103–116 (2017).

Swevers L, Huvenne H, Menschaert G, Kontogiannatos D, Kourti A, Pauchet Y, *et al.*, Colorado potato beetle (Coleoptera) gut transcriptome analysis: Expression of RNA interference-related genes. *Insect Mol Biol* **22**:668–684 (2013).

Swevers L, Liu J, Huvenne H, and Smagghe G, Search for limiting factors in the RNAi pathway in silkmoth tissues and the Bm5 cell line: the RNA-binding proteins R2D2 and Translin. *PLoS One* **6**:e20250 (2011).

Taning CNT, Andrade EC, Hunter WB, Christiaens O, and Smagghe G, Asian Citrus Psyllid RNAi Pathway – RNAi evidence. *Sci Rep* **6**:38082 (2016b).

Taning CNT, Christiaens O, Berkvens N, Casteels H, Maes M, and Smagghe G, Oral RNAi to control *Drosophila suzukii*: laboratory testing against larval and adult stages. *J Pest Sci* **89**:803–814 (2016a).

Tassetto M, Kunitomi M, and Andino R, Circulating immune cells mediate a systemic RNAi-based adaptive antiviral response in *Drosophila*. *Cell* **169**:314–325.e13 (2017).

Tomoyasu Y, Miller SC, Tomita S, Schoppmeier M, Grossmann D, and Bucher G, Exploring systemic RNA interference in insects: a genome-wide survey for RNAi genes in *Tribolium*. *Genome Biol* **9**:R10 (2008).

Ulrich J, Dao VA, Majumdar U, Schmitt-Engel C, Schwirz J, Schultheis D, *et al.*, Large scale RNAi screen in *Tribolium* reveals novel target genes for pest control and the proteasome as prime target. *BMC Genomics* **16**:674 (2015).

Ulvila J, Parikka M, Kleino A, Sormunen R, Ezekowitz RA, Kocks C, *et al.*, Double-stranded RNA is internalized by scavenger receptor-mediated endocytosis in *Drosophila* S2 cells. *J Biol Chem* **281**:14370–14375 (2006).

Upadhyay SK, Chandrashekar K, Thakur N, Verma PC, Borgio JF, Singh PK, *et al.*, RNA interference for the control of whiteflies (*Bemisia tabaci*) by oral route. *J Biosci* **36**:153–161 (2011).

Upadhyay SK, Dixit S, Sharma S, Singh H, Kumar J, Verma PC, *et al.*, SiRNA machinery in whitefly (*Bemisia tabaci*). *PLoS One* **8**:e83692 (2013).

Vatanparast M and Kim Y, Optimization of recombinant bacteria expressing dsRNA to enhance insecticidal activity against a lepidopteran insect, *Spodoptera exigua*. *PLoS One*:e0183054 (2017).

Wang D, Liu Q, Li X, Sun Y, Wang H, and Xia L, Double-stranded RNA in the biological control of grain aphid (*Sitobion avenae* F.). *Funct Integr Genomics* **15**:211–223 (2015b).

Wang GH, Jiang L, Zhu L, Cheng TC, Niu WH, Yan YF, *et al.*, Characterization of Argonaute family members in the silkworm, *Bombyx mori*. *Insect Sci* **20**:78–91 (2013b).

Wang J, Gu L, Ireland S, Garczynski SF, and Knipple DC, Phenotypic screen for RNAi effects in the codling moth *Cydia pomonella*. *Gene* **572**:184–190 (2015a).

Wang J, Wu M, Wang B, and Han Z, Comparison of the RNA interference effects triggered by dsRNA and siRNA *inTribolium castaneum*. *Pest Manag Sci* **69**:781-786 (2013a).

Wang K, Peng Y, Pu J, Fu W, Wang J, and Han Z, Variation in RNAi efficacy among insect species is attributable to dsRNA degradation in vivo. *Insect Biochem Mol Biol* **77**:1–9 (2016).

Wang Y, Zhang H, Li H, and Miao X, Second-generation sequencing supply an effective way to screen RNAi targets in large scale for potential application in pest insect control. *PLoS One* **6**:e18644 (2011).

Wynant N, Duressa TF, Santos D, Van Duppen J, Proost P, Huybrechts R, *et al.*, Lipophorins can adhere to dsRNA, bacteria and fungi present in the hemolymph of the desert locust: A role as general scavenger for pathogens in the open body cavity. *J Insect Physiol* **64**:7–13 (2014a).

Wynant N, Santos D, Subramanyam SH, Verlinden H, and Vanden Broeck J, Drosha, Dicer-1 and Argonaute-1 in the desert locust: Phylogenetic analyses, transcript profiling and regulation during phase transition and feeding. *J Insect Physiol* **75**:20–29 (2015c).

Wynant N, Santos D, Van Wielendaele P, and Vanden Broeck J, Scavenger receptor-mediated endocytosis facilitates RNA interference in the desert locust, *Schistocerca gregaria*. *Insect Mol Biol* **23**:320–329 (2014b).

Wynant N, Santos D, Verdonck R, Spit J, Van Wielendaele P, and Vanden Broeck J, Identification, functional characterization and phylogenetic analysis of double stranded RNA degrading enzymes present in the gut of the desert locust, *Schistocerca gregaria*. *Insect Biochem Mol Biol* **46**:1–8 (2014d).

Wynant N, Verlinden H, Breugelmans B, Simonet G, and Vanden Broeck J, Tissue-dependence and sensitivity of the systemic RNA interference response in the desert locust, *Schistocerca gregaria*. *Insect Biochem Mol Biol* **42**:911–917 (2012).

Xiao D, Gao X, Xu J, Liang X, Li Q, Yao J, *et al.*, Clathrin-dependent endocytosis plays a predominant role in cellular uptake of double-stranded RNA in the red flour beetle. *Insect Biochem Mol Biol* **60**:68–77 (2015).

Xie Y-F, Niu J-Z, Jiang X-Z, Yang W-J, Shen G-M, Wei D, *et al.*, Influence of various stressors to the expression of core genes of the small interfering RNA pathway in the oriental fruit fly, *Bactrocera orsalis*. *Insect Sci* **24**:418-430 (2016).

Xu HJ, Chen T, Ma XF, Xue J, Pan PL, Zhang XC, *et al.*, Genome-wide screening for components of small interfering RNA (siRNA) and micro-RNA (MIRNA) pathways in the brown planthopper. *Nilaparvata lugens* (Hemiptera: Delphacidae). *Insect Mol Biol* **22**:635–647 (2013).

Yang J and Han Z, Efficiency of different methods for dsRNA delivery in cotton bollworm (*Helicoverpa armigera*). *J Integr Agric* **13**:115–123 (2014).

Yokoi K, Kamezaki M, Yoshida T, Tanaka T, and Miura K, Sensitivity to RNA interference-mediated gene silencing in intact and ligated larvae of the armyworm, *Mythimna separata* (Lepidoptera: Noctuidae). *Appl Entomol Zool* **48**:431–439 (2013).

Yoon J-SS, Shukla JN, Gong ZJ, Mogilicherla K, and Palli SR, RNA interference in the Colorado potato beetle, *Leptinotarsa decemlineata*: Identification of key contributors. *Insect Biochem Mol Biol* **78**:78–88 (2016).

Zha W, Peng X, Chen R, Du B, Zhu L, and He G, Knockdown of midgut genes by dsRNA-transgenic plant-mediated RNA interference in the hemipteran insect *Nilaparvata lugens*. *PLoS One* **6**:e20504 (2011).

Zhan S, Merlin C, Boore JL, and Reppert SM, The monarch butterfly genome yields insights into long-distance migration. *Cell* **147**:1171–1185 (2011).

Zhang M, Zhou Y, Wang H, Jones HD, Gao Q, Wang D, *et al.*, Identifying potential RNAi targets in grain aphid (*Sitobion avenae* F.) based on transcriptome profiling of its alimentary canal after feeding on wheat plants. *BMC Genomics* **14**:560 (2013).

Zhang X, Zhang J, and Zhu KY, Chitosan/double-stranded RNA nanoparticle-mediated RNA interference to silence chitin synthase genes through larval feeding in the African malaria mosquito (*Anopheles gambiae*). *Insect Mol Biol* **19**:683–693 (2010).

Zhao C, Alvarez Gonzales MA, Poland TM, and Mittapalli O, Core RNAi machinery and gene knockdown in the emerald ash borer (*Agrilus planipennis*). *J Insect Physiol* **72**:70–78 (2015).

Zhu F, Xu J, Palli R, Ferguson J, and Palli SR, Ingested RNA interference for managing the populations of the Colorado potato beetle, *Leptinotarsa decemlineata*. *Pest Manag Sci* **67**:175–182 (2011).

Chapter 2

Table S2-1. Primers for dsRNA synthesis, cDNA synthesis, and RT-qPCR to investigate dsRNA stability in ECB.

Abbreviations: bp, base pair; cDNA, complementary DNA; dsRNA, double-stranded RNA; RT-qPCR, reverse transcription quantitative real-time PCR; ORF, open reading frame; On, *Ostrinia nubilalis*; Dv, *Diabrotica virgifiera virgifera*,; Av, *Aequorea victoria*; Lgl, lethal giant larvae; GFP, enhanced green fluorescent protein; ECB, European corn borer; WCR, western corn rootworm, %E, percent primer efficiency; F, forward primer; R, reverse primer.

Application of primers	Target gene	Primer pair name	Sequence of primers (5'-3')	Product size (bp)	%E
dsRNA synthesis	*OnLgl*	E800	F: taatacgactcactatagggagCCAACCAGCAGTTGGAGAGT R: taatacgactcactatagggagTGTTTTCGCCGATTTCTTCT	807	
		E500	F: taatacgactcactatagggagCCAACCAGCAGTTGGAGAGT R: taatacgactcactatagggagAGGTAAGGCAACCTCATTGG	506	
		E200	F: taatacgactcactatagggagCCAACCAGCAGTTGGAGAGT R: taatacgactcactatagggagATCTCCTCTCCATCGACGC	205	
		E100	F: taatacgactcactatagggagTATAGACCTGTGCGACCCG R: taatacgactcactatagggagGCAGCCACATTGTCTACGAG	105	
		E50A	F: taatacgactcactatagggagTCGATGGAGAGGAGATCGTT R: taatacgactcactatagggagGAATATGACGCTCTGGGCAT	55	
		E50B	F: taatacgactcactatagggagATGCCCAGAGCGTCATATTC R: taatacgactcactatagggagTTTCGCCCTGTTGTACTGTG	55	
		E50D	F: taatacgactcactatagggagCAGTGTGTGAACACCCCAAA R: taatacgactcactatagggagCCTCGGTTGTAGCCGATTAG	55	
		E50F	F: taatacgactcactatagggagCCAACCAGCAGTTGGAGAGT R: taatacgactcactatagggagGATGTGAAGTGCTCGCCAT	55	
	DvLgl	W800	F: taatacgactcactatagggagAATCGGCAGCTAACAACGG R: taatacgactcactatagggagTGAAGAACGCTGCATGTGAT	805	
		W500	F: taatacgactcactatagggagCTAACCGTTCTTGGCCTGTG R: taatacgactcactatagggagGTCGTTGCTTGGAATCCTCT	505	
		W200	F: taatacgactcactatagggagGGCATTTTTGACCCGTACTC R: taatacgactcactatagggagCGTGTCCTTTCCAAACGAAT	205	
		W100	F: taatacgactcactatagggagCTAACCGTTCTTGGCCTGTG R: taatacgactcactatagggagATTTGACGGTTCCATCTTCG	105	

		W50B	F: taatacgactcactatagggagTCTACACGCCTCAGCTGTCA R: taatacgactcactatagggagTTCCTCCGGTACTCCTGAAA	55	
		W50C	F: taatacgactcactatagggagCAAGCAACGACAATTCTCCA R: taatacgactcactatagggagAACGCTGCATGTGATAGCTG	54	
		W50D	F: taatacgactcactatagggagCAAACGAATAACCCTTTGCC R: taatacgactcactatagggagGGTGCCGCTAACTACCAAAG	52	
		W50E	F: taatacgactcactatagggagCGGGAGTTGCTATTGACAGG R: taatacgactcactatagggagCATCCCAGAATTTGACGGTT	52	
	AvGFP		F: taatacgactcactatagggagTGACCACCCTGACCTAC R: taatacgactcactatagggagTTGATGCCGTTCTTCTGC	305	
cDNA synthesis	*AvGFP*		R: TTGATGCCGTTCTTCTGC	305	
RT-qPCR	*AvGFP*		F: GCCGCTACCCCGACCACATGA R: CGGGTCTTGTAGTTGCCGTCGT	112	93.8

Figure S2-1. Diagram depicting the location of dsRNA constructs of various sizes (800, 500, 200, 100, 50 bp) targeting the lethal giant larvae (Lgl) gene from ECB (On) and WCR (Dv).

Open reading frames are shown in lighter colors, and target regions for each dsRNA are shown as thin colored lines. DsRNAs targeting *OnLgl* are labeled with an "E" and are named based on size. DsRNAs targeting *DvLgl* are labeled with a "W" and similarly named based on size.

Figure S2-2. Diagram depicting the location of 50 bp dsRNA constructs targeting the lethal giant larvae (Lgl) gene from ECB (On) and WCR (Dv).

Open reading frames are shown in lighter colors, and target regions for each dsRNA are shown as thin colored lines. DsRNAs targeting *OnLgl* are labeled with an "E" and dsRNAs targeting *DvLgl* are labeled with a "W." The letters A, B, C, D, E, and F after "50" indicate the locations of different 50-bp dsRNA molecules as shown in different colors in the diagram.

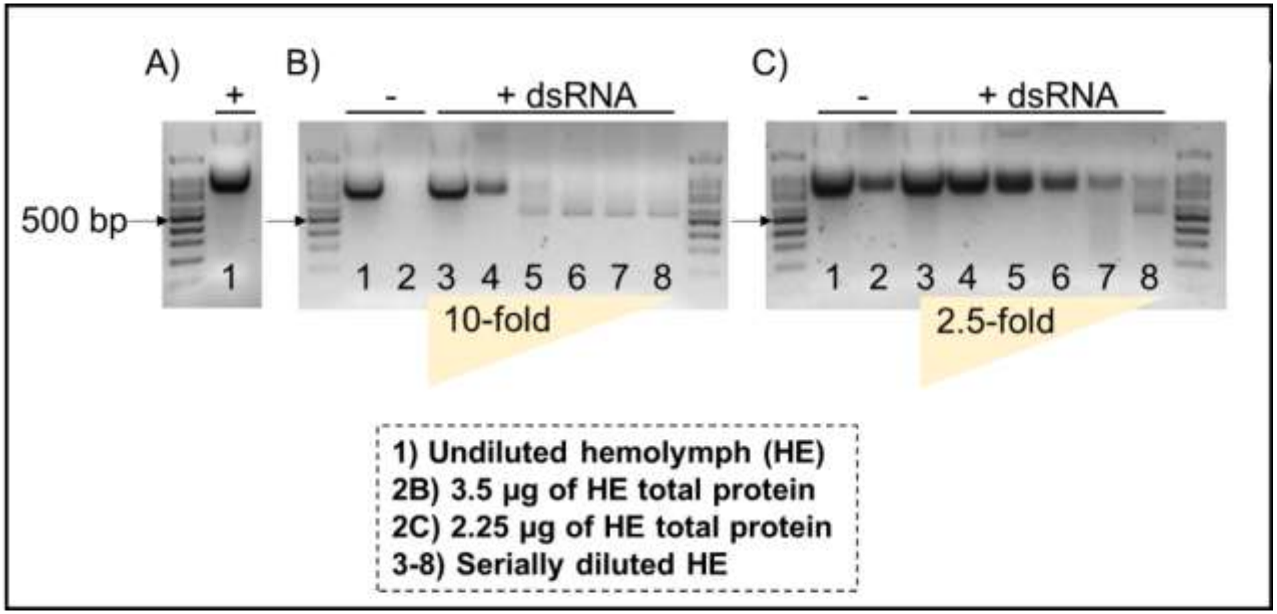

Figure S2-3. Representative gel images showing abnormal migration of dsRNA when combined with hemolymph (HE) extracts from thirty, fifth instar ECB larvae.

The appearance of A) undiluted ECB HE with 250 ng of 500 bp dsRNA targeting *OnLgl*, B) tenfold serial dilutions of ECB HE with (+) and without (-) dsRNA, and C) 2.5-fold serial dilutions of ECB HE with and without dsRNA. Lanes 1 and 2 are no-dsRNA controls containing HE only. The first lanes contain undiluted ECB HE. Lanes B2 and C2 contain 3.5 µg and 5.25 µg of ECB HE total protein, respectively. Lanes 3-8 contain dsRNA with serial dilutions of ECB HE, starting with the highest concentration of ECB HE, undiluted hemolymph in lane 3 and the lowest concentrations in lane 8 of panels B and C. HE appeared as a dark, high molecular weight band which disappeared as the hemolymph was diluted. Conversely, the ds*OnLgl* band (500 bp) appeared as a much lighter band that was only visible when hemolymph was sufficiently diluted.

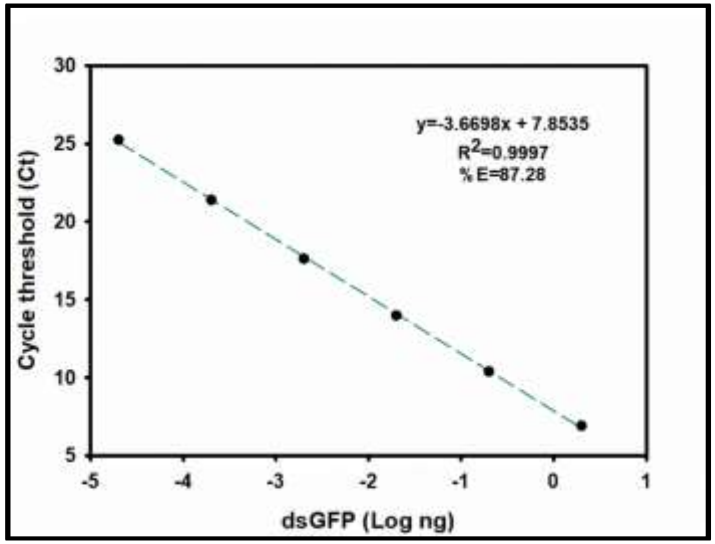

Figure S2-4. Standard curve used for quantification of dsRNA with RT-qPCR.

Ct values corresponding to five serial dilutions of dsRNA targeting *enhanced green fluorescent protein* (ds*GFP*) were plotted against the Log ng of each concentration and subjected to linear regression. The slope and *y*-intercept values were used to convert raw Ct values for each sample into nanograms of ds*GFP* that remained intact after incubation.

Table S2-2. Basic statistical information for *ex vivo* dsRNA incubation experiments under various pH conditions.

The degrees of freedom, test statistic, and *p*-values for each two-sample t-test are presented. Significant differences between treatments are indicated by an asterisks.

pH	Gut contents	Hemolymph
3.0	t(4)= 5.67, p=0.005*	t(4)= 2.08, p=0.172
4.0	t(4)= 4.68, p=0.009*	t(4)= 6.27, p=0.003*
5.0	t(4)= 9.57, p=0.001*	t(4)= 11.37, p<0.001*
6.0	t(4)= 8.24, p=0.001*	t(4)= 5.76, p=0.004*
7.0	t(4)= 5.31, p=0.006*	t(4)= 6.80, p=0.002*
8.0	t(4)= 9.98, p=0.001*	t(4)= 9.11, p=0.001*
9.0	t(4)= 7.26, p=0.002*	t(4)= 4.34, p=0.012*
10.0	t(4)= 6.33, p=0.003*	t(4)= 4.07, p=0.015*

Chapter 3

Table S3-1. Primers for dsRNA synthesis, cDNA synthesis, and RT-qPCR to investigate nucleases in ECB.

Abbreviations: bp, base pair; cDNA, complementary DNA; dsRNA, double-stranded RNA; RT-qPCR, reverse transcription quantitative real-time PCR; ORF, open reading frame; *On, Ostrinia nubilalis; Dv, Diabrotica virgifiera virgifera,; Av, Aequorea victoria; Lgl, lethal giant larvae; GFP, enhanced green fluorescent protein*; ECB, European corn borer; WCR, western corn rootworm, %E, percent primer efficiency; F, forward primer; R, reverse primer; RPS3, *Ribosomal protein S3; EF1a, Elongation factor 1-alpha.*

Application of primers	**Target gene**	**Sequence of primers (5′ to 3′)**	**Product size (bp)**	**%E**
cDNA sequencing	*OndsRNase2*	F: GCCCTGACTACACTGAAGGTG R: ACGCCCCTATTACGGTGACTGATGG	1,454	
	OndsRNase3	F: TAACCCAAGCAATACCTAT R: TATGTAAACCAGGGATGT	1,281	
	OndsRNase4	F: ATGATACATCTGCAAAAACTATTTACTC R: TGTGCCTATTTAAGACCG	1,280	
	OndsRNase1	F: ATGCACTCCGTCGTGGTGTTTC R: GTAAGGGGTCTGCTGAACTAAG	1,342	
	OnREase	F: CACAATGCGGATACGAGC R: CTGCTTACTTACAAATTGGTC	1,878	
	DvdsRNase1	F: ATGGTAAGATATAGGTGTG R: CTAAGCTTGTAAAATACC	1,209	
	DvdsRNase2	F: GGTATTATCGCGGTCTACT R: TGTTATTCATAAATAGCCCG	1,628	
	DvdsRNase3	F: GATGCGATCCATGCATTGT R: GGTCGCAACTATGACTCTTT	1,417	
dsRNA synthesis	*OnLgl*	F: taatacgactcactatagggagCCAACCAGCAGTTGGAGAGT R: taatacgactcactatagggagAGGTAAGGCAACCTCATTGG	506	
	AvGFP	F: taatacgactcactatagggagCTAGAGTGAGCAAGGGCGAG R: taatacgactcactatagggagCTTGAAGTTCACCTTGATGCC	503	

RT-qPCR	*OndsRNase2*	F: AGCAGCCAAGAGTGACTTCC R: GGGCACGGAGATTCTGTTCA	128	97.8
	OndsRNase3	F: ACGGTTGCGGAAATCGGAA R: CCCACTCGGAAAGTGGTGT	132	95.4
	OndsRNase4	F: TCGTTGTTTTCACCGCGAG R: GAAGTCTGTCTTCGCCGCA	123	99.4
	OndsRNase1	F: TGGCGATTTCTACCCTGGC R: CGCGTGCCAAGTACTGACT	131	104.1
	OnREase	F: ACTCCAGGCGAGCCTGTCAA R: GCATCGTCAGCGTCCGGATCCTC	182	n/a
	OnRPS3	F: CTGGCCGAAGATGGTTACTC R: ACCACGGAGGTTAGTTCACG	134	89.2
	OnEF1a	F: CCCGCTAACCTGACCACT R: AAACCACGACGCAACTCC	128	95.3

Fig. S3-1 (*continued on next page*).

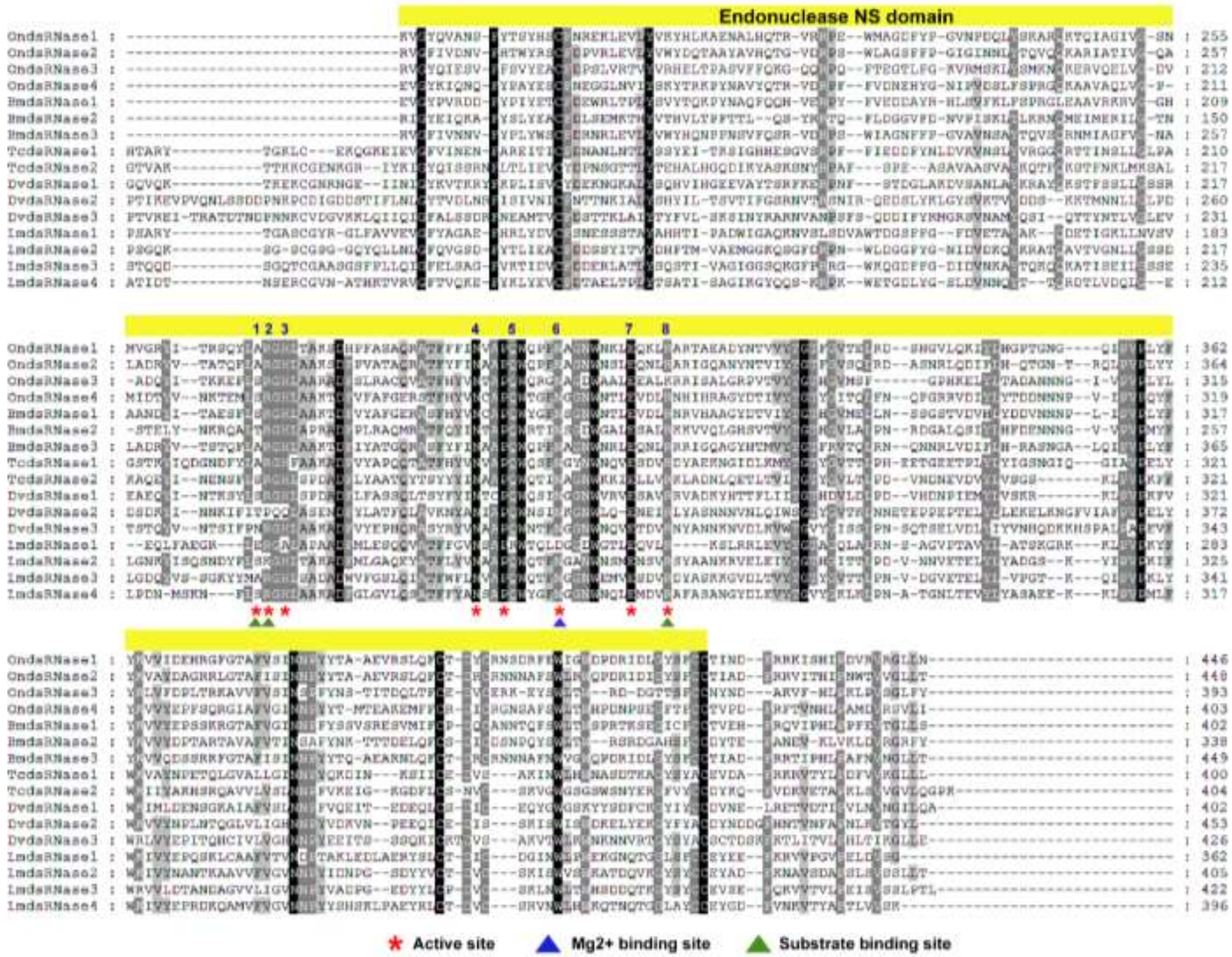

Figure S3-1. Multiple sequence alignments showing conserved domains, residues, and signal peptides in insect dsRNase proteins.

Extracellular secretion (Sec/SPI signal) peptides are indicated in red font and the position of the DNA/RNA non-specific endonuclease **(**endonuclease NS) domain by a yellow bar. The eight amino acid residues that form the active site are indicated by a red astrix and numbered along the top. Amino acid residues that participate in the substrate-binding site and Mg^{2+} binding site are indicated with green and blue triangles, respectively. Black shading indicates 100% identity, dark-grey shading indicates 80–99% identity and light-grey shading indicates 60–79% identity. The species and gene accession number corresponding to each sequence label is as follows: OndsRNase1, *O. nubilalis* (MT524715); OndsRNase2, *Ostrinia nubilalis* (MT524712); OndsRNase3, *O. nubilalis* (MT524713); OndsRNase4, *O. nubilalis* (MT524714); BmdsRNase1, *B. mori* (XP_004922835.1); BmdsRNase2, *Bombyx mori* (NP_001091744.1); BmdsRNase3/AlkNuc, *B. mori* (BAF33251.1); TcdsRNase1, *Tribolium castaneum* (XP_970494.1); TcdsRNase2, *T. castaneum* (XP_015840884.1); DvdsRNase1, *Diabrotica virgifera virgifera* (MT653318); DvdsRNase2, *D. v. virgifera* (MT653319); DvdsRNase3, *D. v. virgifera* (MT653320); LmdsRNase1, *L. migratoria* (ARW74134.1); LmdsRNase2, *L. migratoria* (ARW74135.1); LmdsRNase3, *Locusta migratoria* (KY386893); LmdsRNase4, *L. migratoria* (KY386894).

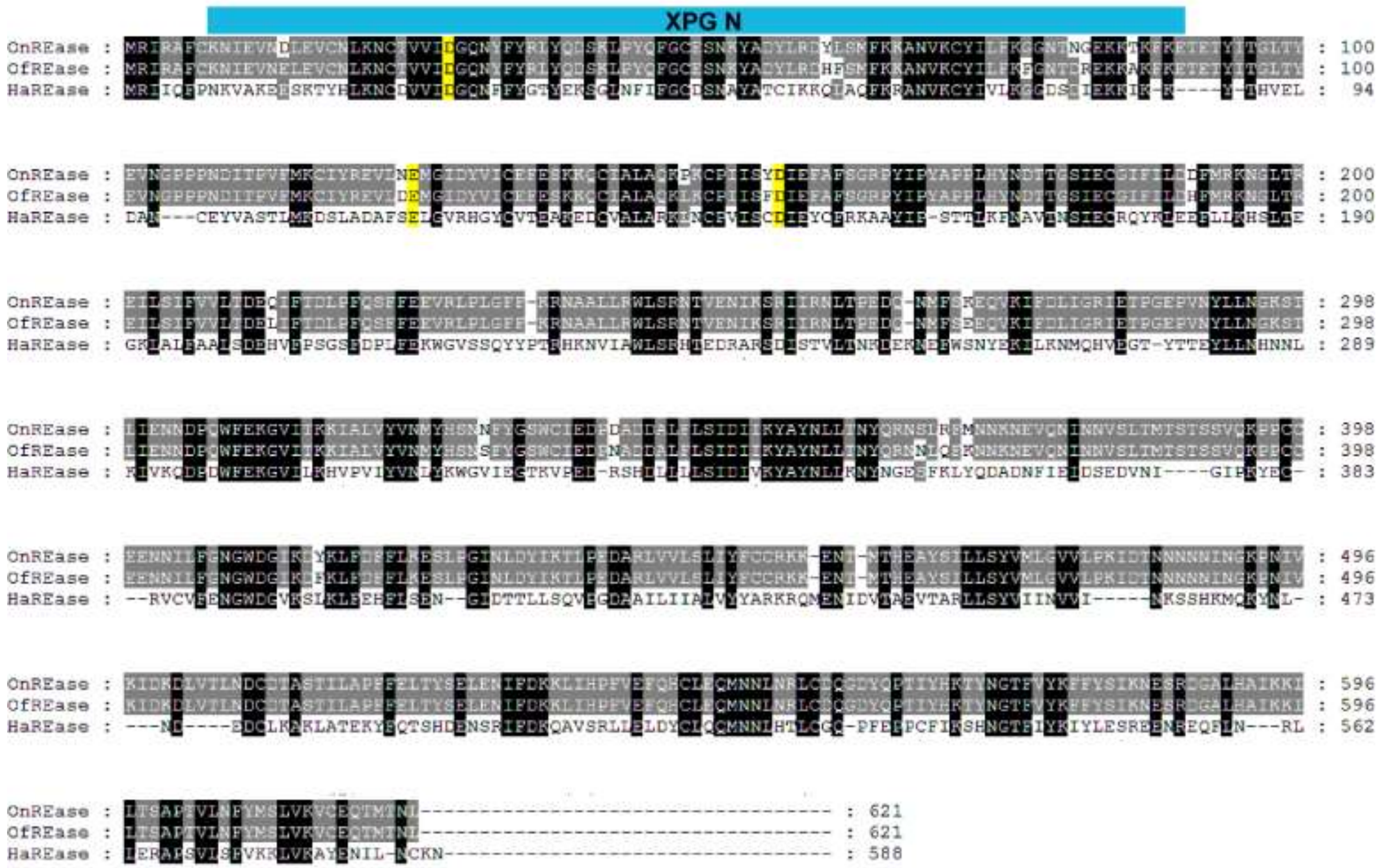

Figure S3-2. Multiple sequence alignments showing conserved domains and residues in insect REase proteins.

The position of the XPG N-terminal domain is indicated by a blue bar and conserved PIN-domain family residues are highlighted. Black shading indicates 100% identity and dark-grey shading indicates 66% identity. The species and gene accession numbers corresponding to each sequence label is as follows: OnREase, *Ostrinia nubialis* (MT524716); OfREase *Ostrinia furnacalis* (XP_028162616.1); HaREase, *Helicoverpa armigera* (XP_021192733.1).

Chapter 4

Table S4-1. Primers for cDNA cloning, dsRNA synthesis, and qPCR to investigate core RNAi machinery genes in ECB.

Abbreviations: bp, base pair; cDNA, complementary DNA; dsRNA, double-stranded RNA; RT-qPCR, reverse transcription quantitative real-time PCR; ORF, open reading frame; On, *Ostrinia nubilalis*; Lgl, lethal giant larvae; GFP, enhanced green fluorescent protein; ECB, European corn borer; %E, percent primer efficiency; F, forward primer; R, reverse primer.

Application of primers	**GenBank number**	**Target gene**	**Sequence of primers (5′ to 3′)**	**Product size (bp)**	**%E**
cDNA cloning	MT921812	*Dcr2, part 1*	F: CAAGGTGCCCTTACAAAT R: GACTCGCATCGTCTTATCCTG	2,000	
	MT921812	*Dcr2, part 2*	F: AGCCGCCTCAGCAATCAG R: TCCACTCGCTCCAGGTTG	1,920	
	MT921812	*Dcr2, part 3*	F: ATTACCGCCGCCATTGAA R: TAGGCAGTGAGATCAAATAAGG	1,584	
	MT981255	*R2D2*	F: TCCAACAACTTGGAACGGC R: GAGGCATTCACTTCTTGGT	999	
	MT524717	*Ago2, part 1*	F: GAATCATTGTTATAGTGCTGTG R: ATCCTGGATCTTCTTCTTGC	1,883	
	MT524717	*Ago2, part 2*	F: CTGAACTGCGTCTGGGTG R: GCAAGGACATCATTGACTATTG	1,715	
dsRNA synthesis	MT467568	*Lgl*	F: taatacgactcactatagggagCCAACCAGCAGTTGGAGAGT R: taatacgactcactatagggagAGGTAAGGCAACCTCATTGG	506	
	LC336974.1	*GFP*	F: taatacgactcactatagggagCTAGAGTGAGCAAGGGCGAG R: taatacgactcactatagggagCTTGAAGTTCACCTTGATGCC	503	
	MT981255	*Dcr2*	F: taatacgactcactatagggagAAGGAGTTGACATTCCGCAG R: taatacgactcactatagggagCGACTGCCAGTTTGTGTGAT	303	
	MT524717	*Ago2*	F: taatacgactcactatagggagATCGCCCAAAGAAGATGCTA R: taatacgactcactatagggagTTACGTCAACGCACTGGATG	303	
	MT981255	*R2D2*	F: taatacgactcactatagggagGGAGCTGTGATTGAGACTGG R: taatacgactcactatagggagCTCAGGCTGGAAGGACTCTG	303	
	LC336974.1	*GFP*	F: taatacgactcactatagggagTGACCACCCTGACCTAC R: taatacgactcactatagggagTTGATGCCGTTCTTCTGC	304	
RT-qPCR	MT921812	*Dcr2*	F: AATTGACGACAGCATCCCGAG R: CCATCACGGTCACTGAGGACAA	155	100.2
	MT524717	*Ago2*	F: GCTTGGGATTAGGACTATCTGG R: CGGGAGCACTTGTAGGTGAA	183	86.9

	MT981255	*R2D2*	F: CTTTCGAGGTGACCTATGTGG R: GACTGGGCATCCTTGCTGTT	129	96.7
	DQ988989	*RPS3*	F: CTGGCCGAAGATGGTTACTC R: ACCACGGAGGTTAGTTCACG	134	89.2
	AF173392	*EF1a*	F: CCCGCTAACCTGACCACT R: AAACCACGACGCAACTCC	128	95.3
	MT467568	*Lgl*	F: TTCCTGGCACCGGTAGACT R: TAGACTCCACGCAGAGGGA	144	97.6

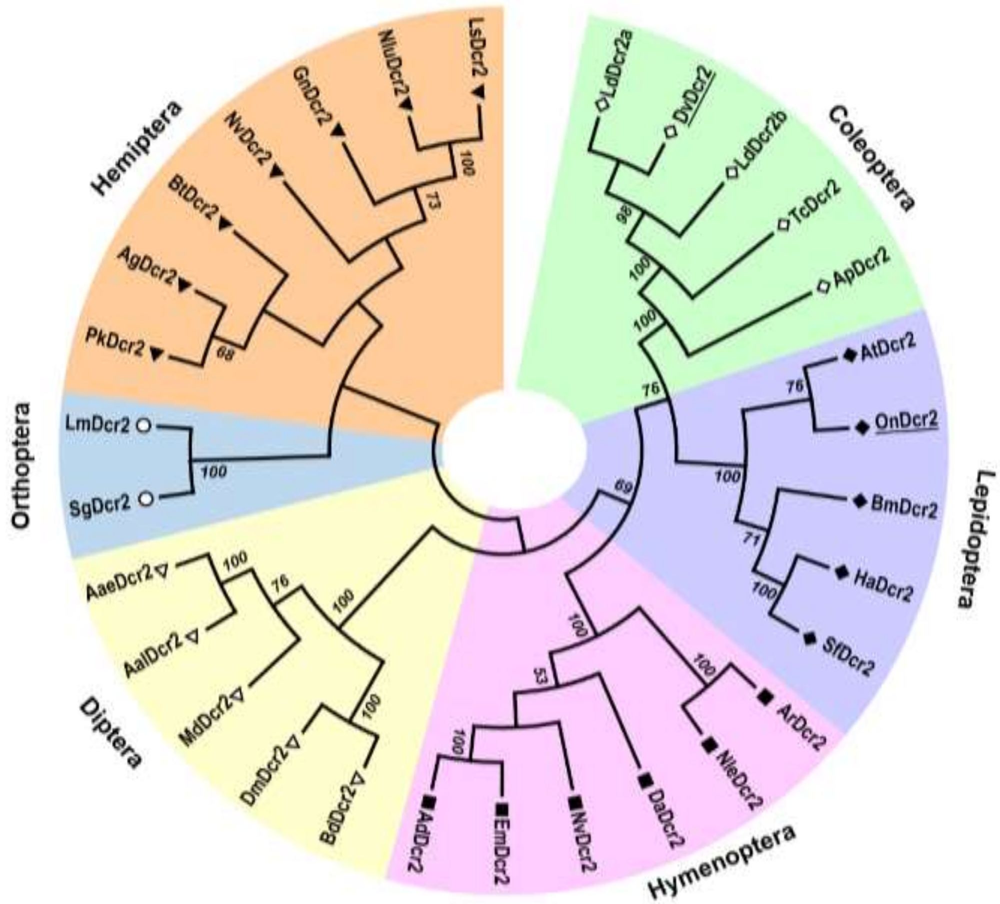

Figure S4-1. Phylogenetic tree showing the relationships between insect Dcr2 proteins.

Bootstrap support is indicated at internal nodes. Different shapes and shading denote different insect orders. The species and gene accession number corresponding to each sequence label is as follows for each order. Coleoptera: LdDcr2a, *Leptinotarsa decemlineata* (AKQ00041.1); DvDcr2, *Diabrotica virgifera virgifera* (AUM60046.1); LdDcr2b, *L. decemlineata (*AKQ00042.1); TcDcr2, *Tribolium castaneum* (NP_001107840.1); ApDcr2, *Agrilus planipennis* (AJF15703.1). Lepidoptera: AtDcr2, *Amyelois transitella* (XP_013192187.1); OnDcr2, *Ostrinia nubilalis* (MT921812); BmDcr2, *Bombyx mori* (NP_001180543.1); HaDcr2, *Helicoverpa armigera* (XP_021197630.1); SfDcr2, *Spodoptera frugiperda* (AVK59442.1). Hymenoptera: ArDcr2, *Athalia rosae* (XP_012265864.1); NleDcr2, *Neodiprion lecontei* (XP_015511858.1); DaDcr2, *Diachasma alloeum* (XP_015124116.1); NvDcr2, *Nasonia vitripennis* (XP_008210323.2); EmDcr2, *Eufriesea Mexicana* (XP_017766061.1); AdDcr2, *Apis dorsata* (XP_006623214.1). Diptera: BdDcr2, *Bactrocera dorsalis* (AHI44612.1); DmDcr2, *Drosophila melanogaster* (AAF57830.2); MdDcr2, *Mayetiola destructor* (AFX89025.1); AalDcr2, *Aedes albopictus* (AEX31250.1); AaeDcr2, *Aedes aegypti* (AAW48725.1); Orthoptera: SgDcr2, *Schistocerca gregaria* (BAX36478.1); LmAgo2a, *Locusta migratoria* (BAW35365.1). Hemiptera: PkDcr2, *Planococcus kraunhiae* (BAX36481.1); AgDcr2, *Aphis glycines* (AFZ74931.1); BtDcr2, *Bemisia tabaci* (AIC07485.1); NvDcr2, *Nezara viridula* (AVK59458.1); GnDcr2, *Graminella nigrifrons* (AIY24625.1); NluDcr2, *Nilaparvata lugens* (AGH30333.1); LsDcr2, *Laodelphax striatella* (AGE12616.1).

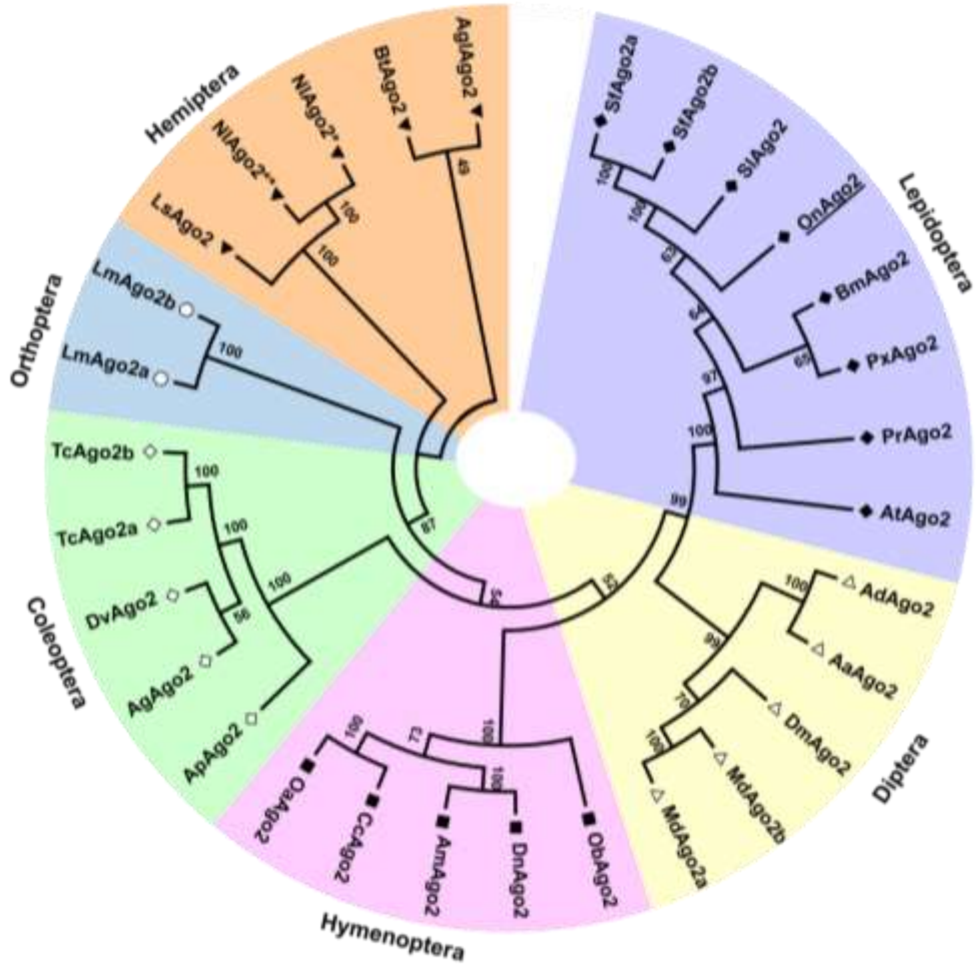

Figure S4-2. Phylogenetic tree showing the relationships between full-length insect Ago2 proteins.

Bootstrap support is indicated at internal nodes. Different shapes and shading denote different insect orders. The species and gene accession number corresponding to each sequence label is as follows for each order. Asterisks (*, **) differentiate unnumbered proteins from the same species. Hemiptera: AglAgo2, *Aphis glycines* (AFZ74933.1); BtAgo2, *Bemisia tabaci* (AHY18683.1); NlAgo2*, *Nilaparvata lugens* (AGE12619.1); NlAgo2**, *N. lugens* (AGH30327.1); LsAgo2, *Laodelphax striatella* (AIY24303.1). Orthoptera: LmAgo2a, *Locusta migratoria* (SXU); LmAgo2b, *L. migratoria* (SXU). Coleoptera: TcAgo2a, *Tribolium castaneum*

(NP_001107842.1); TcAgo2b, *T. castaneum* (NP_001107828.1); DvAgo2, *Diabrotica virgifera virgifera* (AUM60042.1); AgAgo2, *Anoplophora glabripennis* (XP_018569626.1); ApAgo2, *Agrilus planipennis* (AJF15705.1). Hymenoptera: OaAgo2, *Orussus abietinus* (XP_023290372.1), CcAgo2, *Cephus cinctus* (XP_015609184.1); AmAgo2, *Apis mellifera* (XP_395048.4); DnAgo2, *Dufourea novaeangliae* (XP_015438406.1), ObAgo2, *Ooceraea biroi* (XP_011351606.1). Diptera: MdAgo2a, *Mayetiola destructor* (AFX89028.1); MdAgo2a, *M. destructor* (AFX89029.1); DmAgo2, *Drosophila melanogaster* (NP_648775.1); AaAgo2, *Aedes aegypti* (ACR56327.1), AdAgo2, *Anopheles darling* (ETN67307.1). Lepidoptera: AtAgo2, *Amyelois transitella* (XP_013185292.1); PrAgo2, *Pieris rapae* (XP_022113727.1); PxAgo2, *Papilio xuthus* (KPI92855.1); BmAgo2, *Bombyx mori* (NP_001036995.2); OnAgo2, *Ostrinia nubilalis* (MT524717); SlAgo2, *Spodoptera litura* (AHC98010.1); SfAgo2a, *Spodoptera frugiperda* (AVK59454.1); SfAgo2b, *S. frugiperda* (AVK59455.1).

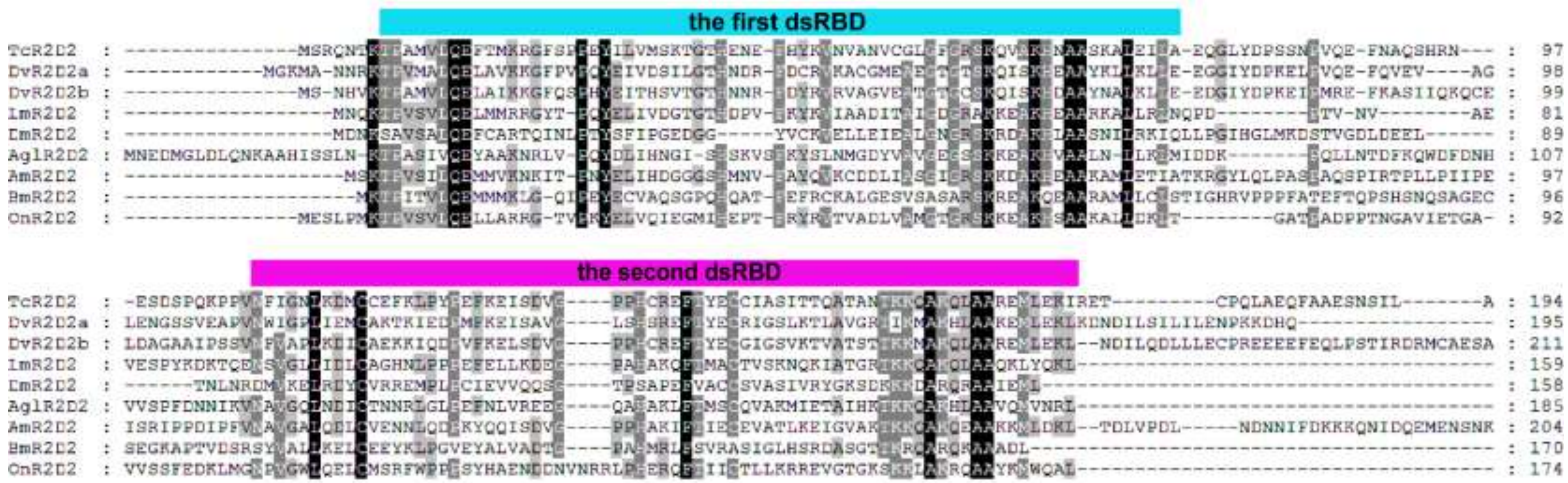

Figure S4-3. Multiple sequence alignment showing conserved domains in R2D2 proteins from insects.
The position of the first and second double-stranded RNA binding (dsRBD) domains are indicated by blue and pink bars, respectively. Black shading indicates 100% identity, dark-grey shading indicates 75–99% identity and light-grey shading indicates 55–74% identity. The species and gene accession number corresponding to each sequence label is as follows: TcR2D2, *Tribolium castaneum* (NP_001128425.1); DvR2D2a, *Diabrotica virgifera virgifera* (XP_028140225.1); DvR2D2b, *D. v. virgifera* (XP_028148994.1**):** LmR2D2, *Locusta migratoria* (SXU); DmR2D2, *Drosophila melanogaster* (FBpp0290544);_AglR2D2, *Aphis glycines* (AFZ74932.1); AmR2D2, *Apis mellifera* (XP_006560091.1); BmR2D2, *Bombyx mori* (NP_001182007.1); OnR2D2, *Ostrinia nubilalis* (MT981255).

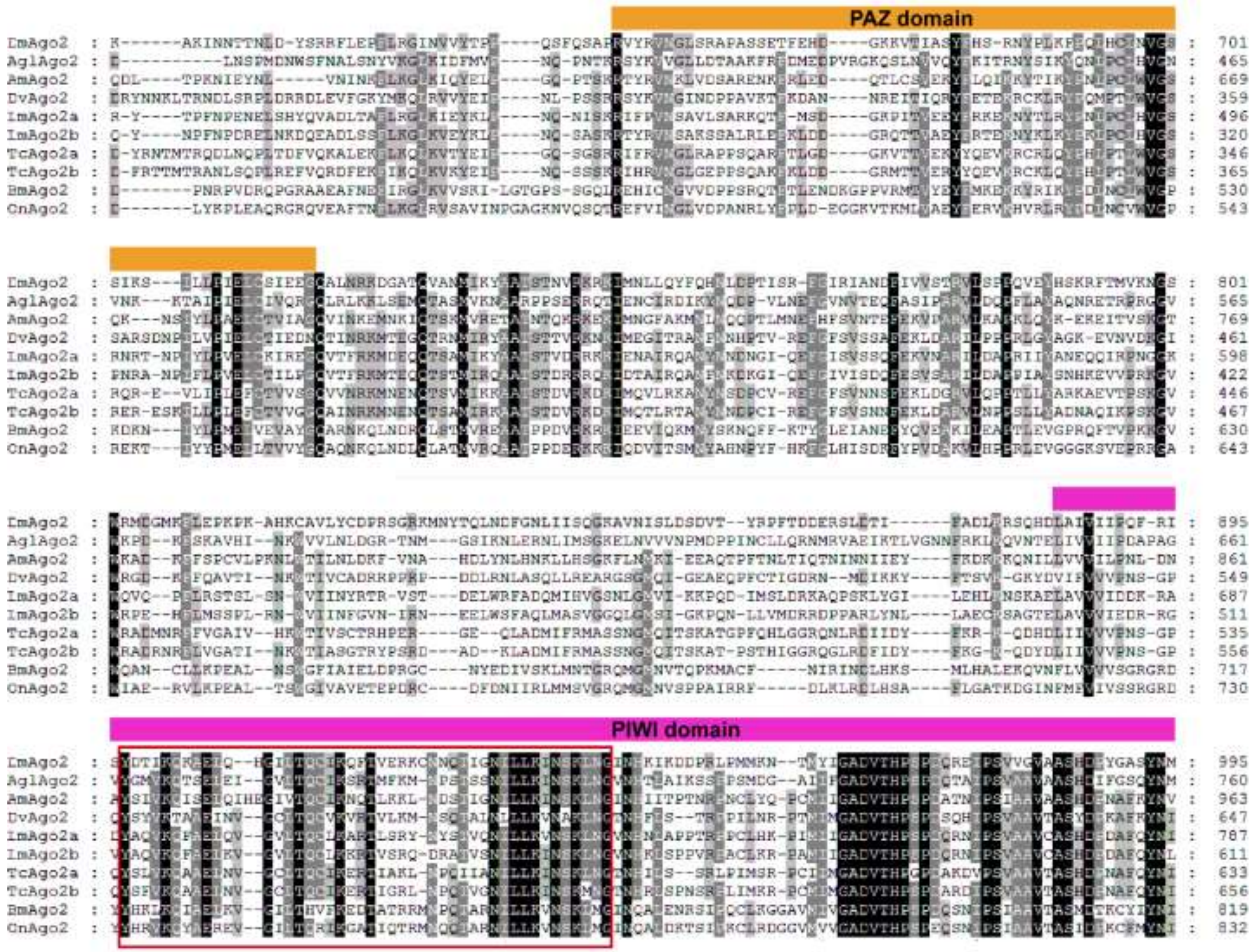

Fig. S4-4 (*continued on next page*).

Figure S4-4. Multiple sequence alignment showing conserved residues and domains in Ago2 proteins from insects.

The position of the PAZ and PIWI domains are indicated by orange and pink bars, respectively. Amino acid residues that form the 5' phosphate-anchoring region are in a red box and residues that form the Ago Asp-Asp-His motif in the active site are highlighted in yellow. Black shading indicates 100% identity, dark-grey shading indicates 80–99% identity and light-grey shading indicates 50–79% identity. The species and gene accession number corresponding to each sequence label is as follows: DmAgo2, *Drosophila melanogaster* (NP_648775.1); AglAgo2, *Aphis glycines* (AFZ74933.1); AmAgo2, *Apis mellifera* (XP_395048.4); DvAgo2, *Diabrotica virgifera virgifera* (AUM60042.1); LmAgo2a, *Locusta migratoria* (SXU); LmAgo2b, *L. migratoria* (SXU); TcAgo2a, *Tribolium castaneum* (NP_001107842.1); TcAgo2b, *T. castaneum* (NP_001107828.1); BmAgo2, *Bombyx mori* (NP_001036995.2); OnAgo2, *Ostrinia nubilalis* (MT524717).

Fig. S4-5 (*continued on next page*).

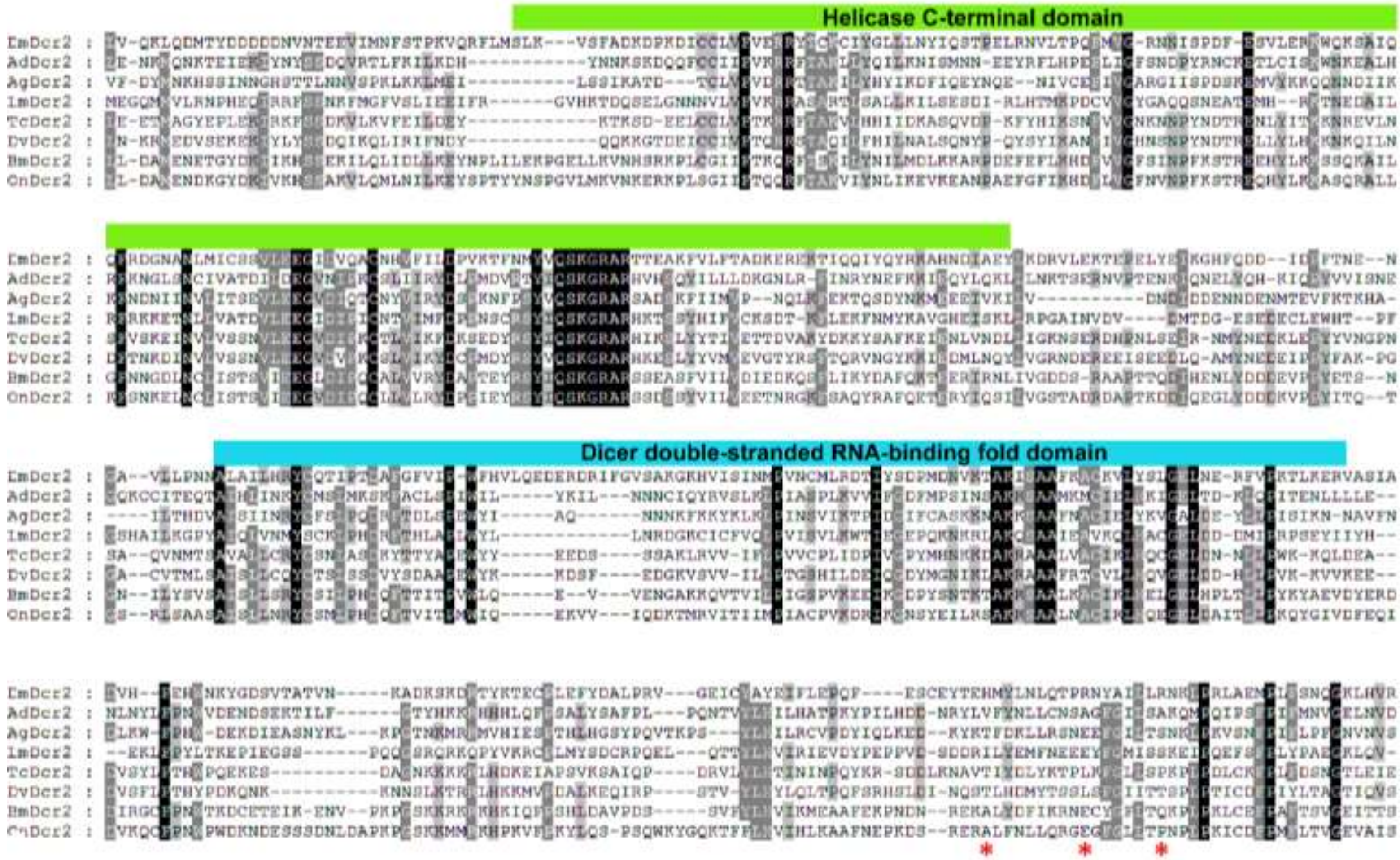

Fig. S4-5 (*continued on next page*).

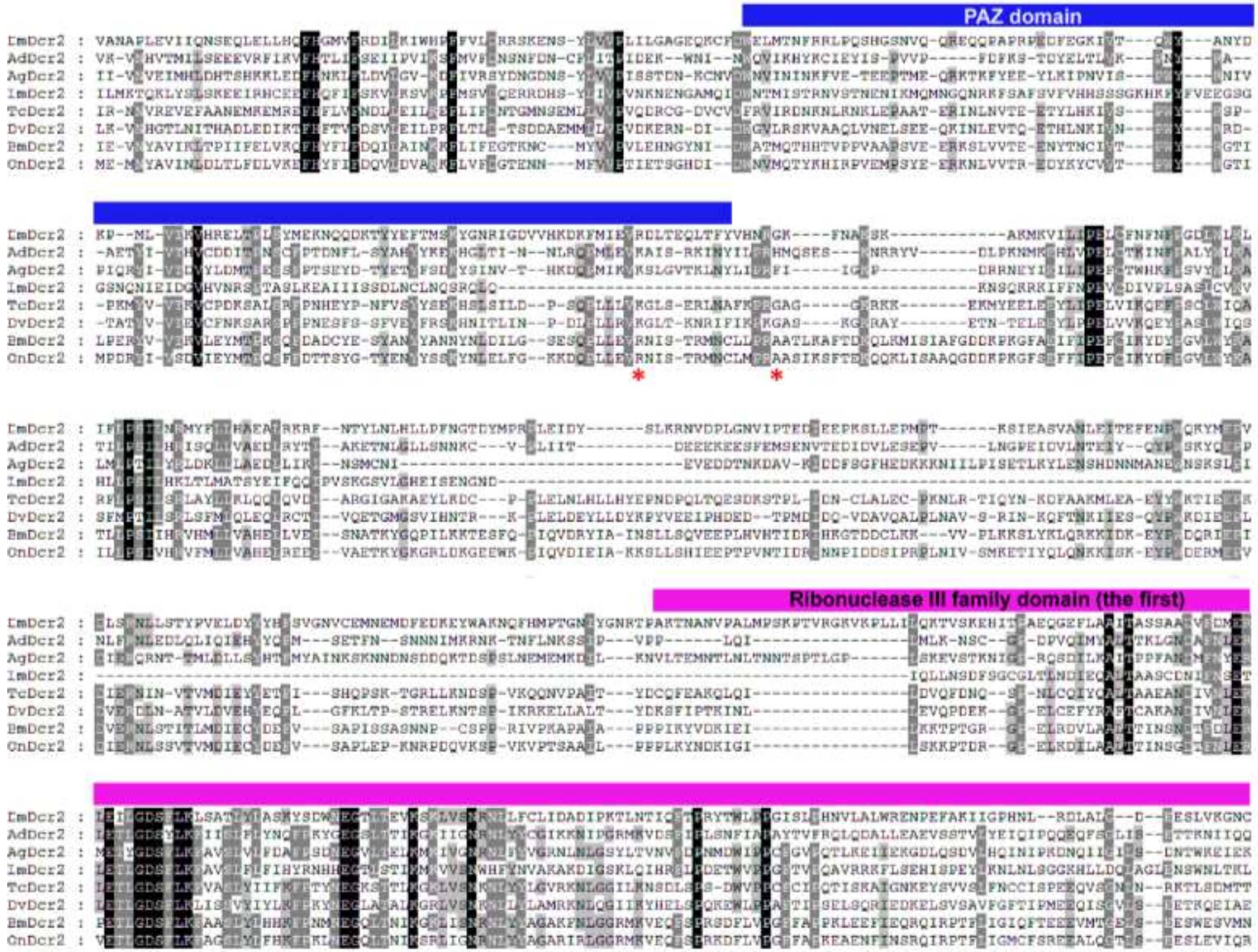

Fig. S4-5 (*continued on next page*).

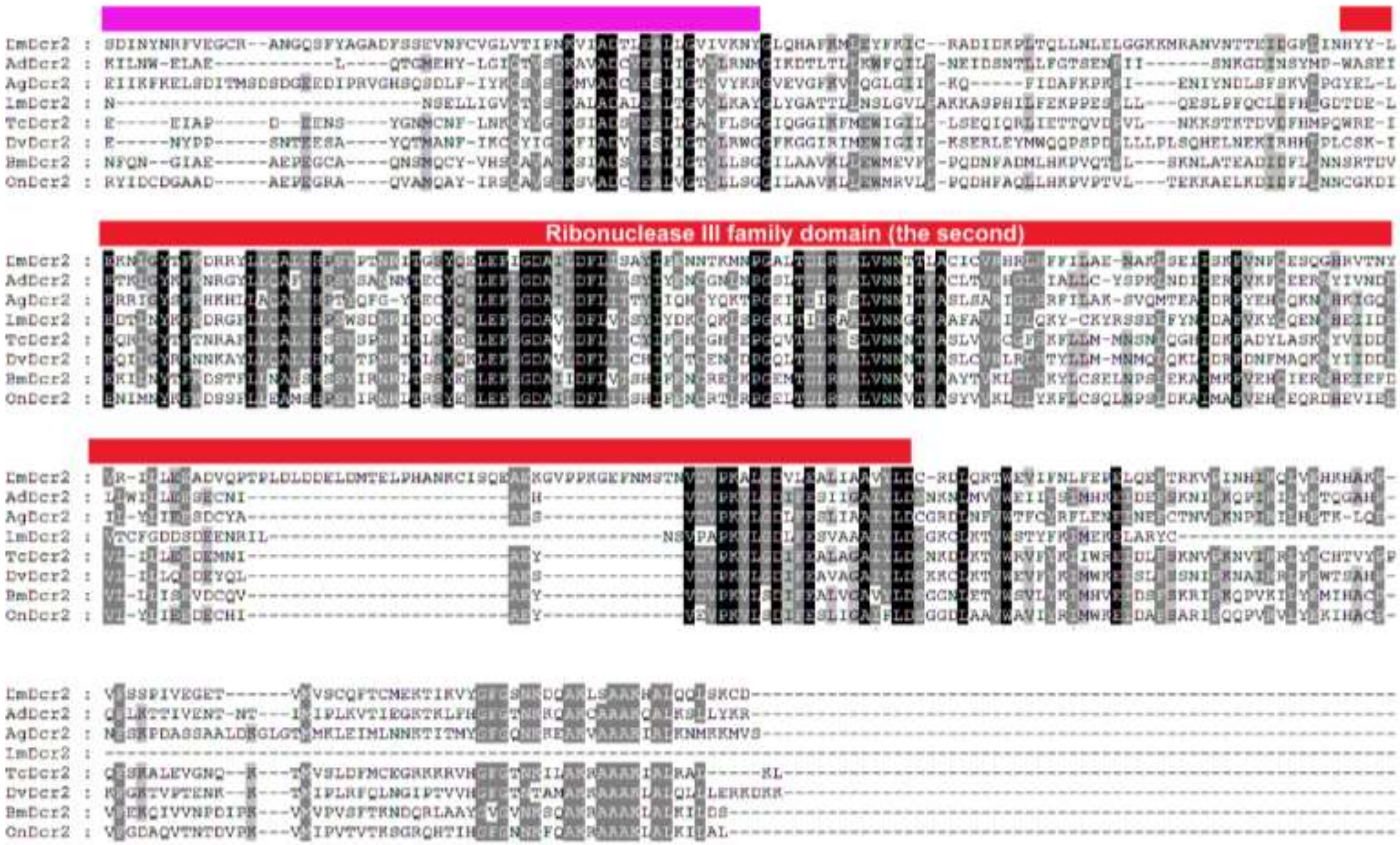

Figure S-5. Multiple sequence alignment showing conserved residues and domains in Dcr2 proteins from insects.

The position of the helicase ATP-binding type-1 domain, the helicase C-terminal domain, the Dicer double-stranded RNA-binding fold domain, the PAZ domain, the first ribonuclease III family domain, and the second ribonuclease III family domain are indicated by yellow, green, aqua, blue, pink, and red bars, respectively. Amino acid residues predicted to form the phosphate binding pocket are indicated with a red asterisk. Black shading indicates 100% identity, dark-grey shading indicates 75–99% identity and light-grey shading indicates 60–74% identity. The species and gene accession number corresponding to each sequence label is as follows: DmDcr2, *Drosophila melanogaster* (AAF57830.2); AdDcr2, *Apis dorsata* (XP_006623214.1); AgDcr2, *Aphis glycines* (AFZ74931.1); LmDcr2, *Locusta migratoria* (BAW35365.1); TcDcr2, *Tribolium castaneum* (NP_001107840.1); DvDcr2, *Diabrotica virgifera virgifera* (AUM60046.1); BmDcr2, *Bombyx mori* (NP_001180543.1); OnDcr2, *Ostrinia nubilalis* (MT921812).

Chapter 5

Table S5-1. Primers for cDNA cloning, dsRNA synthesis, and qPCR used in the comparison of strategies for enhancing efficiency of RNAi in ECB.

Abbreviations: cDNA, complementary DNA; dsRNA, double-stranded RNA; qPCR, quantitative PCR; bp, base pairs; *Lgl*, lethal giant larvae; *GFP*, enhanced green fluorescent protein; *RPS3*, ribosomal protein S3; *Ef1a*, elongation factor-1 alpha; *Cht*, chitinase; *VhaSFD*, V-type proton ATPase subunit H; *Rab7*, Ras-related protein Rab7; *AP50*, assembly protein 50; *Arf72A*, ADP-ribosylation factor 72A; *Chc*, clathrin heavy chain; *Vha16*, V-type proton ATPase 16 kDa proteolipid subunit.

Application of primers	**Target gene**	**Sequence of primers (5' to 3')**	**Product size (bp)**	**Primer efficiency (E%)**
cDNA synthesis	*GFP*	F: none R: TTGATGCCGTTCTTCTGC	305	
dsRNA synthesis	*Lgl*	F: taatacgactcactatagggagCCAACCAGCAGTTGGAGAGT R: taatacgactcactatagggagAGGTAAGGCAACCTCATTGG	506	
	GFP	F: taatacgactcactatagggagCTAGAGTGAGCAAGGGCGAG R: taatacgactcactatagggagCTTGAAGTTCACCTTGATGCC	503	
	Chc	F: taatacgactcactatagggagCCGAGGACATCTCTGTAACAGTGA R: taatacgactcactatagggagCTATCAACACCTGAATGGCAGAGGT	306	
	Arf72A	F: taatacgactcactatagggagCGCCGGAAAGACAACAATTT R: taatacgactcactatagggagCATGTCCTGCTTGTTGGCTA	310	
	Vha16	F: taatacgactcactatagggagAAGTTCAAAATGGCCGAAAA R: taatacgactcactatagggagCCAAGTGGATGAACCCTCTG	286	
	Rab7	F: taatacgactcactatagggagGGATCGTCACCATGCAAATATGGG R: taatacgactcactatagggagGCACTCGTTTCATAGTACGGAATATCA	304	
	AP50	F: taatacgactcactatagggagTCTTCCACATAAAGCGAGCC R: taatacgactcactatagggagCCGATCTGACCAGTCACCTG	310	
	VhaSFD	F: taatacgactcactatagggagCTCGGAGGATAAATCCAGAGTGAAG R: taatacgactcactatagggagATCTACCGACAGGAAGGCGAAGC	304	
	GFP	F: taatacgactcactatagggagTGACCACCCTGACCTAC R: taatacgactcactatagggagTTGATGCCGTTCTTCTGC	304	
qPCR	*Chc*	F: CTGACTACCAAGGCGCTCAT R: AGGCGGCCTGAATATACTTG	130	110.4
	Arf72A	F: GAAGAAGAGCTAGCGAACGC R: AGATCTGGAAGGTTCGGTCG	130	104.9
	Vha16	F: TCCTGATCGCTGGTTCCCT	132	109.6

		R: CATCACCCACGATGCCTATG		
	AP50	F: GTGGCAGGCAAGGTTGTAAT R: GCTGTCAGTGTTGCCAGAGA	129	89.6
	VhaSFD	F: GGCAAGCACATCATCGAGCA R: TGCCGAGGTATTCCCAGTTG	136	105.7
	GFP	F: GCCGCTACCCCGACCACATGA R: CGGGTCTTGTAGTTGCCGTCGT	112	93.8
	RPS3	F: CTGGCCGAAGATGGTTACTC R: ACCACGGAGGTTAGTTCACG	134	89.2
	EF1a	F: CCCGCTAACCTGACCACT R: AAACCACGACGCAACTCC	128	95.3
	Lgl	F: TTCCTGGCACCGGTAGACT R: TAGACTCCACGCAGAGGGA	144	97.6

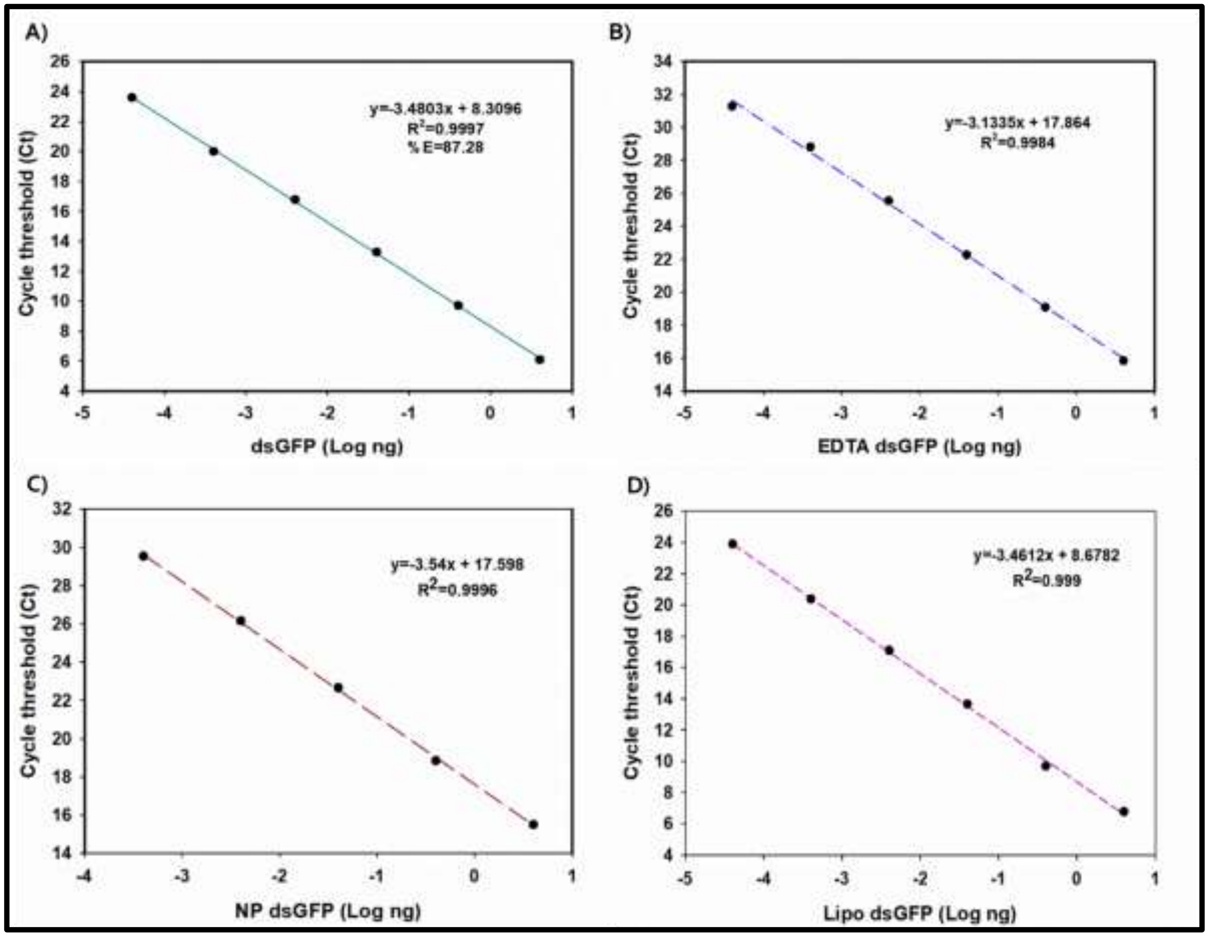

Figure S5-1. Standard curve for the quantification of A) dsRNA, B) EDTA dsRNA, C) NP dsRNA, and D) Lipo dsRNA.

Linear regression of threshold cycle (Ct) values corresponding to five known quantities of ds*GFP*, EDTA ds*GFP*, NP ds*GFP* or Lipo ds*GFP*, and the resulting linear equations that were used to convert raw Ct values for each ds*GFP* sample into nanograms of ds*GFP* recovered and quantified after incubation**.**

Incubation Experiments

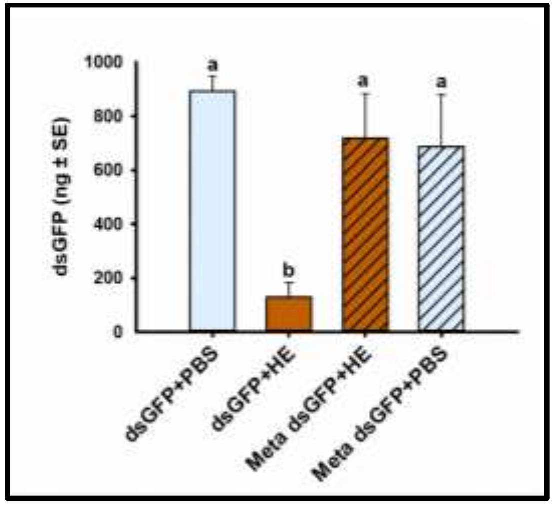

Figure S5-2. Graph showing enhancement of dsRNA stability in hemolymph (HE) due to Metafectene Pro (Meta).

The mean nanograms (ng) of dsRNA targeting the enhanced green florescent protein (*GFP*) gene that were recovered after a 30 min incubation in PBS buffer (control) or tissue extracts harvested from 15 fifth-instar ECB larvae.

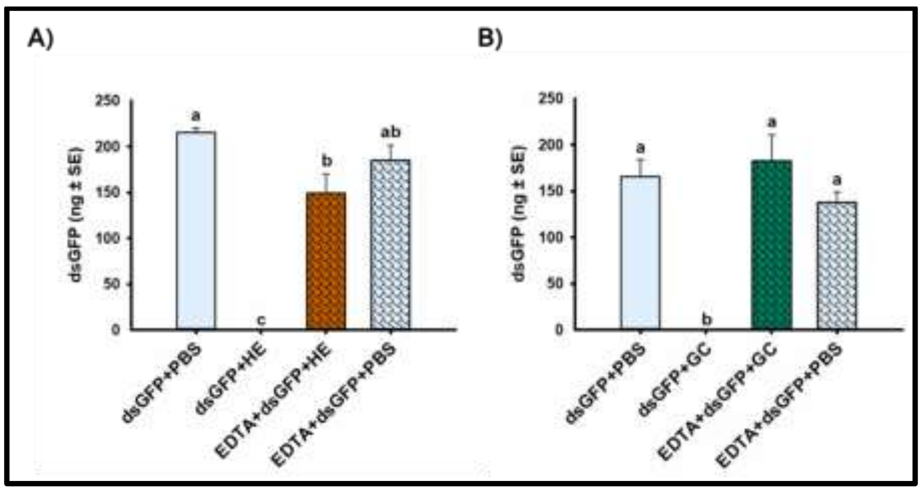

Figure S5-3. Enhancement of dsRNA stability in A) hemolymph (HE) and B) gut contents (GC) and due to 6 mM EDTA.

The mean nanograms (ng) of dsRNA targeting the enhanced green florescent protein (*GFP*) gene that were recovered after a 30 min incubation in PBS buffer (control) or tissue extracts harvested from 15 fifth-instar ECB larvae.

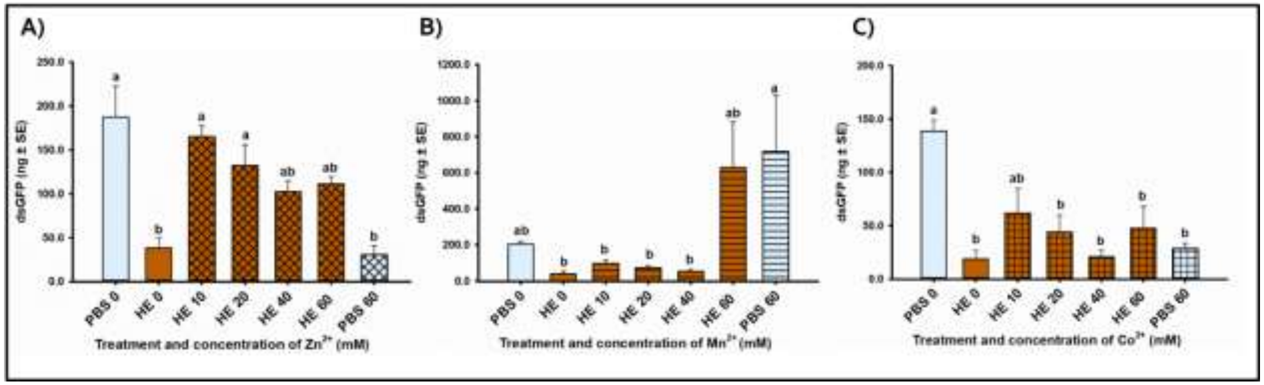

Figure S5-4. Enhancement of dsRNA stability in hemolymph (HE) extracts due to various concentrations of nuclease inhibitor A) Zn^{2+}, but not B) Mn^{+} or C) Co^{2+}.

The mean nanograms (ng) of dsRNA targeting the enhanced green florescent protein (*GFP*) gene that were recovered after a 30 min incubation in PBS buffer (control) or hemolymph harvested from 15 fifth-instar ECB larvae.

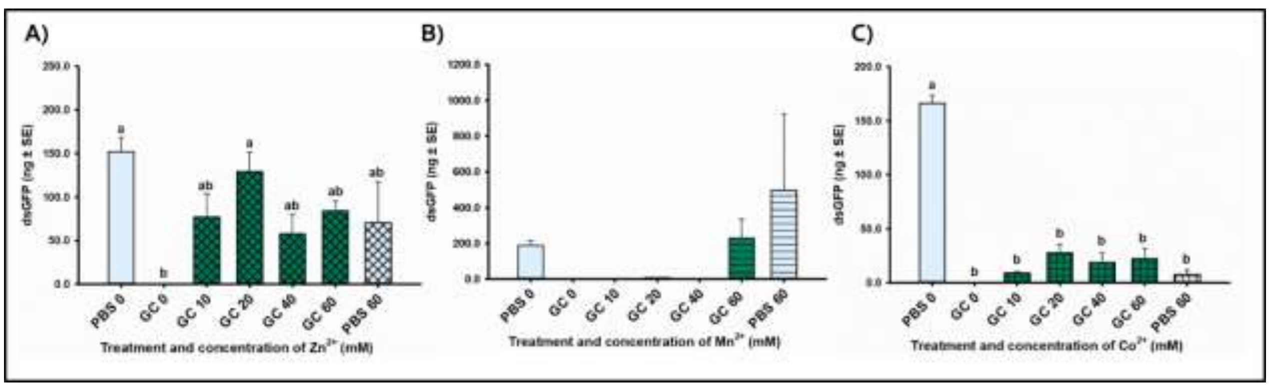

Figure S5-5. Enhancement of dsRNA stability in gut contents (GC) extracts due to various concentrations of nuclease inhibitor A) Zn^{2+}, but not B) Mn^{+} or C) Co^{2+}.

The mean nanograms (ng) of dsRNA targeting the enhanced green florescent protein (*GFP*) gene that were recovered after a 30 min incubation in PBS buffer (control) or gut contents harvested from 15 fifth-instar ECB larvae.

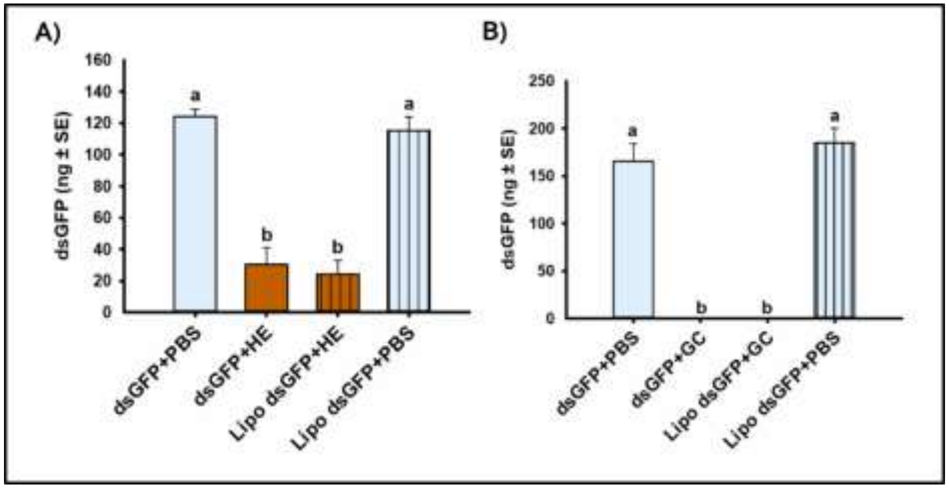

Figure S5-6. Graphs showing no enhancement of dsRNA stability in A) hemolymph (HE) and B) gut content (GC) extracts due to Lipofectamine RNAi Max (Lipo).

The mean nanograms (ng) of dsRNA targeting the enhanced green florescent protein (GFP) gene that were recovered after a 30 min incubation in PBS buffer (control) or tissue extracts harvested from 15 fifth-instar ECB larvae.

Oral RNAi Bioassays

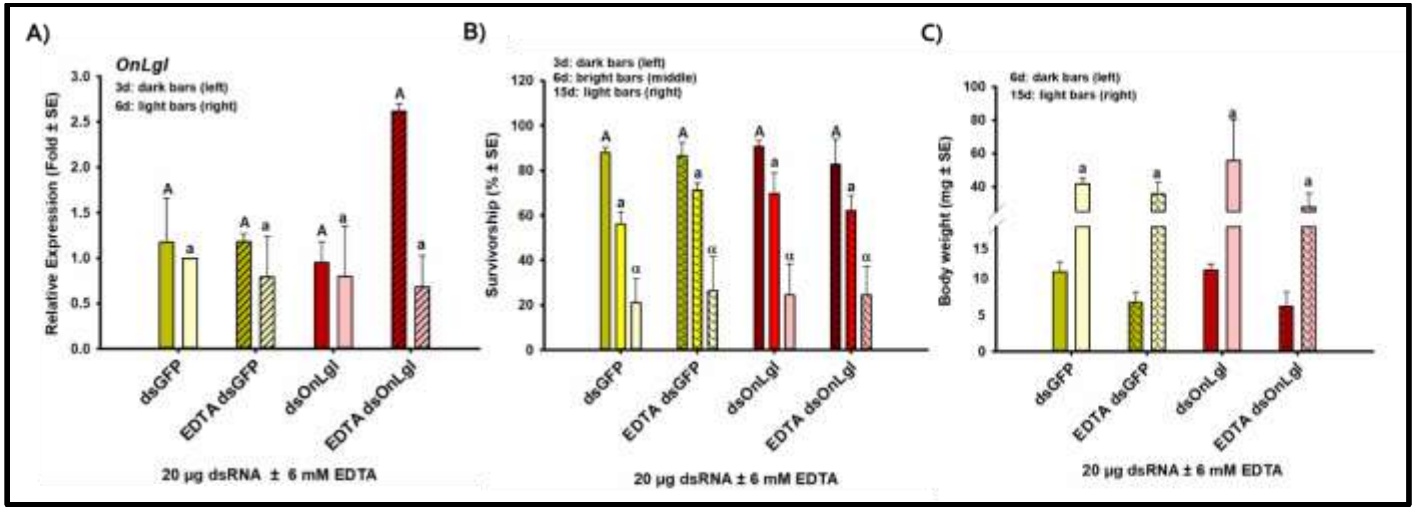

Figure S5-7. RNAi efficiency of 24 h old, unfed, neonate ECB larvae after oral delivery of dsRNA with and without nuclease inhibitor (EDTA).

The mean A) relative expression of the lethal giant larvae (*OnLgl)* target gene B) larval survivorship, and C) body weight, three, six, and fifteen days after the start of feeding of ds*OnLgl* or ds*GFP* incorporated into diet, with and without the addition of 6 mM EDTA. Significant differences between treatments are indicated by the presence of different upper (three day data), lowercase (six day data), and Greek (15 day data) letters.

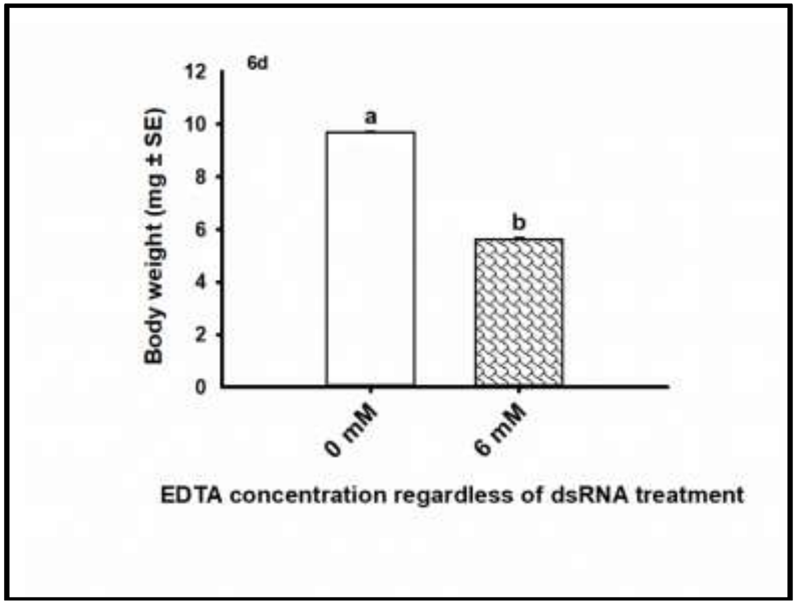

Figure S5-8. Significant effects on body weight of 24 h old, unfed neonate ECB larvae six days after oral delivery of nuclease inhibitor (EDTA) regardless of dsRNA treatment.

Average body weight in milligrams (mg) six days after the start of feeding on ds*OnLgl* or ds*GFP* incorporated into diet with and without 6 mM EDTA. Significant differences between treatments are indicated by the presence of different lowercase letters above bars.

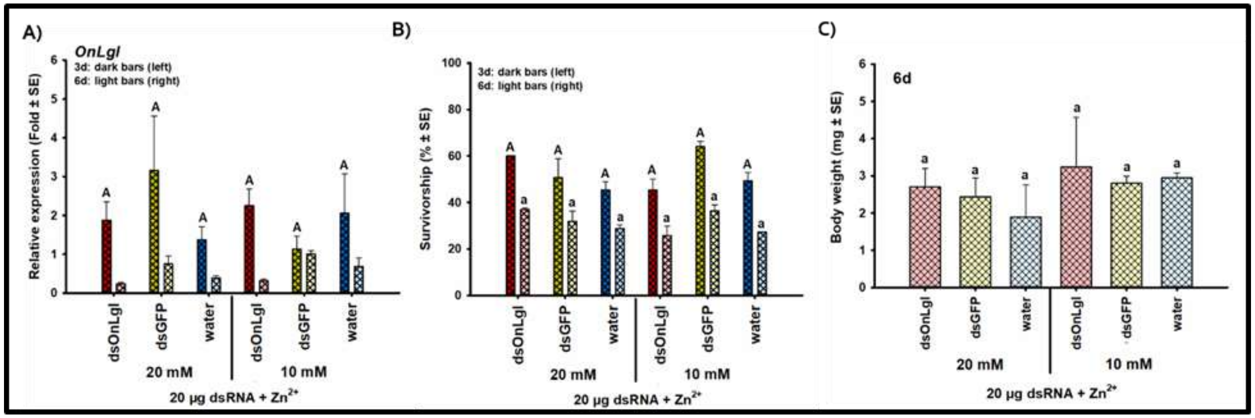

Figure S5-9. RNAi efficiency in 48-h old ECB larvae after oral delivery of dsRNA, with and without nuclease inhibitor (Zn^{2+}).

The mean A) relative expression of the lethal giant larvae (*OnLgl)* target gene B) larval survivorship, and C) body weight, three and six days after the start of feeding of ds*OnLgl* or ds*GFP* incorporated into diet, with 10 or 20 mM Zn^{2+}. Means that do not share a letter are significantly different (3 d and 6 d data with upper and lowercase letters, respectively).

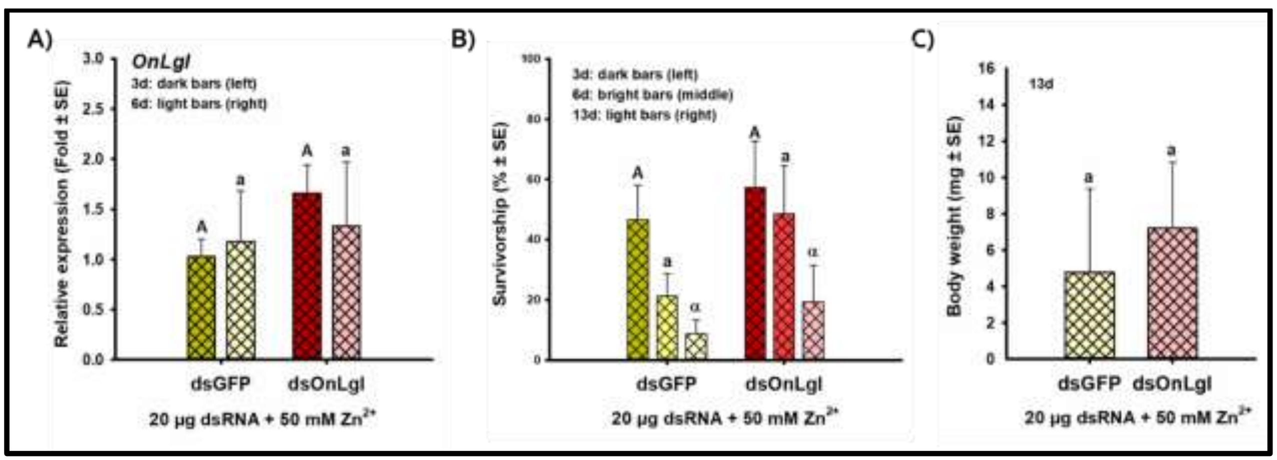

Figure S5-10. RNAi efficiency of 24-h old, unfed, neonate ECB larvae after oral delivery of dsRNA with nuclease inhibitor (50 mM Zn^{2+}).

The mean A) relative expression of the lethal giant larvae (*OnLgl)* target gene B) larval survivorship, and C) body weight, three, six and thirteen days after the start of feeding of ds*OnLgl* or ds*GFP* incorporated into diet with 50 mM RiE-1 Significant differences between treatments are indicated by the presence of different uppercase, lowercase, and Greek letters.

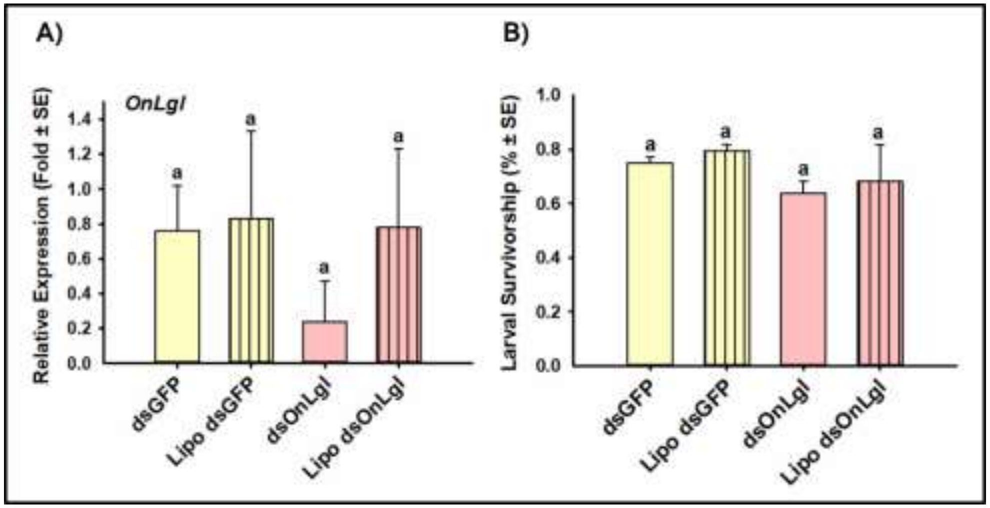

Figure S5-11. RNAi efficiency of 24 h old, unfed, neonate ECB larvae after oral delivery of dsRNA with and without Lipofectamine RNAi Max (Lipo) liposomes.

The mean A) relative expression of the lethal giant larvae (*OnLgl)* target gene B) larval survivorship, and C) body weight, three and six days after the start of feeding on ds*OnLgl* or ds*GFP* incorporated into diet with and without Lipo. Significant differences between treatments are indicated by the presence of different upper and lowercase letters.

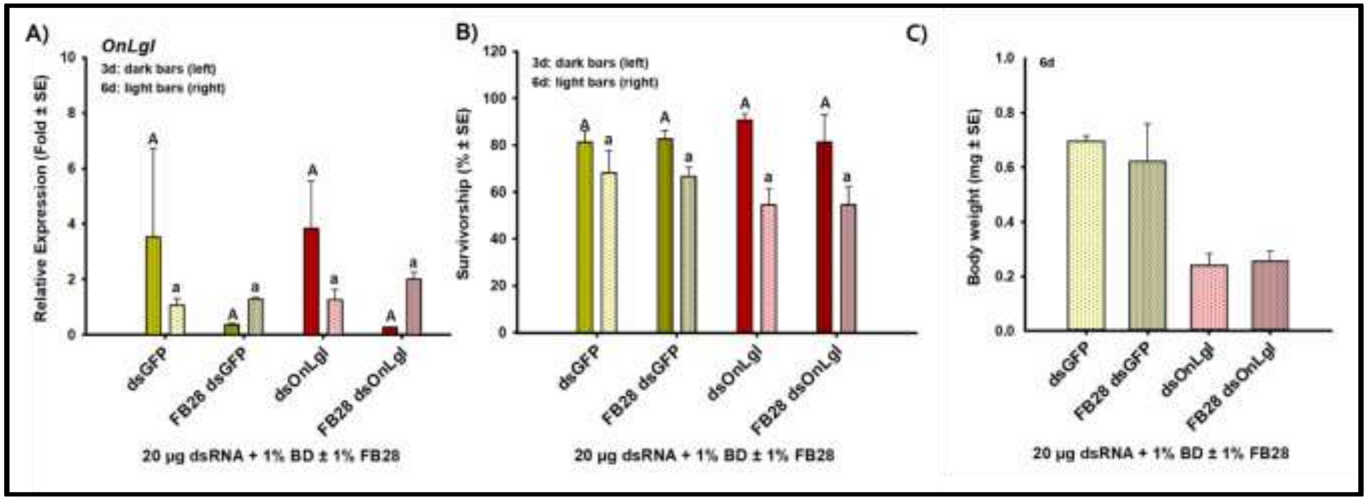

Figure S5-12. RNAi efficiency of 24 h old, unfed, neonate ECB larvae after oral delivery of dsRNA with and without chitin-synthase inhibitor (FB28).

The mean A) relative expression of the lethal giant larvae (*OnLgl)* target gene B) larval survivorship, and C) body weight, three and six days after the start of feeding on ds*OnLgl* or ds*GFP* incorporated into diet with 1% blue dextran (BD) as well as with and without 1% FB28. Significant differences between treatments are indicated by the presence of different upper and lowercase letters.

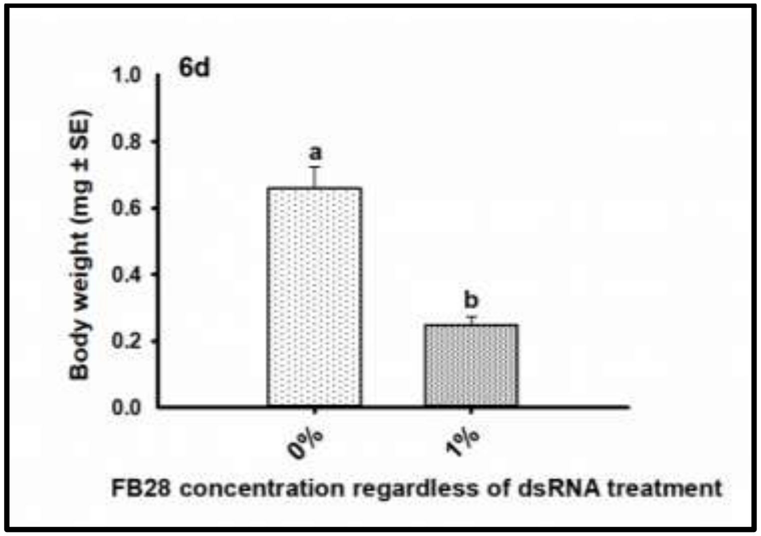

Figure S5-13. Significant effects on body weight after oral delivery of chitin-synthase inhibitor (FB28) regardless of dsRNA treatment.

Average body weight in milligrams (mg) six days after the start of feeding on ds*OnLgl* or ds*GFP* incorporated into diet with 1% blue dextran and either 0% or 1% FB28. Significant differences between treatments are indicated by the presence of different lowercase letters above bars.

Injection RNAi Bioassays

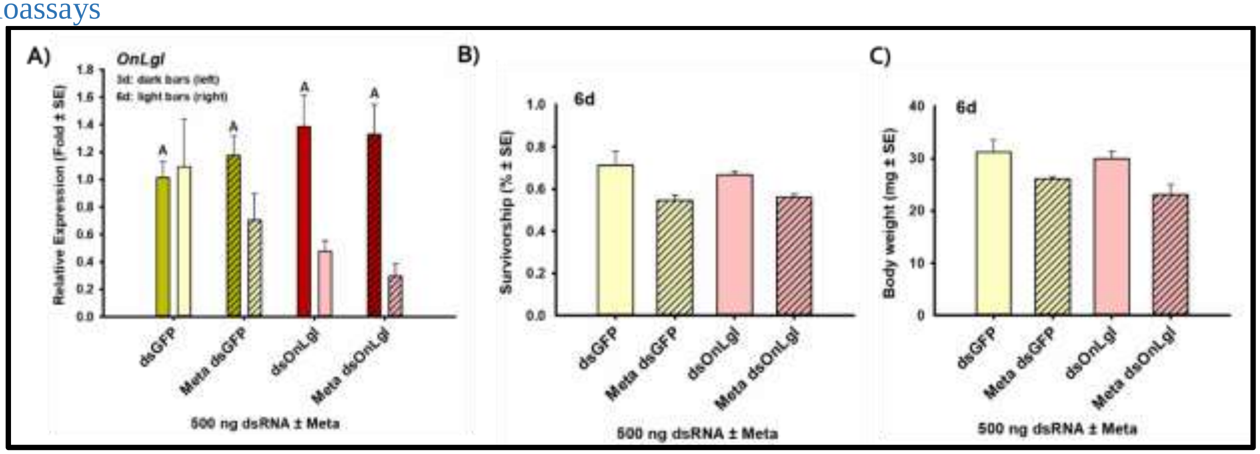

Figure S5-14. RNAi efficiency of third-instar ECB larvae after injection of dsRNA with and without Metafectene Pro (Meta) lipoplexes.

The mean A) relative expression of the lethal giant larvae (*OnLgl)* target gene B) larval survivorship, and C) body weight, three and six days after the start of feeding of ds*OnLgl* or ds*GFP* incorporated into diet with and without encapsulation in Meta lipoplexes. Significant differences between treatments are indicated by the presence of different letters.

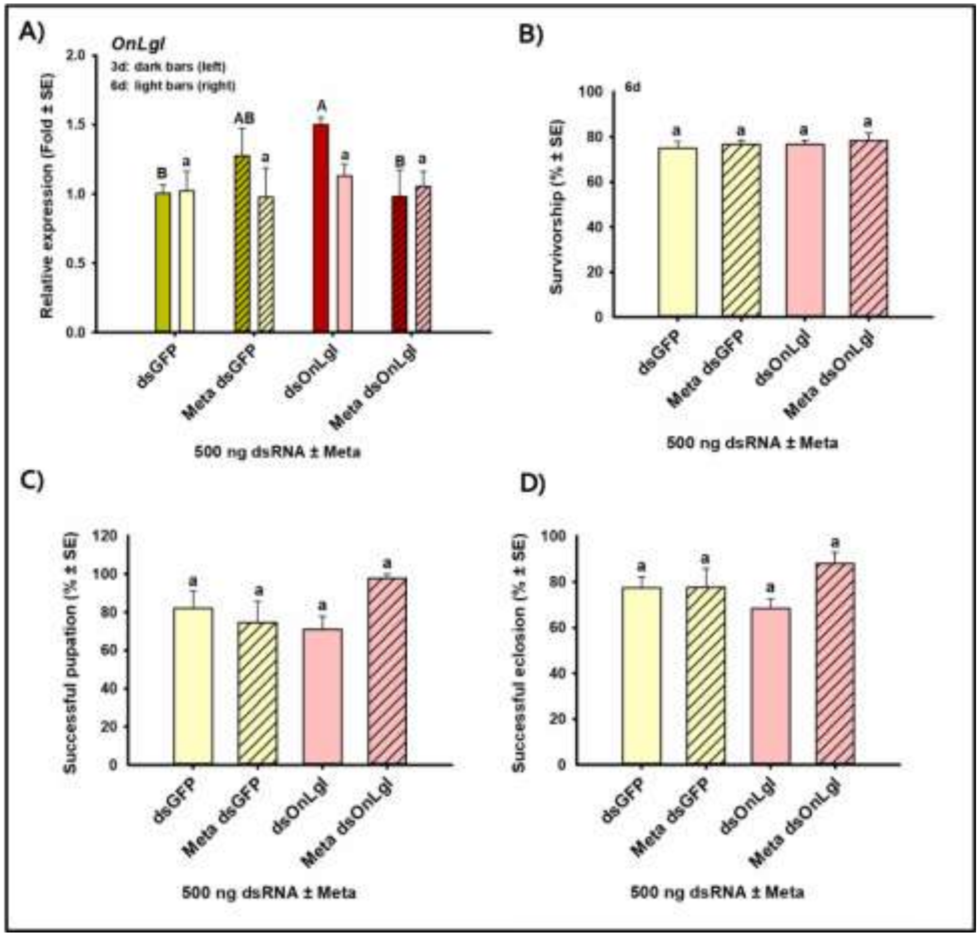

Figure S5-15. RNAi efficiency of wandering ECB larvae after injection of dsRNA with and without Metafectene Pro (Meta) lipoplexes.

The mean A) relative expression of the *OnLgl* target gene three and six days after dsRNA injection into wandering larvae with and without encapsulation of dsRNA in Meta lipoplexes, B) percent of injected larvae to survive six days after injection, C) percent of injected larvae to successfully pupate, D) percent of pupae to successfully eclose into living adult moths. Significant differences between treatments are indicated by the presence of different upper and lowercase letters.

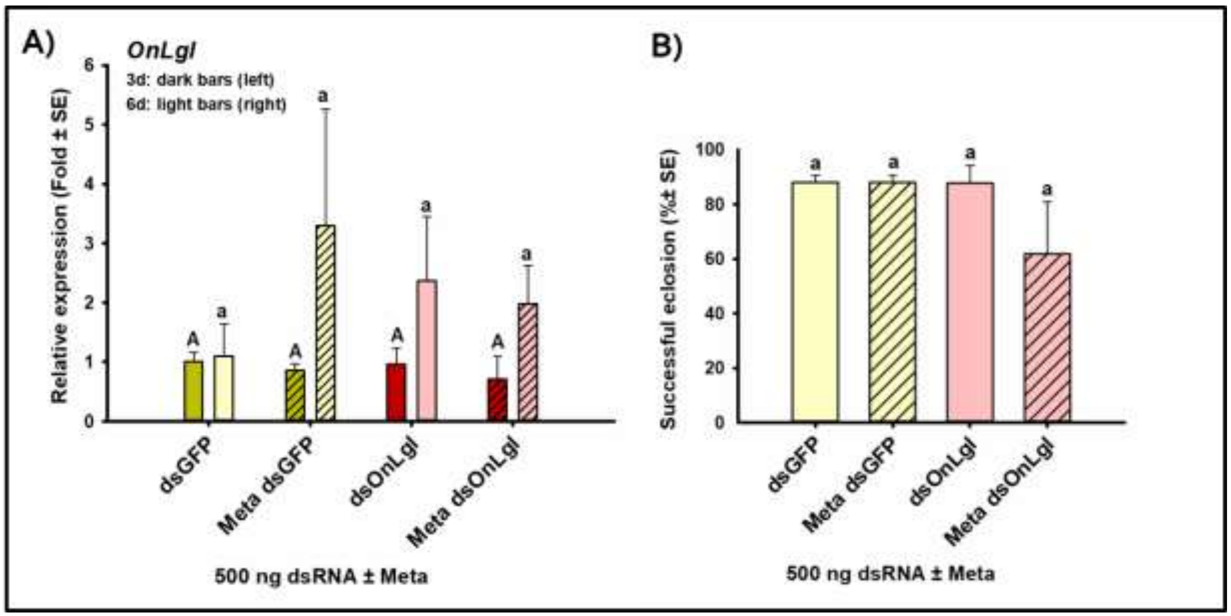

Figure S5-16. RNAi efficiency of 24-48 h old ECB pupae after injection of dsRNA with and without Metafectene Pro (Meta) lipoplexes.

The mean A) relative expression of the *OnLgl* target gene three and six days after dsRNA injection into pupae with and without encapsulation in Meta lipoplexes, and B) percent of injected pupae and successfully eclose into living adult moths, after microinjection of ds*OnLgl* or ds*GFP*, with and without encapsulation of dsRNA in Meta lipoplexes. Significant differences between treatments are indicated by the presence of different lowercase or uppercase letters.

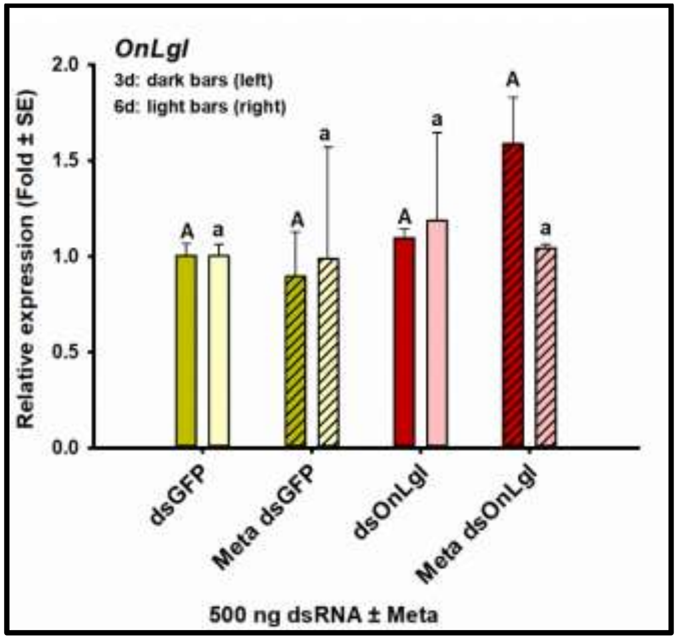

Figure S5-17. RNAi efficiency of >24-h old, adult ECB moths after injection of dsRNA with and without Metafectene Pro (Meta) lipoplexes.

Relative expression of the *OnLgl* target gene three and six days after microinjection of ds*OnLgl* or ds*GFP* with and without encapsulation of dsRNA in Meta lipoplexes. Significant differences between treatments are indicated by the presence of different lowercase or uppercase letters.

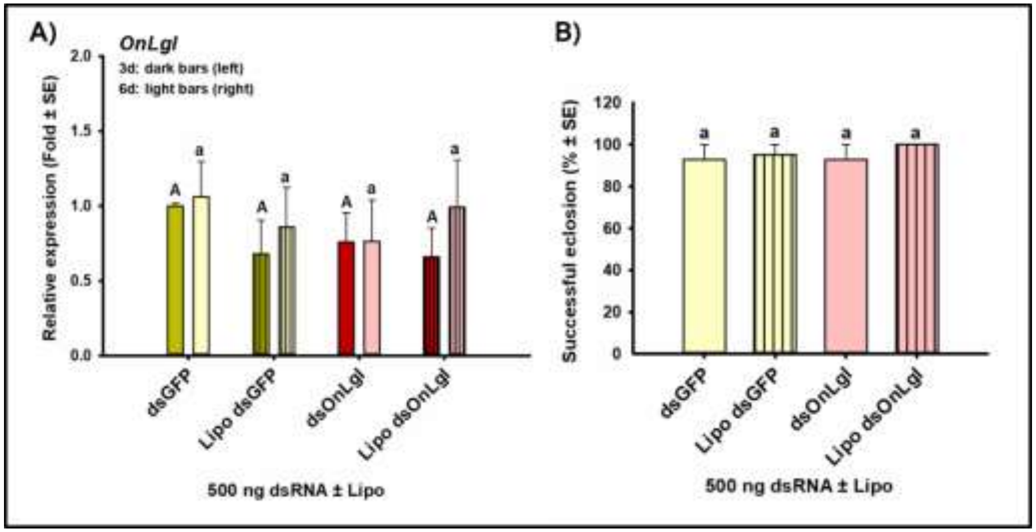

Figure S5-18. RNAi efficiency of 24-48 h old ECB pupae after injection of dsRNA with and without Lipofectamine RNAiMax (Lipo) lipoplexes.

The mean A) relative expression of the *OnLgl* target gene three and six days after dsRNA injection of dsRNA into pupae with and without encapsulation in Lipo lipoplexes, and B) percent of injected pupae and successfully eclose into living adult moths, after microinjection of ds*OnLgl* or ds*GFP*, with and without encapsulation of dsRNA in Lipo lipoplexes. Significant differences between treatments are indicated by the presence of different lowercase or uppercase letters.

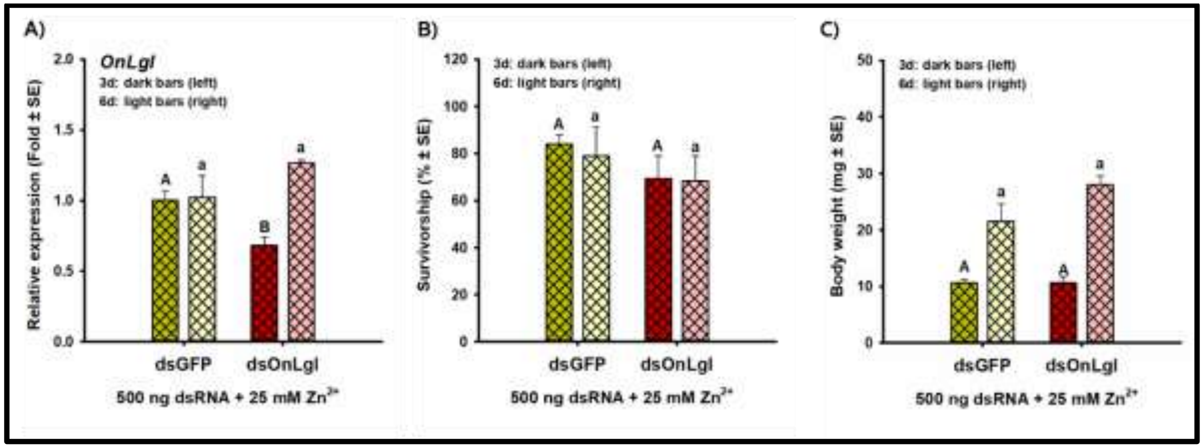

Figure S-19. RNAi efficiency following injection of third-instar ECB larvae with dsRNA and 25 mM nuclease inhibitor (Zn^{2+}).

The mean A) relative expression of the lethal giant larvae (*OnLgl)* target gene B) larval survivorship, and C) body weight, three and six days after injection of ds*OnLgl* or ds*GFP* in conjunction with 25 mM Zn^{2+}. Significant differences between treatments are indicated by the presence of different upper (3 d) and lowercase (6 d) letters.

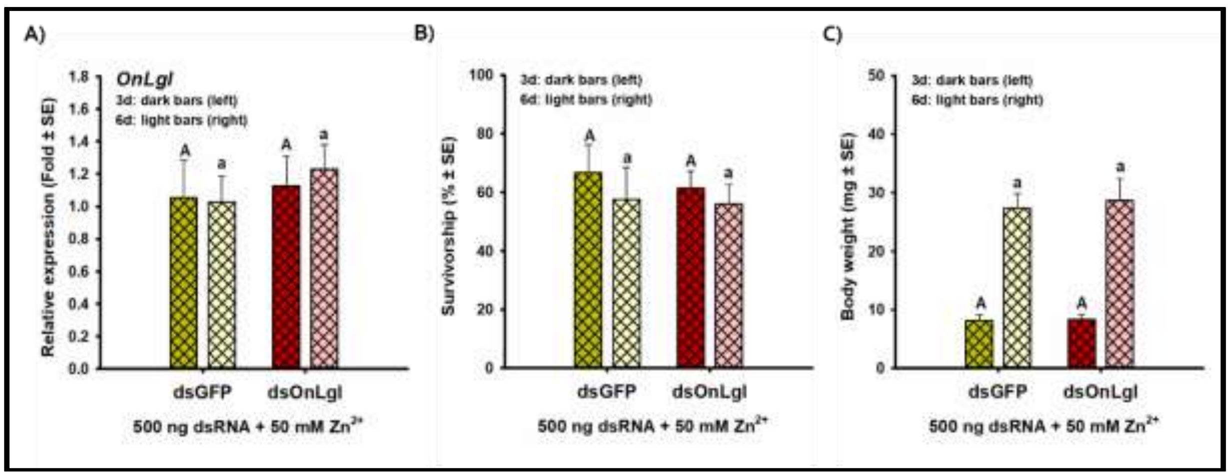

Figure S5-20. RNAi efficiency of third-instar ECB larvae after injection of dsRNA with 50 mM nuclease inhibitor (Zn^{2+}).

The mean A) relative expression of the lethal giant larvae (*OnLgl)* target gene B) larval survivorship, and C) body weight, three and six days after injection of ds*OnLgl* or ds*GFP* with 50 mM Zn^{2+}. Significant differences between treatments are indicated by the presence of different upper and lowercase letters.

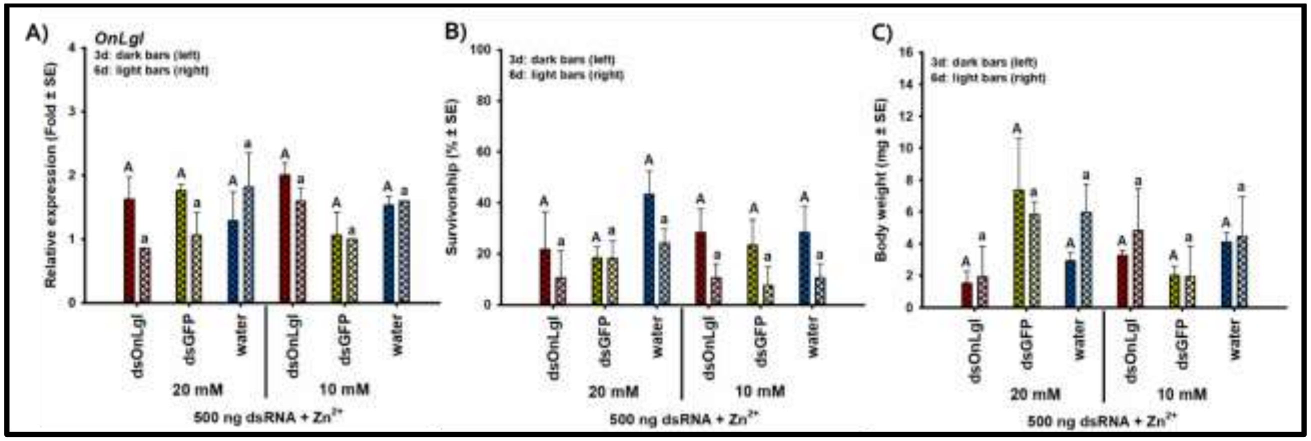

Figure S5-21. RNAi efficiency of 48 h old ECB larvae after injection of dsRNA with and without 10 mM and 20 mM nuclease inhibitor (Zn^{2+}).

The mean A) relative expression of the lethal giant larvae (*OnLgl)* target gene B) larval survivorship, and C) body weight, three and six days three and six days after injection of ds*OnLgl* or ds*GFP* with 10 and 20 mM Zn^{2+}. Significant differences between treatments are indicated by the presence of different upper lowercase letters.

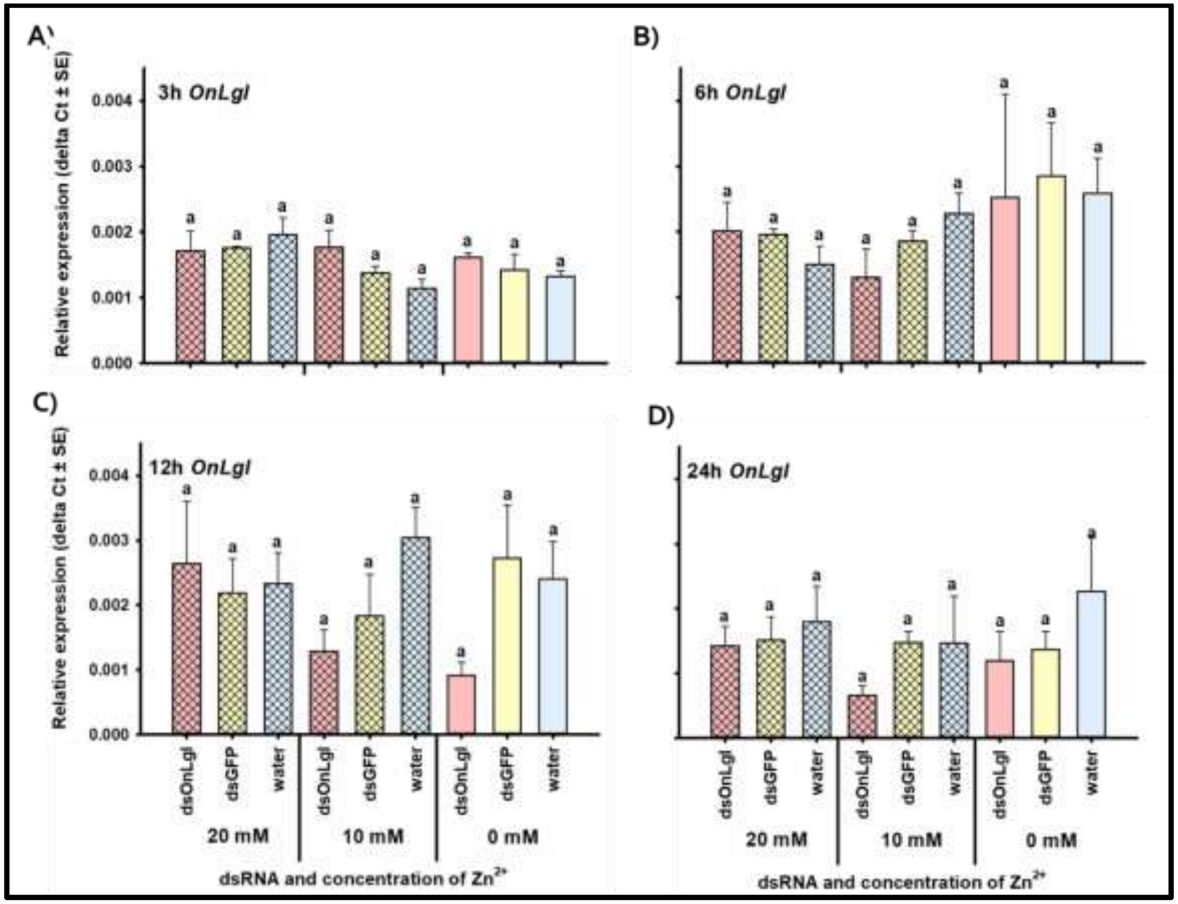

Figure S5-22. Short-term time-dependent expression of *OnLgl* after oral delivery of dsRNA in combination with various concentrations of nuclease inhibitor (Zn^{2+}).

The mean relative expression of the lethal giant larvae (*OnLgl)* target gene after A) three, B) six, C) twelve, and D) twenty-four hours of feeding on diet containing ds*OnLgl* or ds*GFP* as well as 10 or 20 mM Zn^{2+}. Significant differences between treatments are indicated by the presence of different lowercase letters above bars.

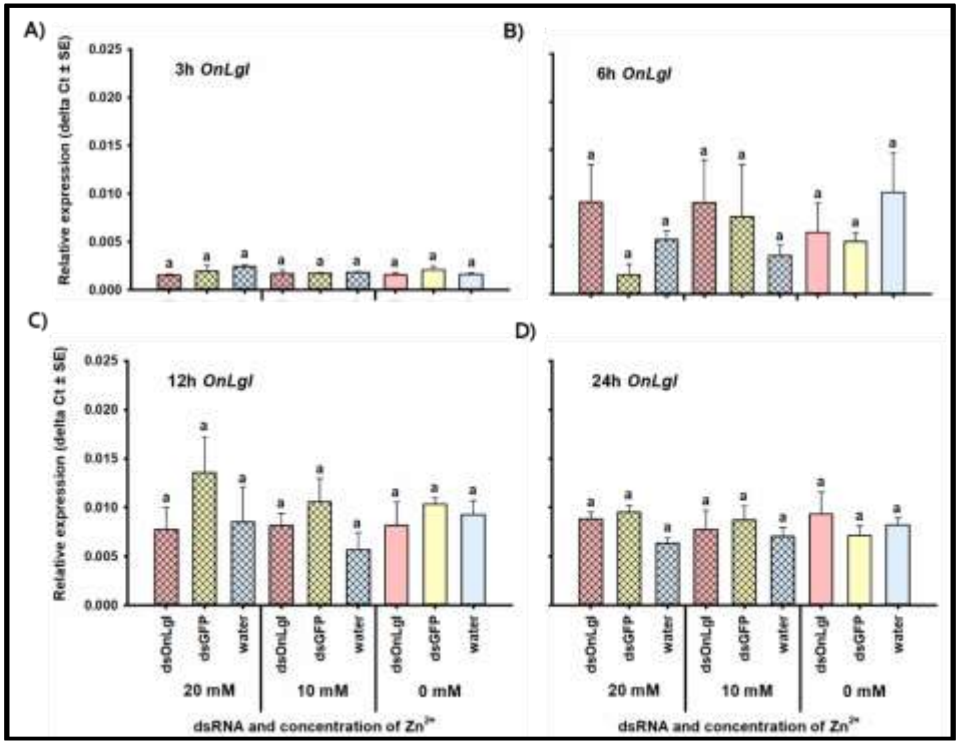

Figure S5-23. Short-term time-dependent expression of *OnLgl* after injection of dsRNA in combination with various concentrations of nuclease inhibitor (Zn^{2+}).

The mean relative expression of the lethal giant larvae (*OnLgl)* target gene A) three, B) six, C) twelve, and D) twenty-four hours after injection of ds*OnLgl* or ds*GFP* as well as 10 or 20 mM Zn^{2+}. Significant differences between treatments are indicated by the presence of different lowercase letters above bars.

Tissue Culture RNAi Assays

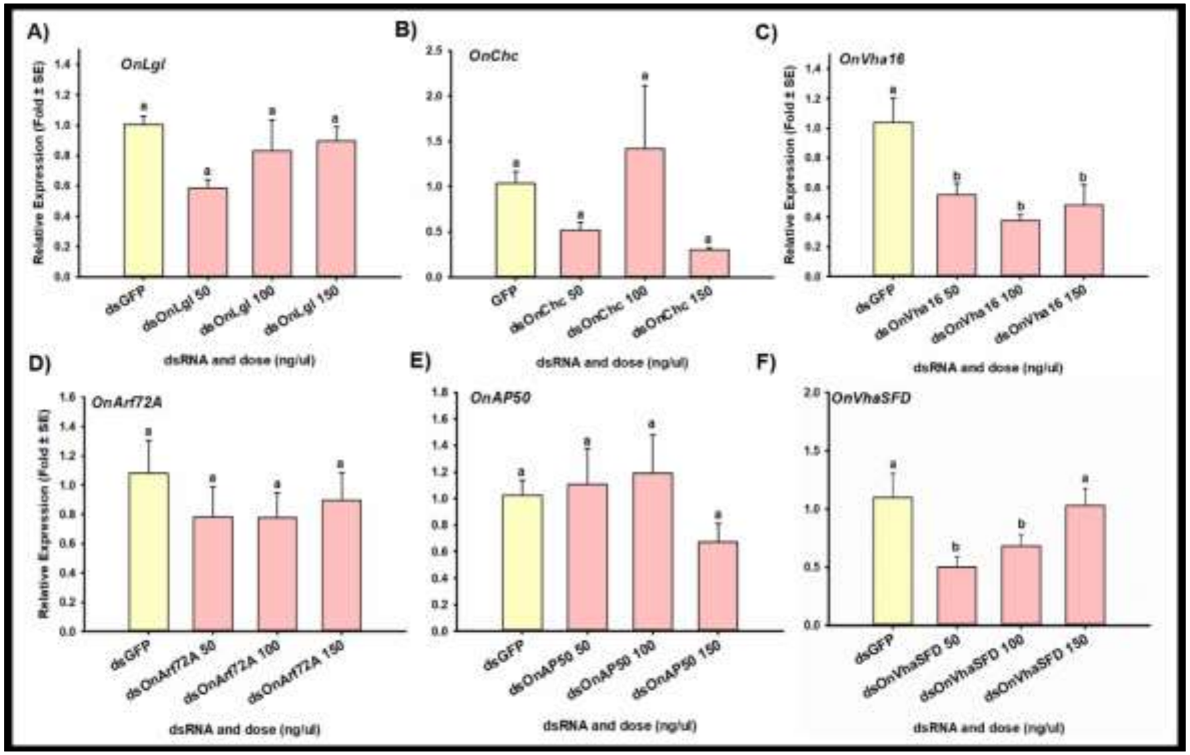

Figure S5-24. Comparison of RNAi efficiency in ECB midgut tissue cultures for multiple target genes after incubation of excised midguts in tissue culture medium containing various concentrations of dsRNA.

The mean relative expression of A) lethal giant larvae (*OnLgl*), B) clathrin heavy chain (*OnChc*), C) V-type proton ATPase 16 kD proteolipid subunit (*OnVha16*), D) ADP ribosylation factor 72A (*OnArf72A*), E) adaptor protein complex 50 (*OnAP50*), and F) V-type proton subunit H (*OnVhaSFD*) after a 24 h incubation of individual excised midguts harvested from fifth instar larvae in tissue culture medium containing 50, 100, or 150 ng/µl of dsRNA targeting each target gene, or *GFP* as a control. Significant differences between treatments are indicated by the presence of different lowercase letters.

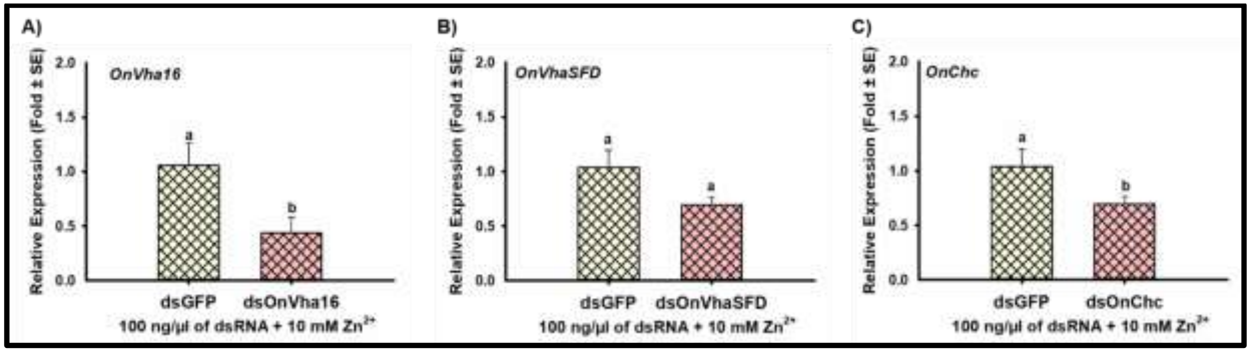

Figure S-25: Enhancement of RNAi efficiency for specific target genes in ECB midgut tissue cultures due to inclusion of nuclease inhibitor Zn^{2+}.

The mean relative expression of the A) V-type proton ATPase 16 kD proteolipid subunit *(OnVha16)*, B) V-type proton subunit H *(OnVhaSDF)*, and C) clathrin heavy chain *(OnChc)* target genes after incubation of excised midguts from fifth-instar ECB larvae in media containing 10 mM Zn^{2+} and either ds*OnVha16*, ds*OnVhaSFD*, or ds*GFP*. Means that do not share a letter are significantly different**.**